NSF/CEE-82104

PB83-194266

DYNAMIC RESPONSE OF JOINTED ROCK MASSES

by

Gregg Alan Scott

B.S., University of Colorado, 1976

A thesis submitted to the

Faculty of the Graduate School of the

University of Colorado in partial fulfillment

of the requirements for the degree of

Master of Science

Department of Civil, Environmental, and

Architectural Engineering

1982

INFORMATION RESOURCES
NATIONAL SCIENCE FOUNDATION

50272-101

68-12

REPORT DOCUMENTATION PAGE	1. REPORT NO. NSF/CEE-82104	2.	3. Recipient's Accession No. PB3 194266

4. Title and Subtitle Dynamic Response of Jointed Rock Masses	5. Report Date 1982
	6.
7. Author(s) G.A. Scott	8. Performing Organization Rept. No.
9. Performing Organization Name and Address University of Colorado Department of Civil, Environmental, and Architectural Engineering Boulder, CA 80309	10. Project/Task/Work Unit No.
	11. Contract(C) or Grant(G) No. (C) CEE8105779 (G)
12. Sponsoring Organization Name and Address Directorate for Engineering (ENG) National Science Foundation 1800 G Street, N.W. Washington, DC 20550	13. Type of Report & Period Covered M.S. Thesis 1982
	14.

15. Supplementary Notes

Submitted by: Communications Program (OPRM)
National Science Foundation
Washington, DC 20550

16. Abstract (Limit: 200 words)

The static behavior of clean rock joints is reviewed and it is determined that the criteria of Patton, Jaeger, Ladanyi and Archambault, and Barton are appropriate for the analysis of rock masses under static loading conditions. An analytical method for three-dimensional limit equilibrium analysis of rock mass bounded by planar discontinuities is discussed, and the means of adapting the method for computer solution are noted. The dynamic shear behavior of clean rock joints is examined and a dynamic limit equilibrium analysis, including provisions for calculating permanent displacements and accounting for dynamic material behavior, is described.

17. Document Analysis a. Descriptors

Rocks	Computers
Dynamic loading	Rock mechanics
Static loading	Displacement
Earthquakes	Mathematical models

b. Identifiers/Open-Ended Terms

Equilibrium analysis	S. Sture, /PI
Rock joints	

c. COSATI Field/Group

18. Availability Statement	19. Security Class (This Report)	21. No. of Pages
NTIS	20. Security Class (This Page)	22. Price

(See ANSI–Z39.18) See Instructions on Reverse

OPTIONAL FORM 272 (4–77)
(Formerly NTIS–35)
Department of Commerce

This thesis for the Master of Science degree by

Gregg Alan Scott

has been approved for the

Department of

Civil, Environmental, and Architectural Engineering

by

Stein Sture

Hon-Yim Ko

Bernard Amadei

Date December 1, 1982

Any opinions, findings, conclusions or recommendations expressed in this publication are those of the author(s) and do not necessarily reflect the views of the National Science Foundation.

Scott, Gregg Alan (M.S., Civil Engineering)
Dynamic Response of Jointed Rock Masses
Thesis directed by Associate Professor Stein Sture

Growing public awareness and demand for safe design and construction of potentially hazardous projects in earthquake prone regions has prompted extensive work in earthquake engineering and research toward determining dynamic material response. However, only recently has research been directed toward determining the dynamic behavior of rock joints.

A servocontrolled dynamic direct shear apparatus has been developed at the University of Colorado, for testing rock joint specimens. Independent normal and shear load actuators are capable of dynamic testing up to a frequency of 10 Hz under load or displacement control. Artificial rough and smooth clean sandstone joint specimens, with nominal shear areas larger than 325 cm^2 (50 in^2), were tested under dry displacement controlled conditions. The response of the samples to dynamic shear excitations under constant normal stress was measured utilizing sensitive instrumentation. Shearing velocity was found to have a significant effect on the strength of clean rock joints.

A computer program was developed for performing dynamic three-dimensional limit equilibrium analyses of potentially unstable rock masses. When evaluating the effects of earthquakes is considered to be important, response history rigid block analyses for rock masses can be performed. Time-varying forces are combined with static forces to determine time-varying resultant forces acting on potentially unstable rock masses. The potential mode of instability and factor of safety are determined at each time step during an earthquake analysis. When the factor of safety drops below 1.0, cumulative permanent displacements can be estimated by double integration of the relative acceleration between the rock mass and its underlying support. Provisions have also been made for including in the analysis dynamic material behavior as determined from the laboratory testing. Accounting for a change in strength with increasing velocity is shown to have a significant effect on cumulative permanent displacements for an example problem of a dam foundation.

Further research is needed to develop comprehensive models for the dynamic behavior of rock joints. Different rock types, effects of water and changes in water pressure, load controlled testing, testing of filled joints, and testing under dynamic normal loads warrant future consideration.

The form and content of this abstract are approved.

Signed Adrian C. Gure
Faculty member in charge of thesis

ACKNOWLEDGEMENTS

The author wishes to thank the following groups and individuals for their roles in the completion of this research:

The U.S. Bureau of Reclamation for support of the research through funding and time allowed for participation.

Larry Von Thun for his constant support and interest in the technical work.

Professors Stein Sture, Hon-Yim Ko, and Bernard Amadei for their advice and direction.

The National Science Foundation for their funding support.

The people in the laboratories at the University of Colorado including Mark Gould for his development work and testing.

A special thanks to his wife Ricka for her help, support, and understanding during completion of this work.

CONTENTS

TABLES

Table

FIGURES

Figure

Figure

Figure

CHAPTER I

INTRODUCTION

1.1 Background

Growing public awareness and demand for the safe design and construction of potentially hazardous projects, such as large dams in earthquake prone regions, has prompted extensive work in earthquake engineering and research toward determining dynamic material response. It has been established that saturated cohesionless soils exhibit significant changes in pore pressure, deformation, and strength characteristics when subjected to cyclic or dynamic excitations. This behavior has been observed both in the field and under laboratory conditions, as summarized by Seed [25], Hardin [14], Woods [32], Finn [9], and Silver [26]. As a result of this behavior, earth structures have failed when subjected to earthquake ground motions, although pseudostatic analyses show them to be stable. The Madison Canyon (Montana) landslide, triggered by the 1959 Hebgen Lake earthquake may represent similar phenomena in rock. A buttress of jointed dolomite collapsed due to the shaking and allowed a landslide containing 33 000 000 m^3 (43 000 000 yd^3) of material to occur. Sliding occurred along the foliation of a schist above the dolomite dipping at 50° toward the canyon. Twenty-seven people lost their lives [1]. No major engineering accidents are known to have resulted from failure of a rock mass subjected to earthquake loading. However, many large dams are founded on nearly saturated rock in seismically active areas. It is therefore important to understand potential foundation response during earthquake conditions.

It is generally accepted that the behavior of a rock mass is controlled to a large extent by the presence of discontinuities [11, 15]. These discontinuities may include bedding planes, foliation, geologic contacts, joints, seams, shear zones, and faults. The catastrophic abutment failure of the 61-m (200-ft) high arch Malpasset Dam in southern France occurred by sliding of a rock wedge on an upstream dipping fault plane. The disaster, which occurred in 1959, resulted in the deaths of over 420 people [17]. Similarly, the catastrophic landslide which occurred at Vajont Dam in Italy resulted in 240 000 000 m^3 (314 000 000 yd^3) of material sliding along the limestone bedding of the reservoir rim. The slide, which occurred in 1963, resulted in a wave of water overtopping the 265-m (870-ft) high arch dam by 100 m (330 ft). About 2,600 people were killed downstream. The arch dam, however, did not fail [17]. The shear strength and shear deformation characteristics of discontinuities are, therefore, often critical to the stability of a rock mass. State-of-the-art determination of these characteristics usually involves extensive in situ and laboratory tests conducted at loading rates appropriate for static conditions. Stability analyses are conducted incorporating static loads, material properties, and effective stresses computed utilizing a steady-state seepage water pressure distribution [7]. Response of the rock mass to design earthquakes is considered by estimating appropriate ground-motion parameters and external dynamic loads. Stability analyses may be pseudostatic or include estimation of two-dimensional permanent cumulative displacements occurring when the strengths of rock discontinuities are exceeded for short periods of time during a response history earthquake analysis [22, 13, 30]. However, because little is known about the dynamic behavior of rock discontinuities, the material characteristics obtained from static tests are utilized, and no change to the steady-state water pressure distribution is considered.

Only recently has research been directed towards determining dynamic properties of rock discontinuities. Crawford and Curran [5] developed a servocontrolled direct shear apparatus for dynamically testing rock joints. Test results on saw cut joint specimens indicate changes in shear strength occur with changing shear velocity. This has been shown to be an important consideration when estimating permanent displacements of rock masses during earthquakes [6].

Similar research was conducted at the University of Colorado laboratories under the sponsorship of the U.S. Bureau of Reclamation and the National Science Foundation. A servocontrolled dynamic direct shear apparatus was developed, capable of testing specimens in load or displacement control. Artificial rough and smooth clean sandstone joint specimens were tested under dry displacement controlled conditions. The response of the samples to the dynamic excitations was measured utilizing sensitive instrumentation and recorded using a data acquisition system. Details of the direct shear apparatus and testing are described by Gould [12].

1.2 Scope of Work

The results of the testing performed by Gould [12] are examined and compared to the work of Crawford and Curran [5]. Changes in the shear strength of rock joints as the result of dynamic loading are discussed. The development of a computer program for performing dynamic three-dimensional limit equilibrium earthquake analyses of rock masses is also discussed. Provisions for calculating cumulative permanent displacements of a rock mass where the factor of safety drops below 1.0 for short periods of time during an earthquake are included. The effects of dynamic material behavior as determined from the laboratory testing may also be included. The stability of a dam foundation during an earthquake is examined, including the effects of dynamic material behavior on calculated permanent displacements.

Chapter II contains a review of the static behavior of clean rock joints. Chapter III discusses an analytical method for three-dimensional limit equilibrium analysis of a rock mass bounded by planar discontinuities. The dynamic shear behavior of clean rock joints is discussed in Chapter IV. Chapter V contains a description of dynamic limit equilibrium analysis including provisions for calculating permanent displacements and accounting for dynamic material behavior. Conclusions, suggestions for further study, and a summary are contained in Chapter VI.

CHAPTER II

REVIEW OF STATIC SHEAR BEHAVIOR OF CLEAN ROCK JOINTS

2.1 Introduction

The shear strength of rock discontinuities is the most important consideration in determining the stability of a rock mass for near surface projects where a kinematically possible mode of instability exists. Many investigators have proposed empirical criteria for the shear strength of clean joints. However, only the most widely accepted models will be reviewed here.

2.2 Smooth Planar Discontinuities

Consider a smooth and planar joint, resulting from a preferred orientation of the rock structure, subjected to a uniform normal stress, σ, and shear stress, τ, as shown in Figure 2.1. If the incipient joint is initially cemented and the shear stress is increased until the rock slides along the joint, the resulting shear stress vs. shear deformation curve would be similar to that shown in Figure 2.2. The peak strength occurs just prior to the point where bond is broken, after which the shear stress falls to residual strength. The residual and peak strengths would have been the same if the sample had been unbonded prior to testing. Identical samples tested at different normal stresses will exhibit increasing peak and residual strength with

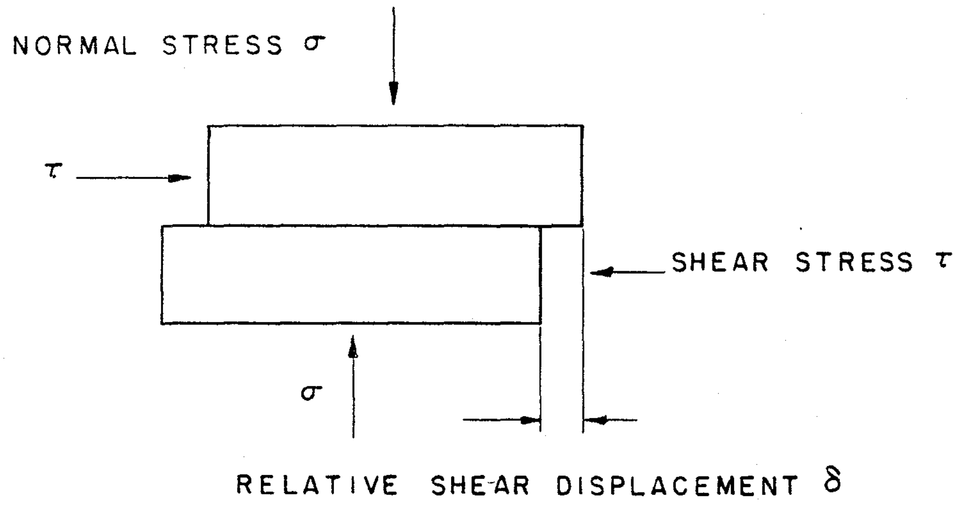

Figure 2.1 Smooth Joint Under Direct Shear Conditions.

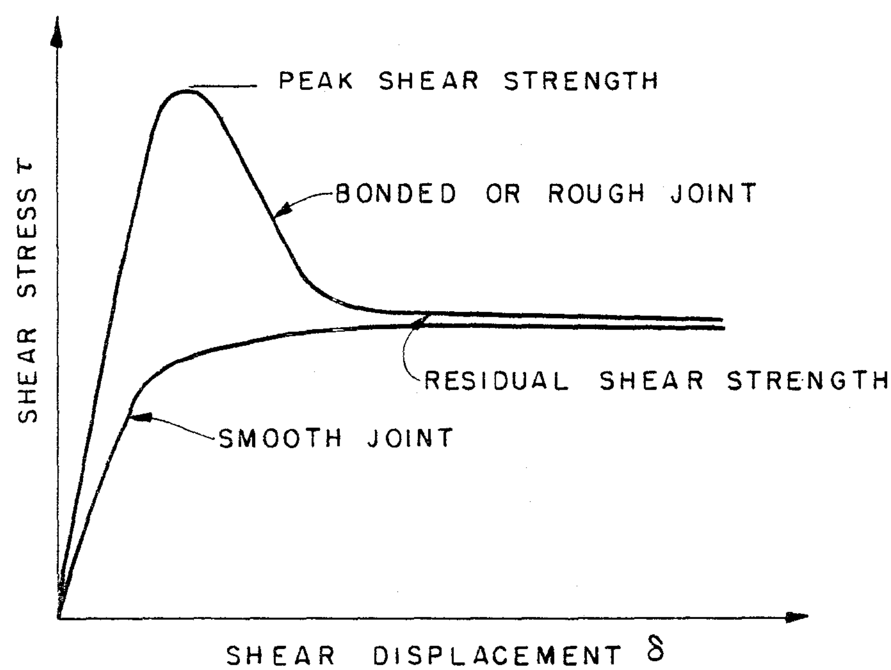

Figure 2.2 Typical Shear Stress vs. Shear Deformation Curves.

increasing normal stress. The resulting strength envelopes, developed by plotting shear strength vs. normal stress, would be similar to those shown in Figure 2.3. The peak strength representative of bonded joints may be defined by the linear equation:

$$\tau = C + \sigma \tan \phi_p \tag{2.1}$$

in which C is the cohesion or strength of the sample under zero normal stress, defined by the shear stress intercept, and $\tan \phi_p$ is the slope of the peak strength envelope. The strength of unbonded smooth joints is given by:

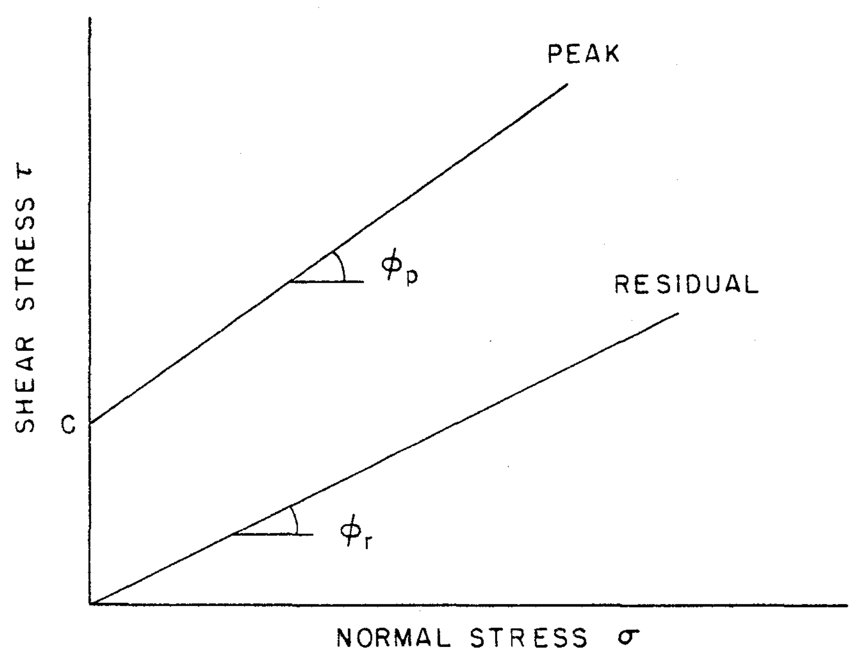

Figure 2.3 Typical Shear Strength Envelopes.

$$\tau = \sigma \tan \phi_r \qquad (2.2)$$

in which $\tan \phi_r$ is the slope of the residual strength envelope, which indicates zero strength at zero normal stress. Equations (2.1) and (2.2) are often referred to as the Mohr-Coulomb failure criterion.

2.3 Rough Discontinuities

The shear stress vs. shear displacement curve for an unbonded rough joint specimen tested under constant normal stress might look similar to that shown in Figure 2.2 for bonded smooth joints. However, since the joint is open, it has essentially zero shear strength at zero normal stress. Tests at different normal stresses would indicate generally increasing shear strength with increasing normal stress. However, the resulting failure envelope would be nonlinear. Intuitively, the effects of roughness on shear strength should be normal stress dependent. At low normal stresses, dilation or riding up on asperities occurs during shearing of a rough joint. At high normal stresses, shearing through asperities occurs, since the work required to shear through the asperities is less than the work required to override them.

2.3.1 Patton's Criterion

Patton [23] is often credited as being the first to quantify the effects of roughness on the shear strength of open joints. Figure 2.4 shows an idealized schematic of a rough open joint in direct shear. For asperities uniformly inclined at an angle i to the direction of shearing, it can be shown trigonometrically that the following relationship applies, assuming that the asperities are rigid and not sheared [15].

$$\tau = \sigma \tan(\emptyset + i) \tag{2.3}$$

Patton verified that this equation is valid at low normal stresses with laboratory tests on artificial joints whose roughness was

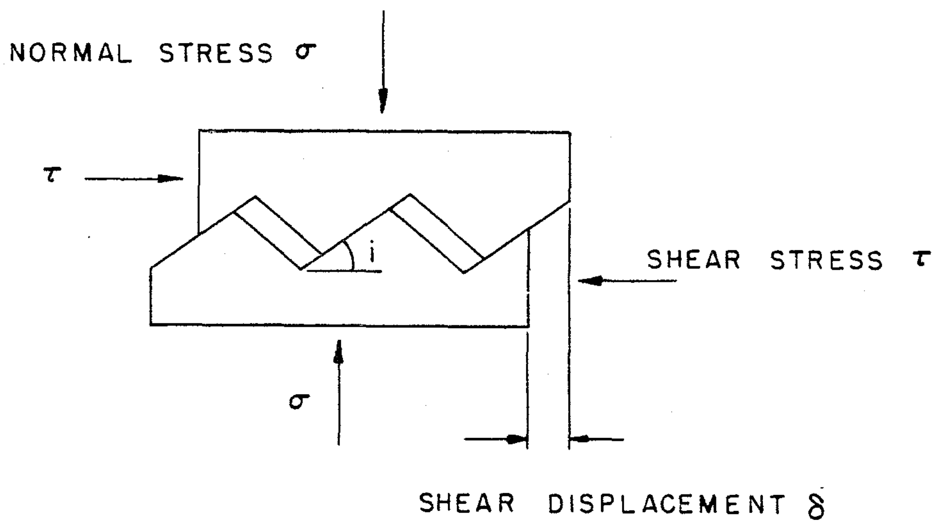

Figure 2.4 Rough Joint Under Direct Shear Conditions.

simulated using regularly inclined teeth. At higher normal stresses, the resulting failure envelopes became nonlinear, with the slope of the line approaching that corresponding to the residual friction angle of the material. Patton suggested that a nonlinear, or bilinear envelope such as that shown in Figure 2.5, is appropriate for the shear strength of rough joints.

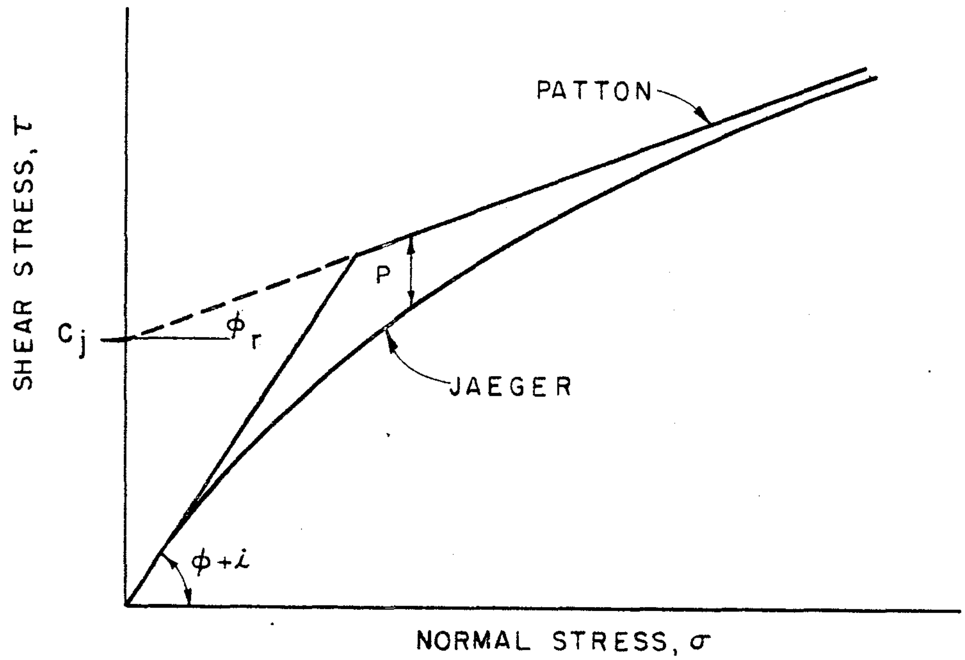

(a) Failure Envelopes.

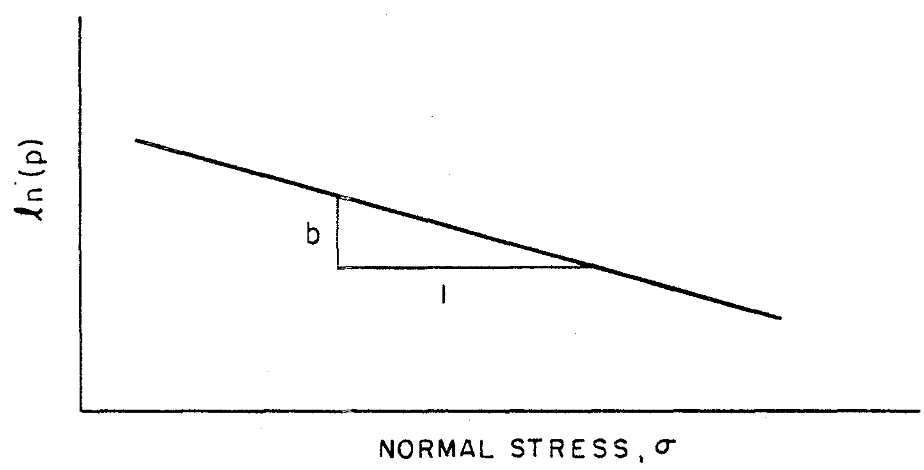

(b) Graphical Construction for Jaeger's Criterion.

Figure 2.5 Patton's [23] and Jaeger's [16] Failure Criteria for Rough Joints.

2.3.2 Jaeger's Criterion

Jaeger [16] proposed a continuously variable empirical shear strength equation as a more appropriate model for actual rock joints. The equation is written as:

$$\tau = C_j\ (1 - e^{-b\sigma}) + \sigma \tan \phi_r \tag{2.4}$$

where C_j is the shear strength (cohesion) derived from the asperities, ϕ_r is the residual friction angle of the wall rock, and b is an empirical curve fitting parameter. The parameter b can be determined from test data by sketching lines asymptotic to the peak strength envelope as shown in Figure 2.5. A parameter, p, can be calculated as:

$$p = C_j + \sigma \tan \phi_r - \tau \tag{2.5}$$

The slope of the line ln(p) plotted against normal stress, σ, is then equal to b as shown in Figure 2.5. It should be noted that at high normal stress, equation (2.4) reduces to the form:

$$\tau = C_j + \sigma \tan \phi_r \tag{2.6}$$

2.3.3 Ladanyi and Archambault's Criterion

Ladanyi and Archambault [18] also recognized the shortcomings of the bilinear failure envelope when applied to joints other than those with regularly inclined teeth. They suggested that a curved envelope is more appropriate and proposed a gradual transition from dilation at low normal stresses to shearing through asperities at high normal stresses. The following equation for peak shear strength, shown graphically in Figure 2.6, was proposed:

$$\tau = \frac{\sigma(1 - a_s)(\dot{v} + \tan \phi_m) + a_s \tau_r}{1 - (1 - a_s)\dot{v} \tan \phi_m} \qquad (2.7)$$

in which a_s is the fraction of the joint surface sheared through asperities, $\dot{v}$ is the dilation rate at peak shear strength (change in normal displacement/change in shear displacement), τ_r is the shear strength of intact rock material, and ϕ_m is the angle of frictional sliding resistance along the contact surfaces of the asperities. It was suggested that the shear strength for intact rock be represented by the criterion proposed by Fairhurst [8].

$$\tau_r = C_o \frac{m - 1}{n} (1 + n \frac{\sigma}{C_o})^{1/2} \qquad (2.8)$$

in which C_o is the uniaxial compressive strength of the asperities, n is the ratio of uniaxial compressive to uniaxial tensile strength of the asperities, and $m = (1 + n)^{1/2}$. Hoek and Bray [15, p. 87] indicate that n is approximately 10 for most hard rocks. The values of a_s and $\dot{v}$ are not always readily available. Therefore, Ladanyi and Archambault proposed the following empirical relationships based on laboratory test data:

$$\dot{v} = (1 - \frac{\sigma}{C_o})^{k_2} (\tan i) \qquad (2.9)$$

$$a_s = 1 - (1 - \frac{\sigma}{C_o})^{k_1} \qquad (2.10)$$

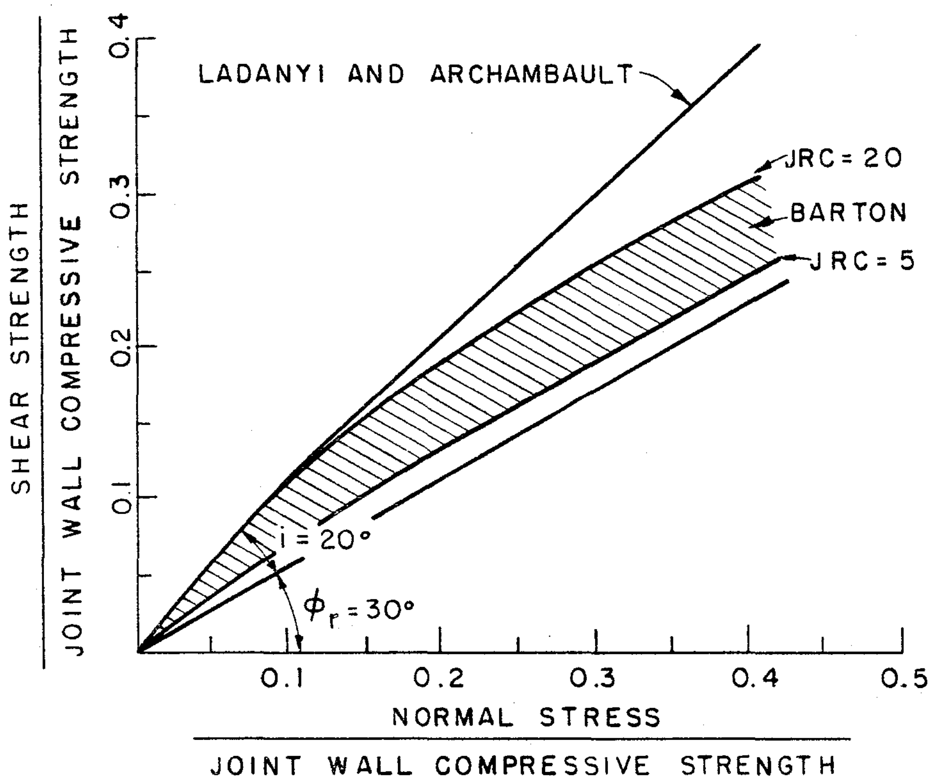

Figure 2.6 Ladanyi and Archambault's [18], and Barton's [3] Failure Criteria for Rough Joints.

in which k_1 is approximately equal to 1.5 and k_2 is approximately equal to 4 for their laboratory data. It should be noted that at very low normal stresses, when no shearing through asperities occurs ($\dot{v}$ = tan i, $a_s = 0$), equation (2.7) reduces to the form of equation (2.3). Similarly, at very high normal stresses, when the asperities are completely sheared ($a_s = 1$), equation (2.7) reduces to the shear strength of intact rock.

2.3.4 Barton's Criterion

Barton [2] and Barton and Choubey [3] proposed an alternate method for predicting the curved shear strength envelope for rough joints. The following empirical equation, shown graphically in Figure 2.6, was determined from laboratory tests:

$$\tau = \sigma \tan \left[\mathrm{JRC} \log_{10} (\mathrm{JCS}/\sigma) + \phi_r \right] \tag{2.11}$$

in which JCS is the joint wall compressive strength, usually determined from Schmidt rebound hammer tests for natural joints, and JRC is an empirical curve fitting coefficient related to the joint roughness. JRC varies from about 5 for smooth nearly planar joints to 20 for rough undulating joints. Barton and Bandis [4] recommend that JRC be determined from tilt or push tests, where the normal stress is induced by the self-weight of the specimen. The tests should be performed on joints of the natural block size, or block size formed by all intersecting joint sets, of a given rock mass. Barton and Choubey suggest that equation (2.11) is valid as long as the calculated strength does not exceed $\sigma \tan 70°$.

2.4 Water Pressure and Effective Stress

The effects of water pressure on the strength of a rock joint are usually accounted for by the effective stress law [7, 11, 15]. The total normal stress acting across the joint is reduced by the water pressure, u, to yield the effective normal stress. For most hard rocks, the material strength characteristics are not significantly affected by the presence of water and the reduction in shear strength is almost entirely a result of reduced effective normal stress [15]. Goodman and Onishi [10] performed undrained direct shear tests on laboratory joint samples. At high normal stresses during shearing, the joint water pressure was found to increase in the compressing joint, with a net loss in strength according to the effective stress law until slip. At the point of slip, dilation occurred and the water pressure dropped. At low normal stresses, the joints dilated practically from the onset of shearing, in some cases inducing negative water pressures.

2.5 Conclusions

The shear strength criteria reviewed in previous sections are appropriate for the analysis of rock masses under static loading conditions. The limit equilibrium approach for the analysis of rock masses bounded by planar discontinuities, described in the next chapter, utilizes shear strengths of the discontinuities and water forces acting normal to them.

Rather than developing new criteria for the behavior of rock joints subjected to dynamic loading, a first approach would be to study the deviations from static behavior that occur. This approach will be pursued in Chapter IV.

CHAPTER III

THREE-DIMENSIONAL LIMIT EQUILIBRIUM ANALYSIS

3.1 Introduction

Three-dimensional limit equilibrium analyses are widely accepted as one means of studying the stability of rock masses such as slopes and dam foundations [7, 11, 15, 20]. The general approach is to first identify discontinuities forming potentially unstable blocks or wedges. Forces acting on a potentially unstable rock mass are then determined. Normal forces acting on potential sliding planes are computed and the possibility of sliding along a discontinuity or the intersection of two discontinuities under the applied loads is checked. The factor of safety against sliding is computed by dividing the resistance that may ultimately be developed on planes with compressive normal forces, by the driving component of the resultant force. Thus, the factor of safety reflects the resistance that could be developed if failure was imminent and not the mobilized resistance under nonfailure conditions. The assumption is made that the rock block or wedge is rigid and does not deform under the applied loads. As a result of this restriction, no shear resistance is considered to develop in the resisting discontinuities transverse to the potential direction of sliding (see Figure 3.1). Therefore, the maximum normal force, and thus the maximum shear resistance, is considered to develop on

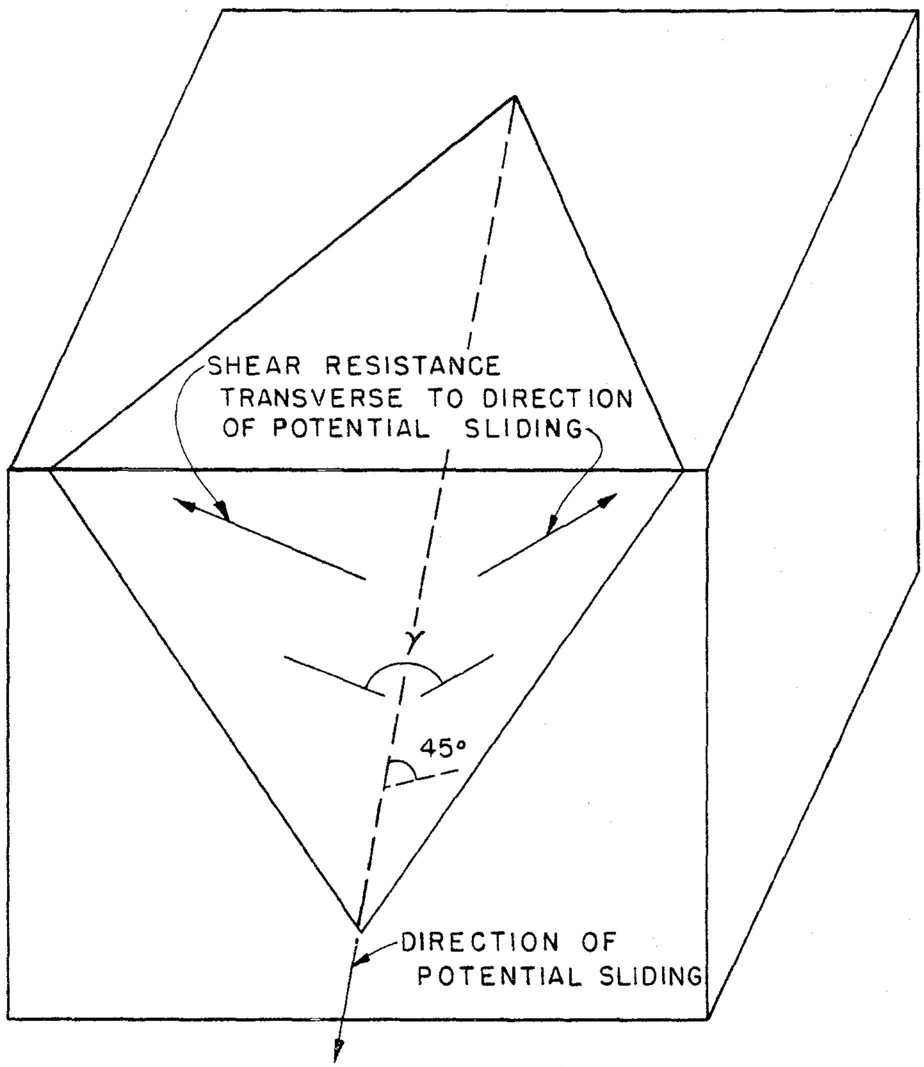

Figure 3.1 Shear Resistance Transverse to Direction of Potential Sliding for Two Plane Wedge.

potential sliding planes. Mahtab and Goodman [21] performed three-dimensional finite element studies of rock slopes, representing discontinuities with planar joint elements. It was found that for large ratios of constant joint normal stiffness to joint shear stiffness, the calculated normal stresses approach those given by the rigid block method as shown in Figure 3.2. Since rock discontinuities usually exhibit large normal stiffness relative to their shear stiffness, the rigid block method of analysis is appropriate in most cases.

Three-dimensional analytical solutions to the rigid block limit equilibrium problem have been proposed [13, 19, 31]. However, most have been adapted to only three potential sliding planes. Von Thun [29] suggested a generalized solution to handle any number of potential sliding planes. The method, which has not been previously documented in detail, will be presented here.

3.2 Three-Dimensional Vector Description of a Plane

The orientation of a planar discontinuity can be defined by two angles, strike and dip, as shown in Figure 3.3. The strike angle, S, is defined by the azimuth angle measured clockwise from north to the horizontal projection of the plane [15]. The dip angle, D, is measured from horizontal at a right angle to the strike, down to the right looking in the direction of the strike. For the discussion that follows, the strike and dip vectors are defined such that their cross product, defining a vector normal to the plane, is directed into the potentially unstable rock block. A right hand coordinate system is established such that the x and y axes define a horizontal plane and the +z axis is directed vertically downward (see Figure 3.3). If θ is the clockwise angle

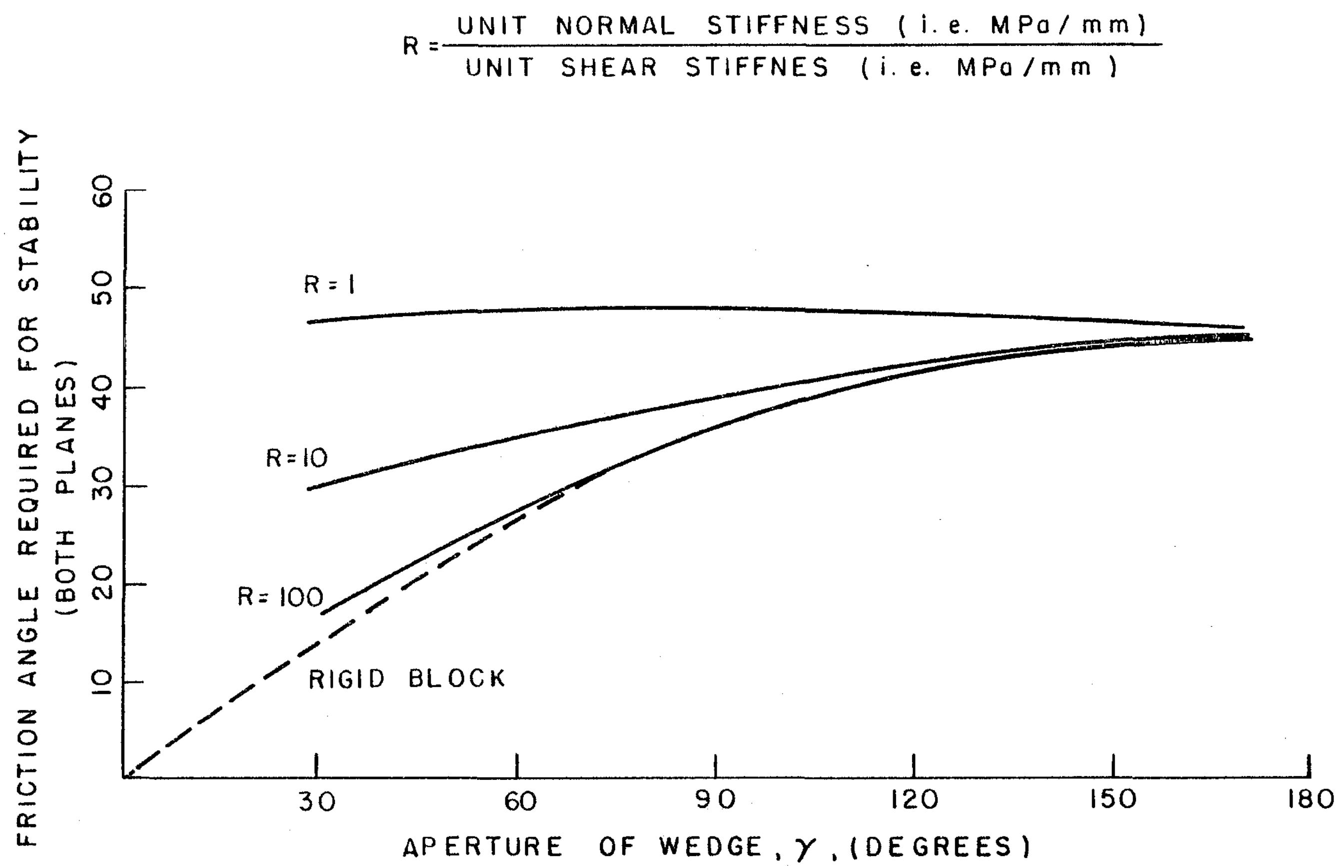

Figure 3.2 Influence of Stiffness Ratio on the Sliding Stability of Two Plane Wedge with Intersection Plunging at 45° [21].

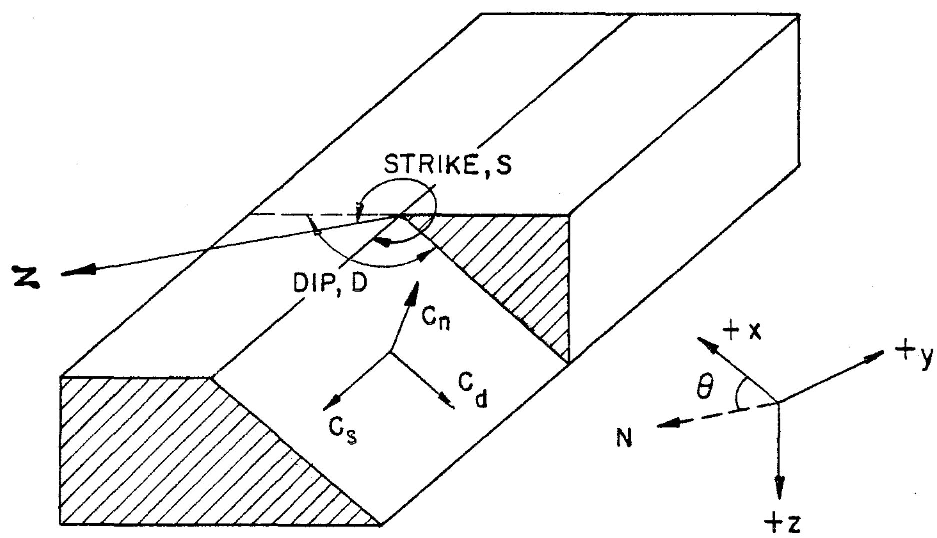

Figure 3.3 Definition of Strike and Dip of a Planar Discontinuity, and Coordinate System.

from north to the +x axis, the direction cosines of the strike unit vector (see Figure 3.3) are given by:

$$\{C_s\} \ ; \ C_{sx} = \cos(S - \theta), \ C_{sy} = \sin(S - \theta), \ C_{sz} = 0.0 \qquad (3.1)$$

The direction cosines of the dip unit vector (see Figure 3.3) are given by:

$$\{C_d\} \ ; \ C_{dx} = -C_{sy}\cos(D), \ C_{dy} = C_{sx}\cos(D), \ C_{dz} = \sin(D) \qquad (3.2)$$

The cross product of the strike and dip unit vectors results in a unit vector normal to the plane:

$$C_{nx} = (C_{sy})(C_{dz}) - (C_{sz})(C_{dy})$$
$$C_{ny} = (C_{sz})(C_{dx}) - (C_{sx})(C_{dz})$$
$$C_{nz} = (C_{sx})(C_{dy}) - (C_{sy})(C_{dx})$$
$$\text{or } \{C_n\} = [C_s] \times [C_d] \qquad (3.3)$$

A matrix [C] containing the direction cosines of the strike, dip, and normal unit vectors is defined as:

$$[C] = \begin{bmatrix} C_{sx} & C_{sy} & C_{sz} \\ C_{dx} & C_{dy} & C_{dz} \\ C_{nx} & C_{ny} & C_{nz} \end{bmatrix} \qquad (3.4)$$

3.3 Potential Sliding on a Plane

The components of water force acting on each plane are determined by:

$$\begin{Bmatrix} F_{wx} \\ F_{wy} \\ F_{wz} \end{Bmatrix} = U \begin{Bmatrix} C_{nx} \\ C_{ny} \\ C_{nz} \end{Bmatrix} \qquad (3.5)$$

where U is the water force acting normal to the plane. The total force components acting on the potentially unstable block, including dead load, water loads, and external forces, are summed and represented by a vector:

$$\{F_r\} = \begin{Bmatrix} F_{rx} \\ F_{ry} \\ F_{rz} \end{Bmatrix} \qquad (3.6)$$

The resultant force is resolved into components normal and parallel to each plane that defines a potentially unstable rock wedge by:

$$\{T\} = \begin{Bmatrix} T_1 \\ T_2 \\ T_3 \end{Bmatrix} = - [C] \ \{F_r\} \tag{3.7}$$

where T_1 is the force parallel to the strike, T_2 is the force parallel to the dip, and T_3 is the force parallel to the normal unit vector as shown in Figure 3.4 (a). The negative sign in equation (2.6) results in a positive force being directed out of the block, and a compressive normal force is then positive. The total shear force acting on the plane is given by:

$$F_{st} = (T_1{}^2 + T_2{}^2)^{1/2} \tag{3.8}$$

The global components of the shear force, shown in Figure 3.4 (b), are then determined as:

$$\{F_s\} = \{F_{sx} \ F_{sy} \ F_{sz}\} = \{T_1 \ T_2\} \begin{bmatrix} C_{sx} & C_{sy} & C_{sz} \\ C_{dx} & C_{dy} & C_{dz} \end{bmatrix} \tag{3.9}$$

When the normal force on a plane is compressive, potential sliding along that plane is considered, providing the orientation of the shear force does not direct movement into another plane. This is checked by solving the following equation:

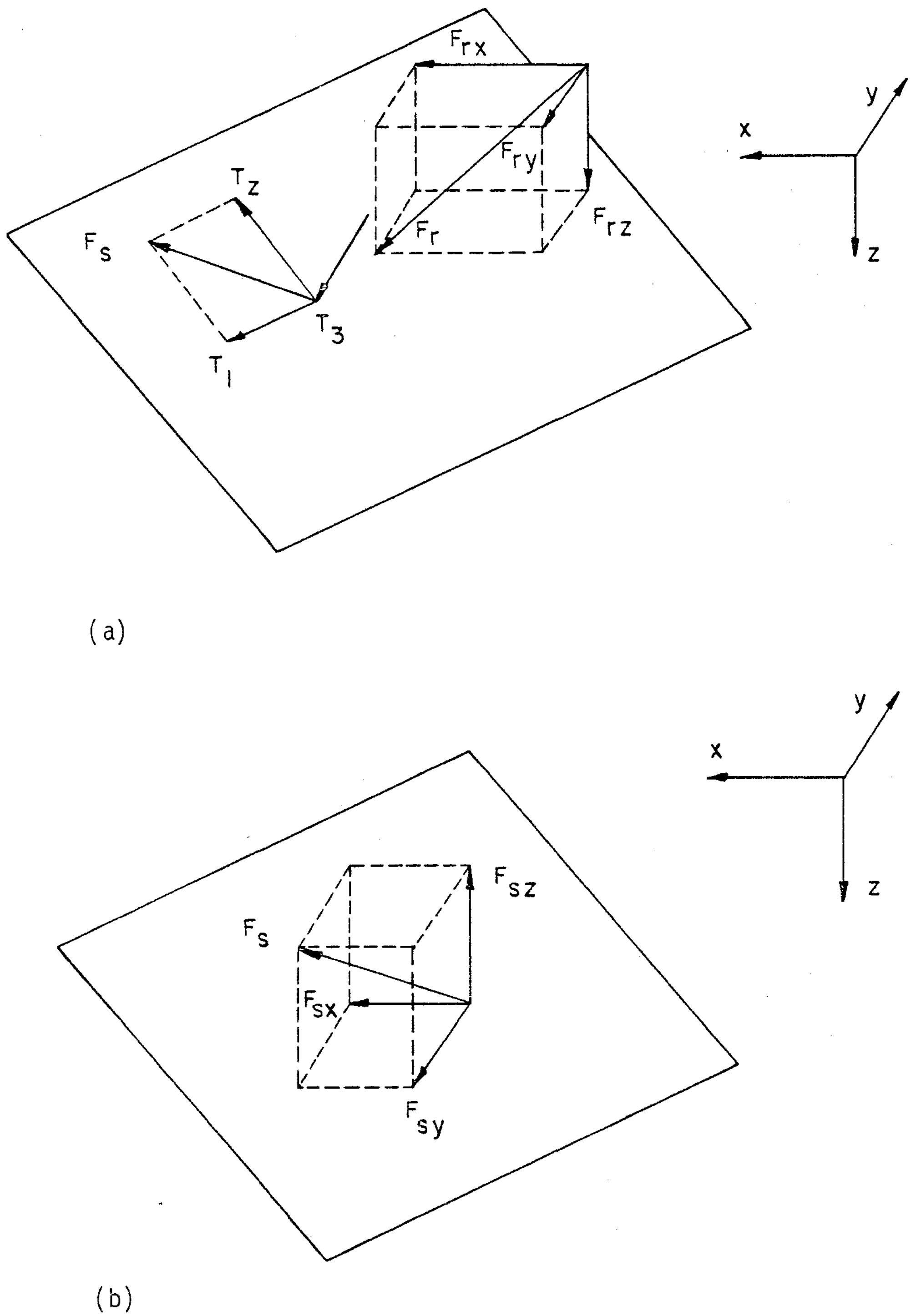

Figure 3.4 Resolution of Forces on a Plane.

$$K = \{F_s\}\begin{Bmatrix} C'_{nx} \\ C'_{ny} \\ C'_{nz} \end{Bmatrix} = \{F_s\}\{C'_n\} \tag{3.10}$$

in which C'_n contains the direction cosines for the normal of a plane potentially blocking movement. If K is greater than zero, movement is blocked. However, movement along the intersection of two planes is possible. If movement is not blocked the factor of safety against sliding is computed as:

$$S_f = \frac{R_n}{F_{st}} \tag{3.11}$$

where R_n is the maximum resisting force based on the shear strength, and normal force or average normal stress acting across the plane.

3.4 Potential Sliding on the Intersection of Two Planes

The intersection of two planes is defined by the cross product of their normals.

$$\begin{aligned} J_x &= (C_{ny})(C'_{nz}) - (C_{nz})(C'_{ny}) \\ J_y &= (C_{nz})(C'_{nx}) - (C_{nx})(C'_{nz}) \\ J_z &= (C_{nx})(C'_{ny}) - (C_{ny})(C'_{nx}) \\ \text{or } \{J\} &= [C_n] \times [C'_n] \end{aligned} \tag{3.12}$$

Since the normals may not be orthogonal, the direction cosines of a unit vector in the direction of the intersection are computed by normalizng the intersection vector.

$$J_{xyz} = (J_x^2 + J_y^2 + J_z^2)^{1/2} \tag{3.13}$$

$$C_{ix} = J_x/J_{xyz}$$

$$C_{iy} = J_y/J_{xyz}$$

$$C_{iz} = J_z/J_{xyz}$$

$$\text{or } \{C_i\} = \{J\}/J_{xyz} \tag{3.14}$$

A matrix [N] containing the direction cosines of the normals to the two planes and their intersection is defined as:

$$[N] = \begin{bmatrix} C_{nx} & C_{ny} & C_{nz} \\ C'_{nx} & C'_{ny} & C'_{nz} \\ C_{ix} & C_{iy} & C_{iz} \end{bmatrix} \tag{3.15}$$

The components of force perpendicular to each plane and along their intersection are calculated as:

$$\{Q\} = \begin{Bmatrix} Q_1 \\ Q_2 \\ Q_3 \end{Bmatrix} = -[N^T]^{-1}\{F_r\} \tag{3.16}$$

where Q_1 is the force normal to the first plane, Q_2 is the force normal to the second plane, and Q_3 is the force along their intersection as shown in Figure 3.5. Restraint against movement is checked as in the case of sliding along one plane, except that:

$$\{F_s\} = Q_3\{C_i\} \tag{3.17}$$

If movement is not blocked, the factor of safety is computed as:

$$S_f = \frac{R_n + R_n'}{Q_3} \tag{3.18}$$

in which R_n and R_n' are the maximum resisting forces for the two planes, based on the shear strengths, and normal forces or average normal stresses acting across the planes.

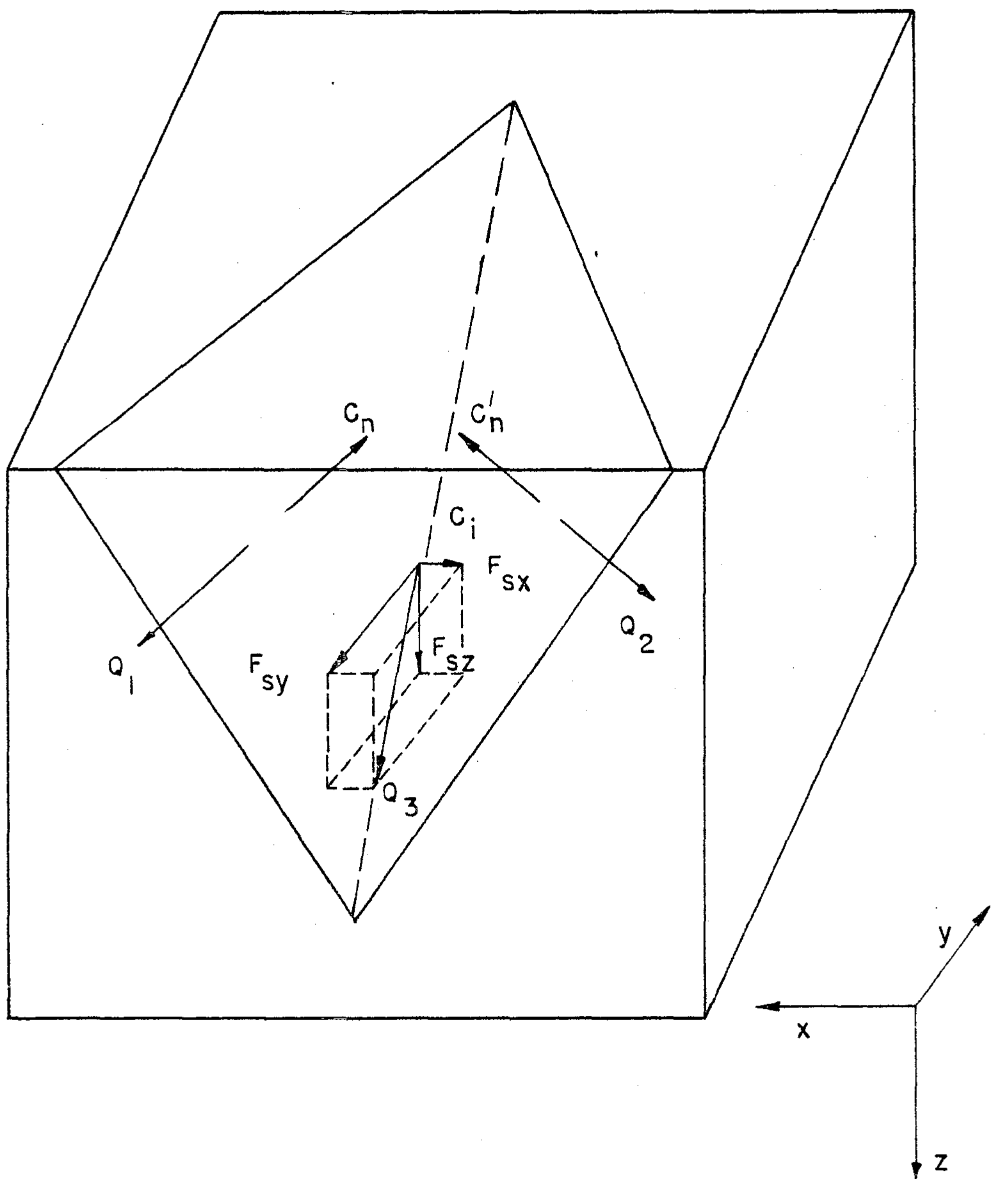

Figure 3.5 Resolution of Forces on Two Planes.

If a compressive normal force is not found to exist across any plane, the rock wedge is considered to be lifted. Similarly, if movement is completely blocked, the rock wedge is considered to be stable.

3.5 Displacement Compatibility for Shear Strengths

Von Thun [28] demonstrated the importance of determining shear strengths at compatible shear displacements when considering composite sliding planes. The same consideration applies for sliding on the intersection of two planes. Consider the shear stress vs. shear deformation curves for two discontinuities, shown in Figure 3.6. The peak shear strength of the first discontinuity occurs at a much smaller shear displacement than the second. Thus, simple addition of peak shear strengths is not appropriate for the case of sliding along the intersection of the two discontinuities. The shear strengths utilized in an analysis must, therefore, be developed in conjunction with compatible shear displacements.

3.6 Conclusions

The method of analysis described in this chapter can be readily adapted to computer solution. If the appropriate forces acting on a rigid block are digitized for each time step during an earthquake, a response history analysis can be performed for that block. The potential mode of instability and factor of safety can be computed for each time step during the earthquake, utilizing a computer program. Additional details of this type of dynamic analysis will be discussed in Chapter V.

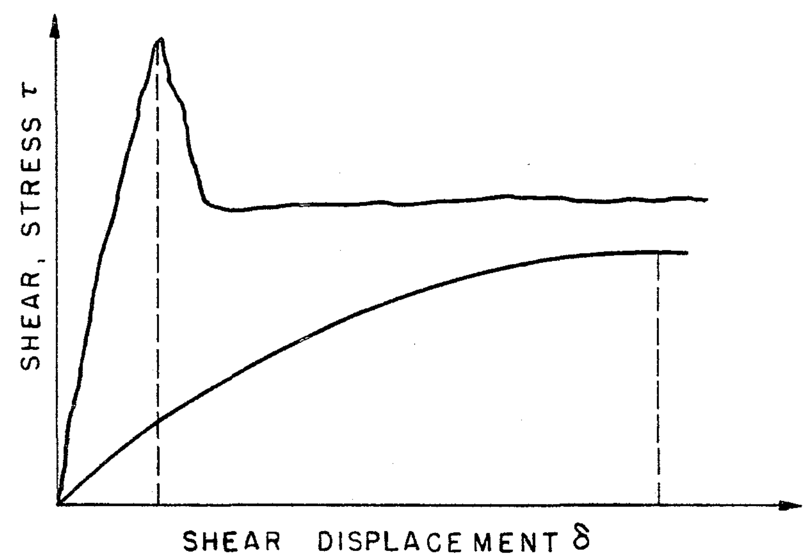

Figure 3.6 Shear Stress vs. Shear Deformation for Two Joints.

CHAPTER IV

DYNAMIC SHEAR BEHAVIOR OF CLEAN ROCK JOINTS

4.1 Experimental Program

Crawford and Curran [5] have studied the effects of relative velocity on the shear resistance of rock discontinuities in the laboratory. A servocontrolled dynamic direct shear machine was developed for the research, capable of testing specimens approximately 200 mm (8 in) square. The machine has three degrees of freedom (two translations and one rotation) with independently controlled horizontal and vertical actuators, each having a capacity of 250 kN (56 kips). Artificial saw cut joints in four rock types, summarized in Table 4.1, were lapped with silicon carbide grit and displaced at various constant shear velocities under various constant normal loads. Similar research was initiated at the University of Colorado, Boulder, Colorado, prior to the publication of Crawford and Curran's results. The experimental program, sponsored by the National Science Foundation and the U.S. Bureau of Reclamation, is discussed in the following sections.

4.1.1 Test Apparatus

A dynamic direct shear apparatus has been developed in the laboratories of the Department of Civil, Environmental, and Architectural Engineering at the University of Colorado, Boulder,

Table 4.1 Summary of Rocks Tested by Crawford and Curran [5]

Rock Type	Uniaxial Compressive Strength (MPa)	Shore Hardness
Black syenite	97	68
Grey dolomite	142	47
Buff sandstone	198	80
Pink granite	160	62

Colorado. A detailed description of the apparatus and its performance characteristics is given by Gould [12]. The apparatus consists of independent servocontrolled horizontal and vertical loading actuators, reaction frames, and shear box fixtures as shown schematically in Figures 4.1 through 4.3. A sample with maximum dimensions of about 200 x 200 x 100 mm (8 x 8 x 4 in), and with a maximum shear area of about 400 cm^2 (64 in^2), is potted in the upper and lower shear box compartments using a sulphur capping compound. The shear box compartments are then bolted to support plates and the actuators. The upper shear box compartment is restrained against horizontal motion by roller bearings on the top support plate which rest against the specimen reaction frames. The specimen reaction frames are connected to a stiff and strong structural floor with oversize stiff bolts. The bottom support plate rests on two rows of roller bearings with seven bearings in each row. The applied shear force thus causes horizontal movement of the lower part of the specimen, relative to the top part, in the direction of the roller bearings.

Closed-loop servocontrolled MTS (MTS Systems Corporation) actuators are used to apply the shear and normal force. Stiff load reaction frames, bolted to the structural floor, permit application of the forces to the specimen. The normal force

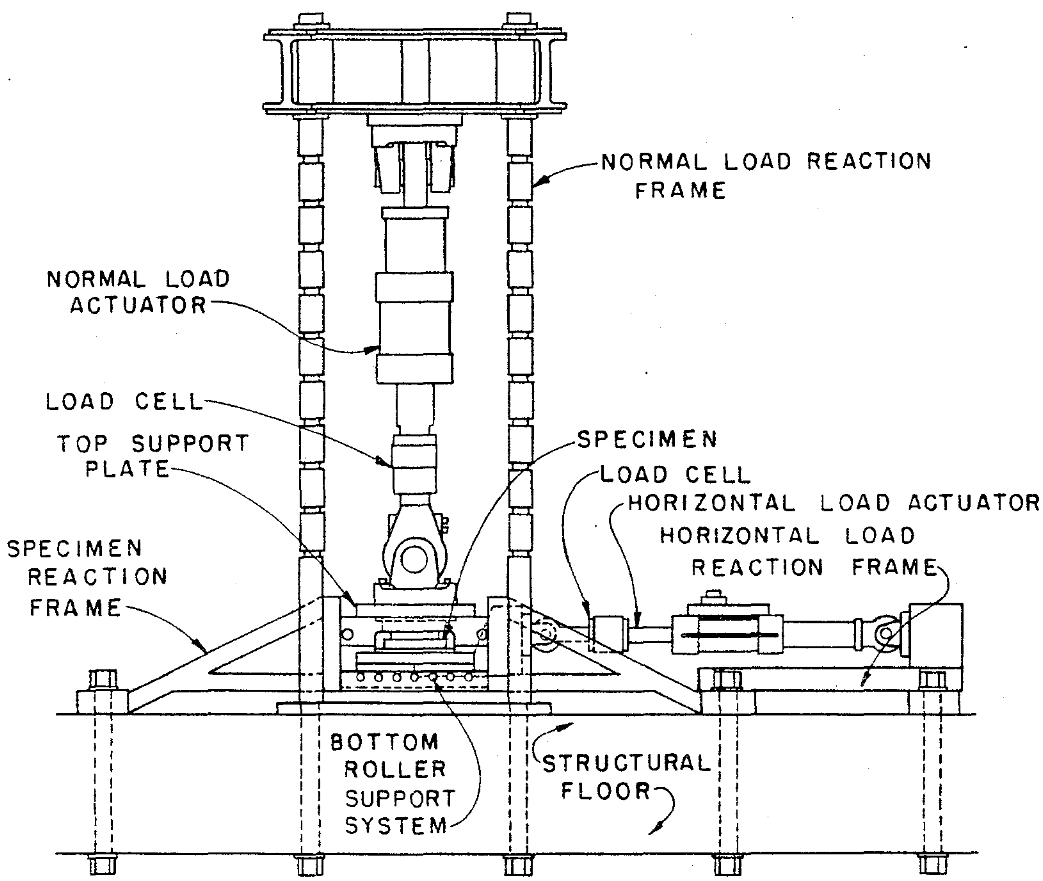

Figure 4.1 Dynamic Direct Shear Apparatus (Side View Schematic).

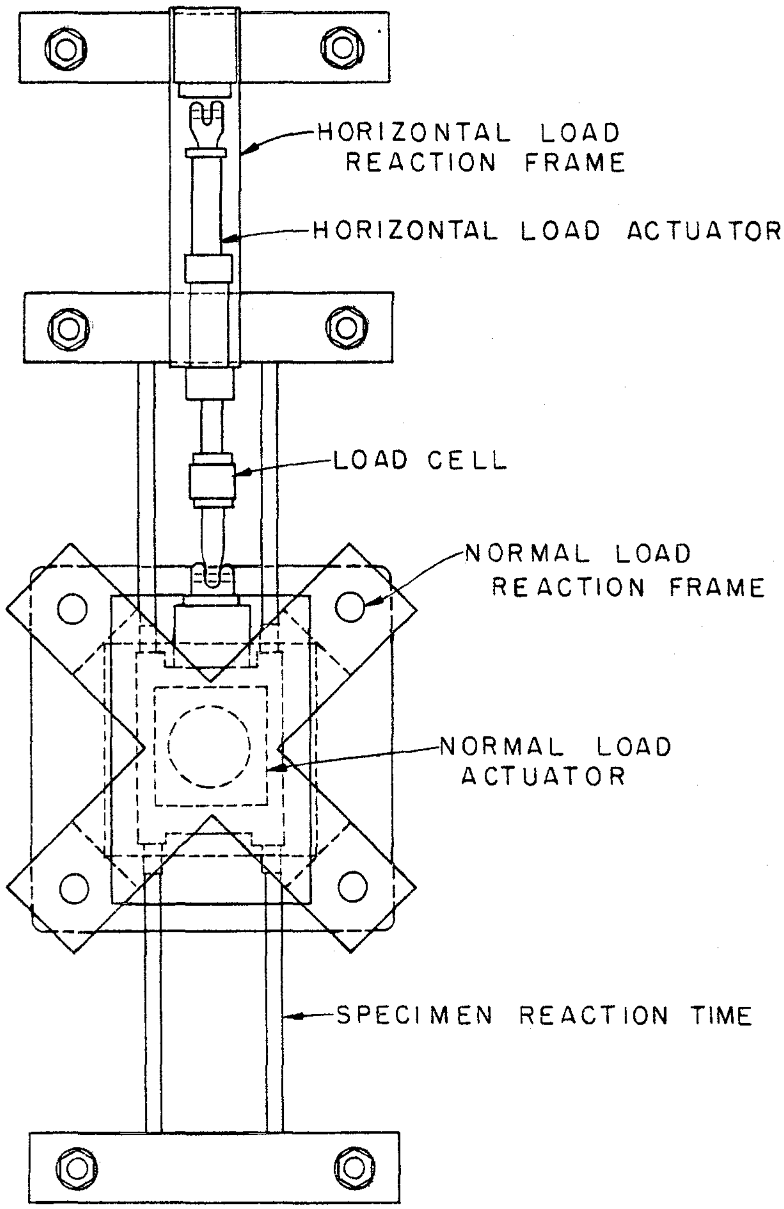

Figure 4.2 Dynamic Direct Shear Apparatus (Schematic Overhead View).

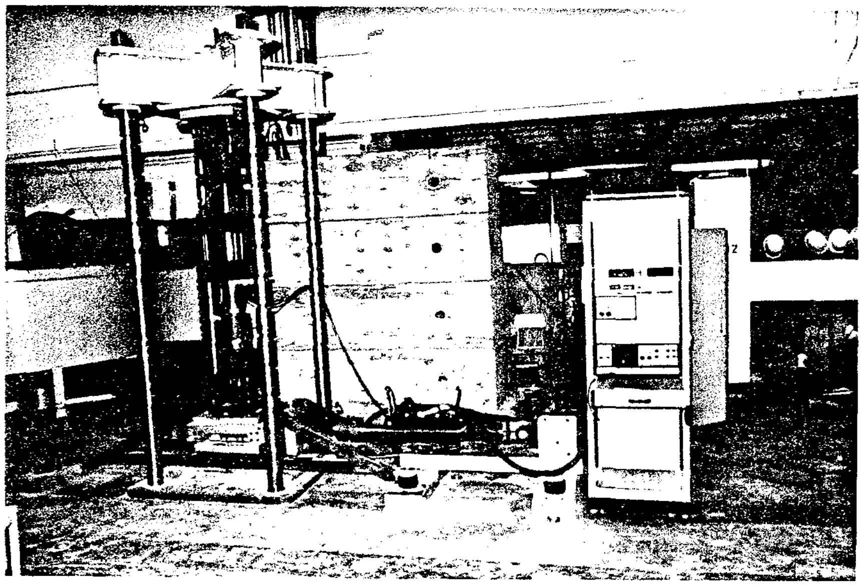

Figure 4.3 Dynamic Direct Shear Apparatus (Assembled with Control Unit).

actuator has a capacity of 736 kN (165 kips) and the shear force actuator has a capacity of 156 kN (35 kips). Each actuator is equipped with a load cell for measuring the applied force and an internal LVDT (linearly varying differential transducer) for monitoring stroke. Several loading patterns are possible through the use of a digital function generator. Each actuator can be operated in the load controlled or displacement controlled mode. Realistically, frequencies up to 10 Hz can be applied. With the normal actuator in load control, the apparatus has four degrees of freedom. These include vertical translation, horizontal translation in the direction of shearing, rotation about a horizontal axis perpendicular to the direction of shearing, and rotation about a horizontal axis parallel to the direction of shearing. In addition, slight horizontal translation perpendicular to the direction of shearing is allowed. The shearing load and specimen reaction are applied co-linear with the shearing plane, thus reducing moments applied to the specimen.

4.1.2 Sample Preparation

Dynamic direct shear tests were performed on homogeneous Loveland Sandstone. The uniaxial compressive strength of the rock, measured from five NX core specimens according to ASTM (American Society for Testing Materials) standards ranged from 136 to 168 MPa (19 700 to 24 400 lb/in^2) and averaged 156 MPa (23 000 lb/in^2). Artificial joints were created in the laboratory for testing under controlled conditions. Six-inch-diameter cores were fractured by the Brazilian split cylinder method to create rough tension joints. The fractured cores were then cut into 4-inch cubical shaped blocks with the fracture surface parallel to one set of the cube's faces. Four cubical blocks were glued together with epoxy to form a 200 x 200 x 100 mm (8 x 8 x 4 in) specimen with a nominal shear area of 400 cm^2 (64 in^2) as shown in Figure 4.4. Care was taken when joining the cubical shaped blocks to assure a common shearing plane with perfectly mated upper and lower surfaces. Smooth joint surfaces were prepared by gluing four unfractured cubical blocks together and subsequently sawing and grinding smooth a 400-cm^2 (64-in^2) shear surface. The lower edges of the shear plane perpendicular to direction of

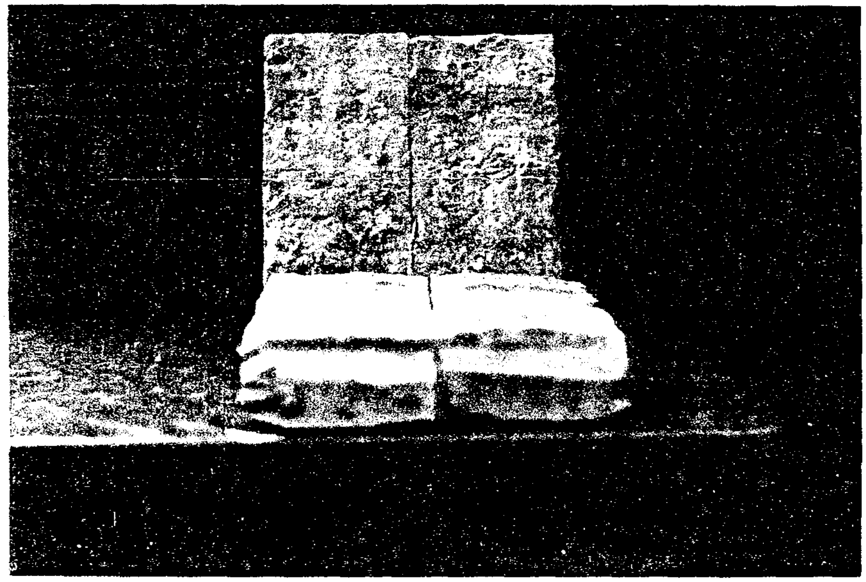

Figure 4.4 Typical Direct Shear Sample.

shearing were beveled for all samples to prevent tensile failure near the edge and keep the nominal normal stress constant. However, a nominal shear area greater than 325 cm^2 (50 in^2) was maintained. Additional details of the samples are discussed by Gould [12].

4.1.3 Monitoring System and Data Acquisition

The normal load and shear load are monitored during a dynamic test using the load cells on the MTS actuators. The vertical translation is monitored with the internal LVDT of the normal load actuator. However, because of the small flexibility of the shear force transmission system, LVDT's are attached directly to the top and bottom of the sample, as shown in Figure 4.5, to measure the relative shear deformation.

The normal load, normal displacement, shear load, and relative shear displacement are recorded with an HP (Hewlett Packard) data acquisition system controlled by an HP desk top computer. The equipment, shown in Figure 4.6, is capable of scanning and recording at the rate of 400 readings per second. The desk top computer records the data on magnetic cassette tape for postprocessing data reduction. Additional details of the monitoring and data acquisition system are discussed by Gould [12].

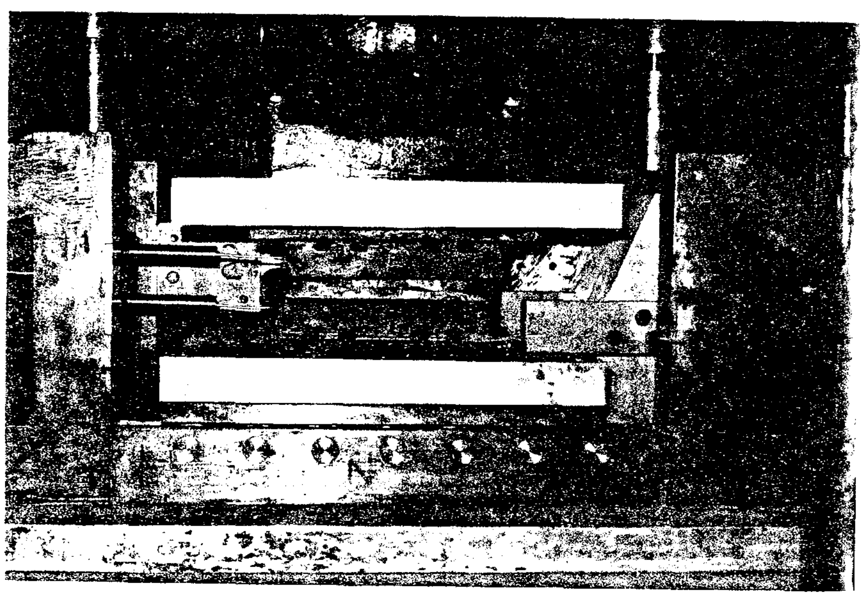

Figure 4.5 LVDT's for Measuring Shear Deformation.

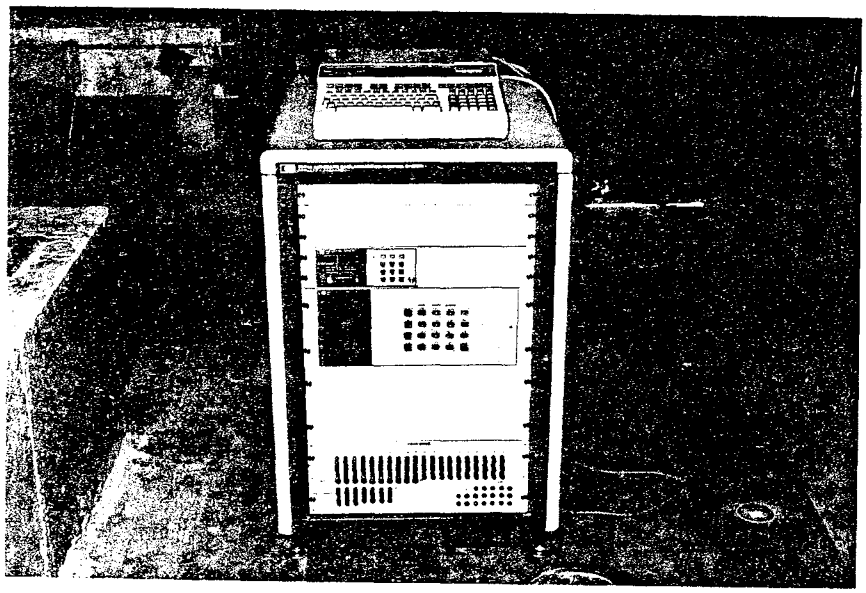

Figure 4.6 Data Acquisition System.

4.1.4 Test Program

Initial tests were conducted in shear displacement control under relatively constant normal stresses on dry joint samples. Sinusoidal shear displacements were applied to the samples at various amplitudes and frequencies under various normal stresses. The test schedule for each specimen is illustrated in Table 4.2. The sequence of testing is shown by the numbers in parentheses. Five rough samples labeled A, B, C, D, and E were tested in the main test program. Typical plots of shear stress vs. shear displacement are shown in Figures 4.7 through 4.11. Small fluctuations in normal stress were accounted for by the working assumption that the shear strength varies linearly with normal stress,

Table 4.2 Schedule for Dry Displacment Controlled Tests

Frequency	Shear Displacement \ Normal Stress	10 lb/in^2 0.069 MPa	30 lb/in^2 0.207 MPa	100 lb/in^2 0.690 MPa	10 lb/in^2 0.069 MPa	30 lb/in^2 0.207 MPa	100 lb/in^2 0.690 MPa	10 lb/in^2 0.069 MPa	30 lb/in^2 0.207 MPa	100 lb/in^2 0.690 MPa	500 lb/in^2 3.45 MPa
0.01 Hz	±0.05 in (±0.127 cm)	1-1 (1)	1-2 (8)	1-3 (15)	1-4 (22)	1-5 (29)	1-6 (36)	1-7 (43)	1-8 (50)	1-9 (57)	1-10 (64)
0.1 Hz	±0.05 in (±0.127 cm)	2-1 (2)	2-2 (9)	2-3 (16)	2-4 (23)	2-5 (30)	2-6 (37)	2-7 (44)	2-8 (51)	2-9 (58)	2-10 (65)
1.0 Hz	±0.05 in (±0.127 cm)	3-1 (3)	3-2 (10)	3-3 (17)	3-4 (24)	3-5 (31)	3-6 (38)	3-7 (45)	3-8 (52)	3-9 (59)	3-10 (66)
10.0 Hz	±0.05 in (±0.127 cm)	4-1 (4)	4-2 (11)	4-3 (18)	4-4 (25)	4-5 (32)	4-6 (39)	4-7 (46)	4-8 (53)	4-9 (60)	4-10 (67)
0.01 Hz	±0.1 in (±0.254 cm)	5-1 (5)	5-2 (12)	5-3 (19)	5-4 (26)	5-5 (33)	5-6 (40)	5-7 (47)	5-8 (54)	5-9 (61)	5-10 (68)
0.1 Hz	±0.1 in (±0.254 cm)	6-1 (6)	6-2 (13)	6-3 (20)	6-4 (27)	6-5 (34)	6-6 (41)	6-7 (48)	6-8 (55)	6-9 (62)	6-10 (69)
1.0 Hz	±0.1 in (±0.254 cm)	7-1 (7)	7-2 (14)	7-3 (21)	7-4 (28)	7-5 (35)	7-6 (42)	7-7 (49)	7-8 (56)	7-9 (63)	7-10 (70)

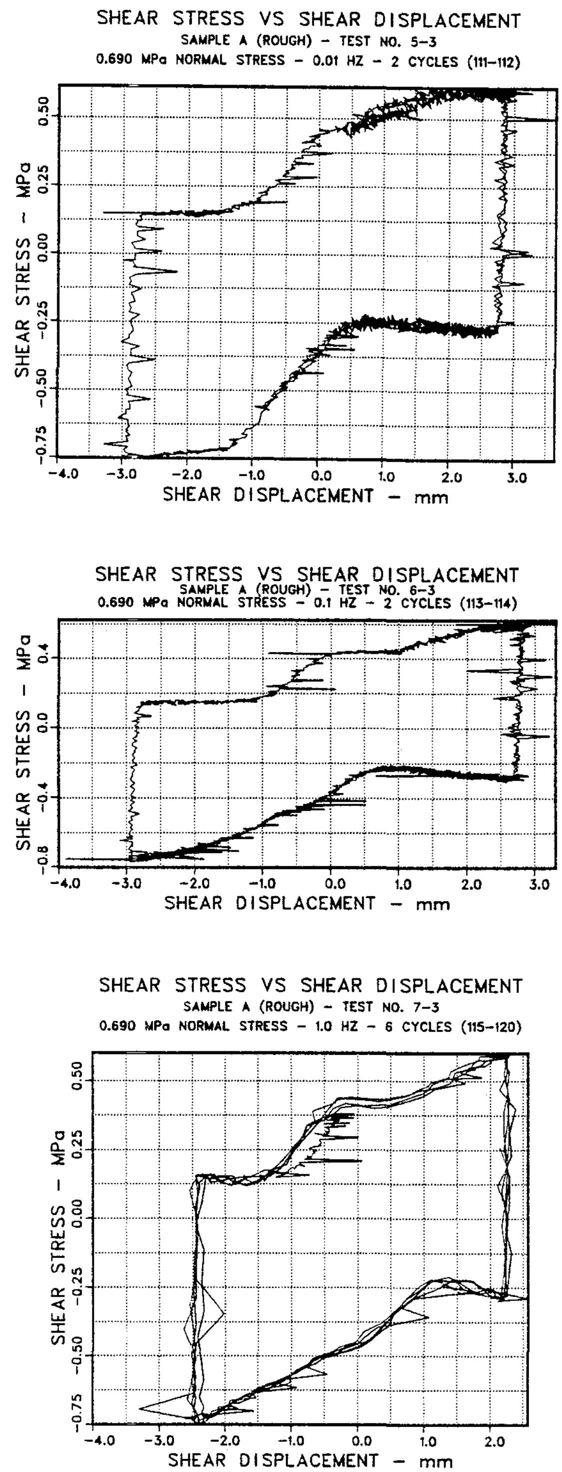

Figure 4.7 Typical Shear Stress vs. Shear Displacement Curves for Sample A.

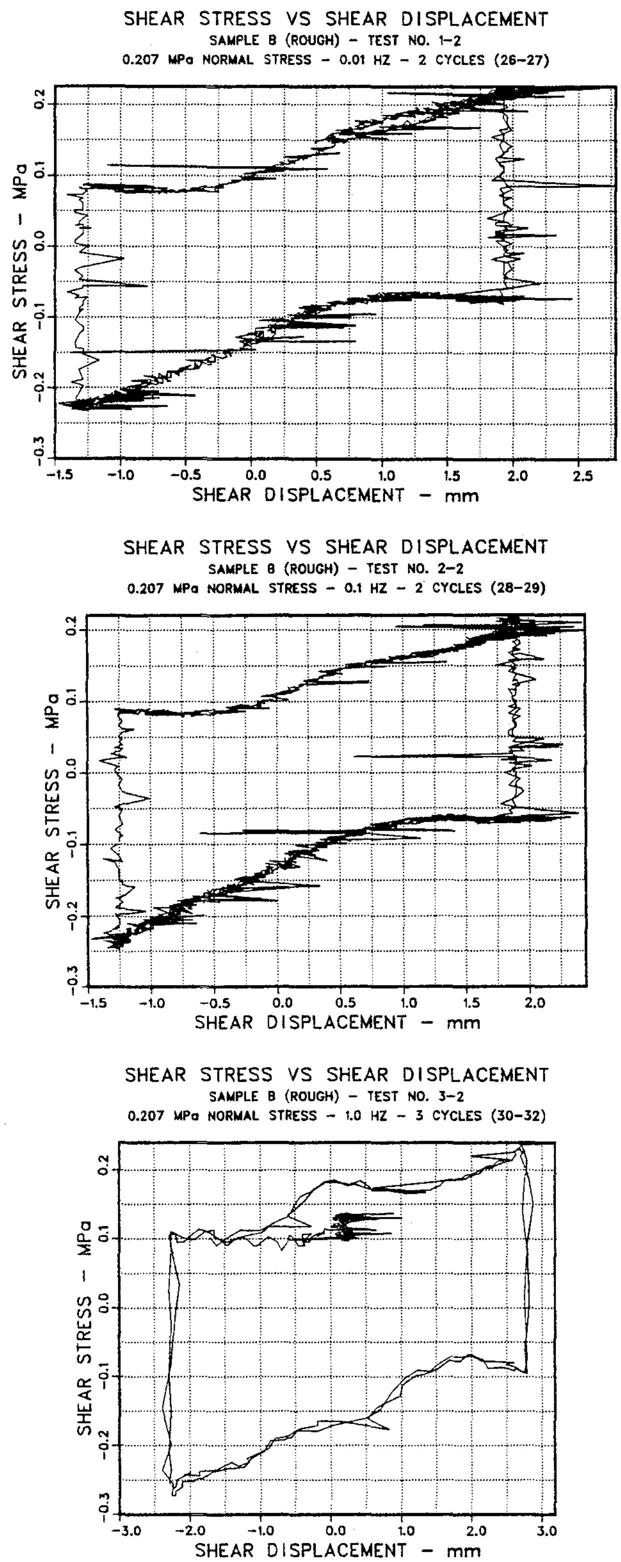

Figure 4.8 Typical Shear Stress vs. Shear Displacement Curves for Sample B.

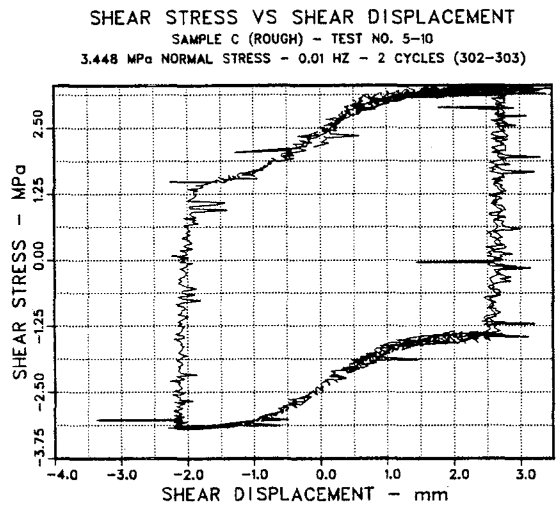

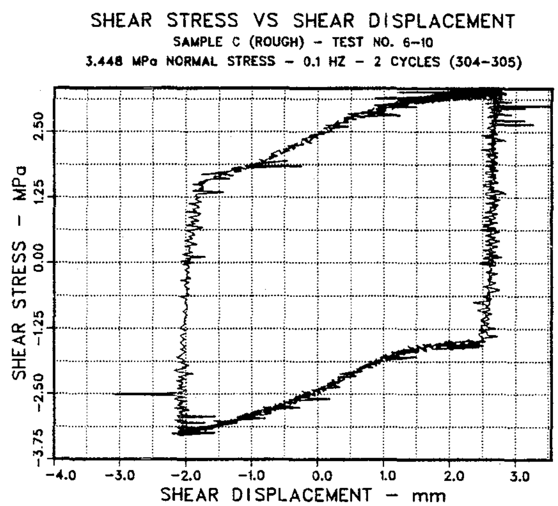

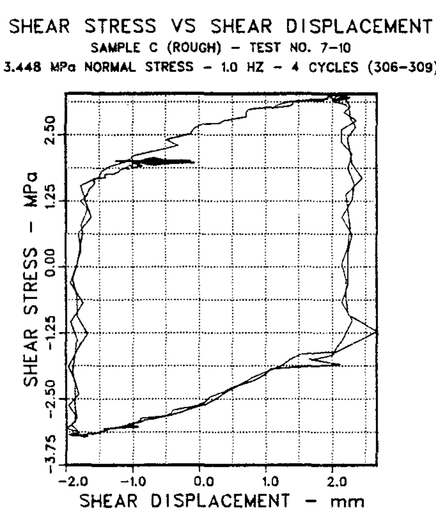

Figure 4.9 Typical Shear Stress vs. Shear Displacement Curves for Sample C.

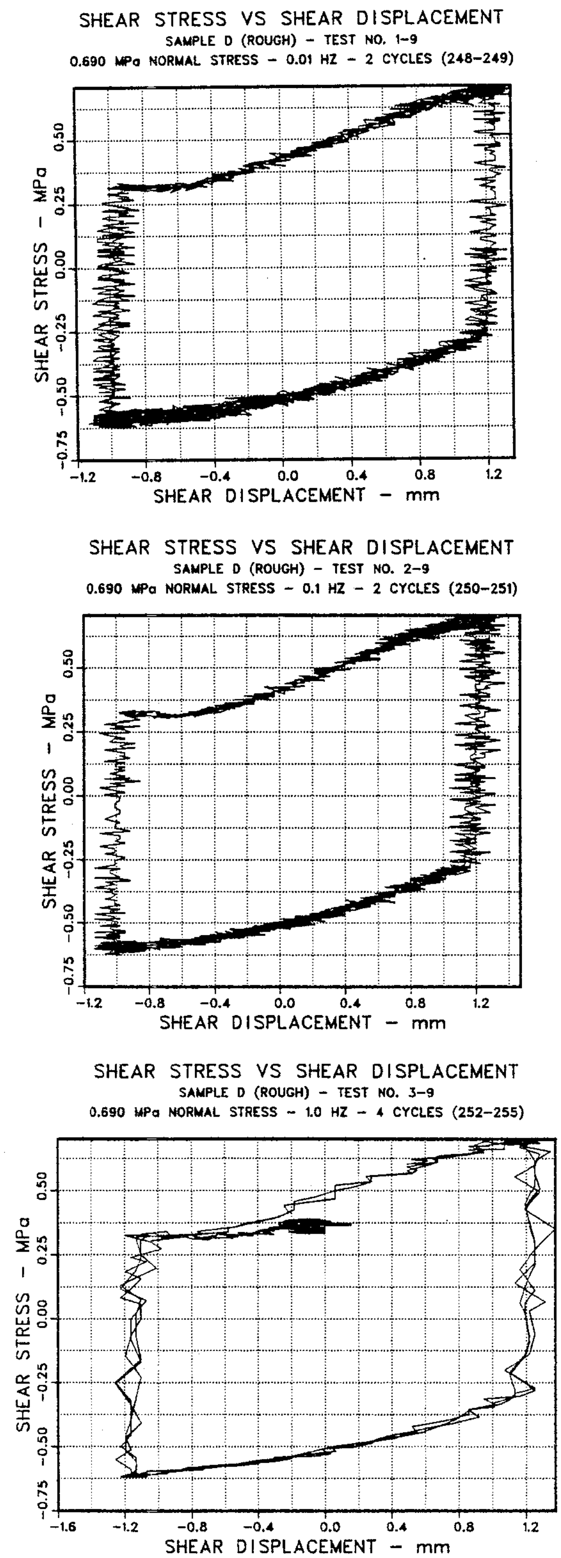

Figure 4.10 Typical Shear Stress vs. Shear Displacement Curves for Sample D.

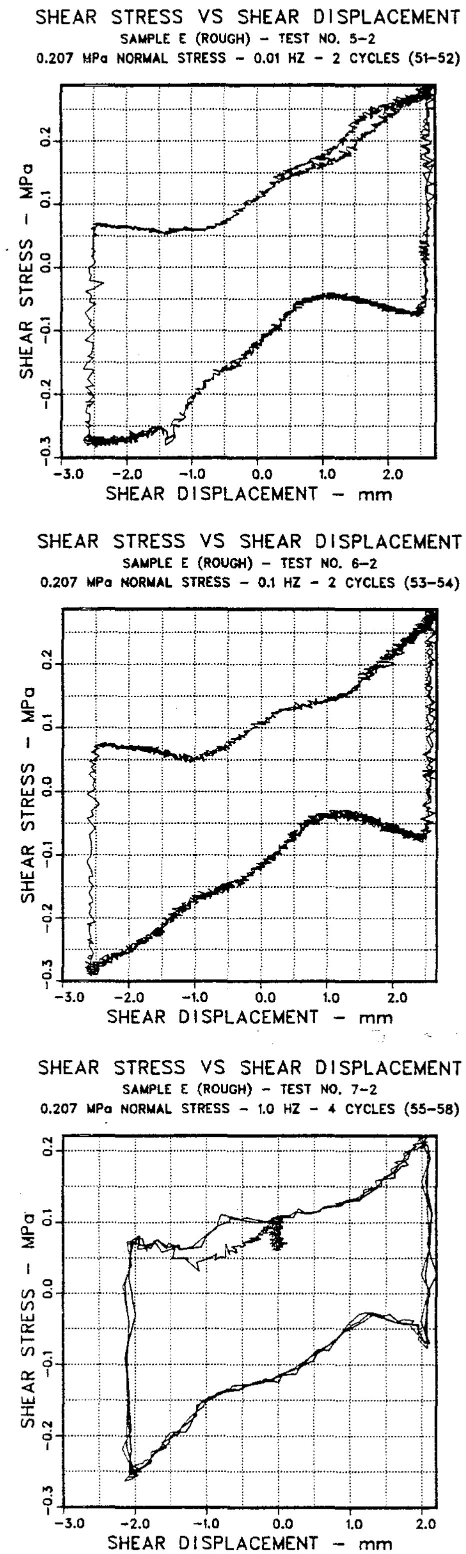

Figure 4.11 Typical Shear Stress vs. Shear Displacement Curves for Sample E.

within the range of normal stress fluctuation. The shear stress was normalized to the assumed constant normal stress by the relationship:

$$\tau = \tau_m \frac{\sigma_{test}}{\sigma_{actual}} \tag{4.1}$$

where σ_{test} is the assumed constant normal stress, σ_{actual} is the actual normal stress, and τ_m is the measured shear stress. The tests at 0.069 MPa (10 lb/in^2) normal stress had very large percentages of normal load fluctuation and may be of limited value. Similarly, tests at 10 Hz could not be completely recorded by the data acquisition system. One group of tests at 10 Hz was recorded with a Honeywell visicorder strip chart recorder, and the data were reduced manually.

4.2 Velocity Effects

Crawford and Curran [5] concluded that in general the shear resistance of harder rocks decreases with increasing velocity greater than a variable critical velocity, and the shear resistance of softer rocks increases with increasing shear velocity up to a critical velocity. Data from the testing of Crawford and Curran [5] are shown in Figures 4.12 and 4.13. The average strength at a given velocity is normalized with respect to the "static" strength, or strength at the lowest velocity for a given sample and normal stress. The normalized strength is then plotted against shearing velocity. Only the tests on dolomite indicate that the shearing velocity effects are normal stress

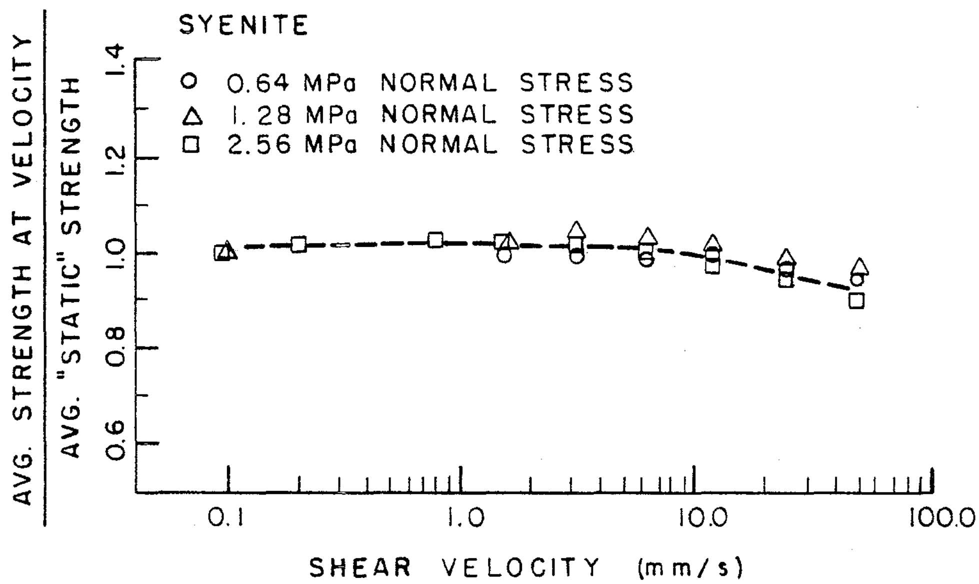

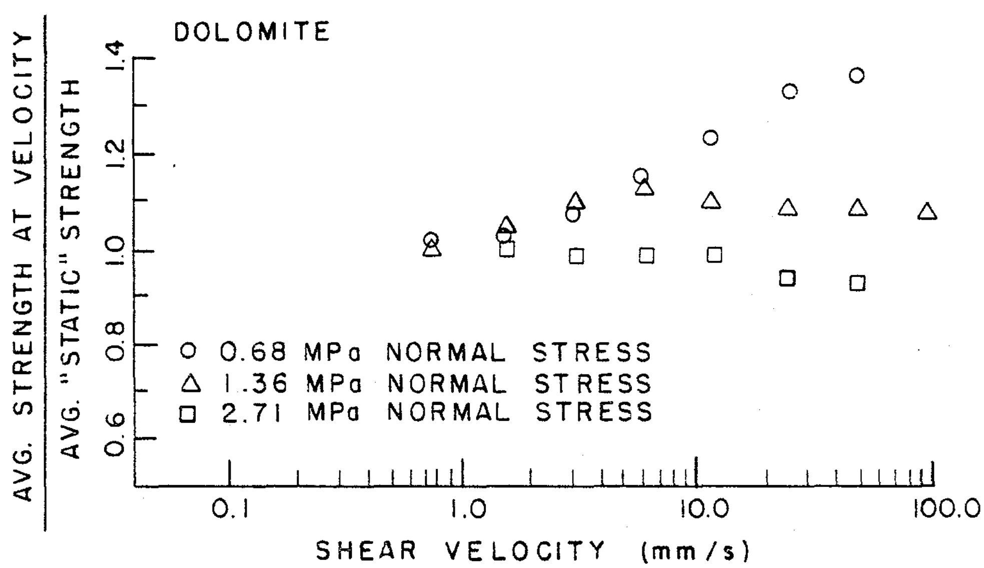

Figure 4.12 Normalized Shear Strength vs. Shear Velocity for Tests on Syenite and Dolomite [5].

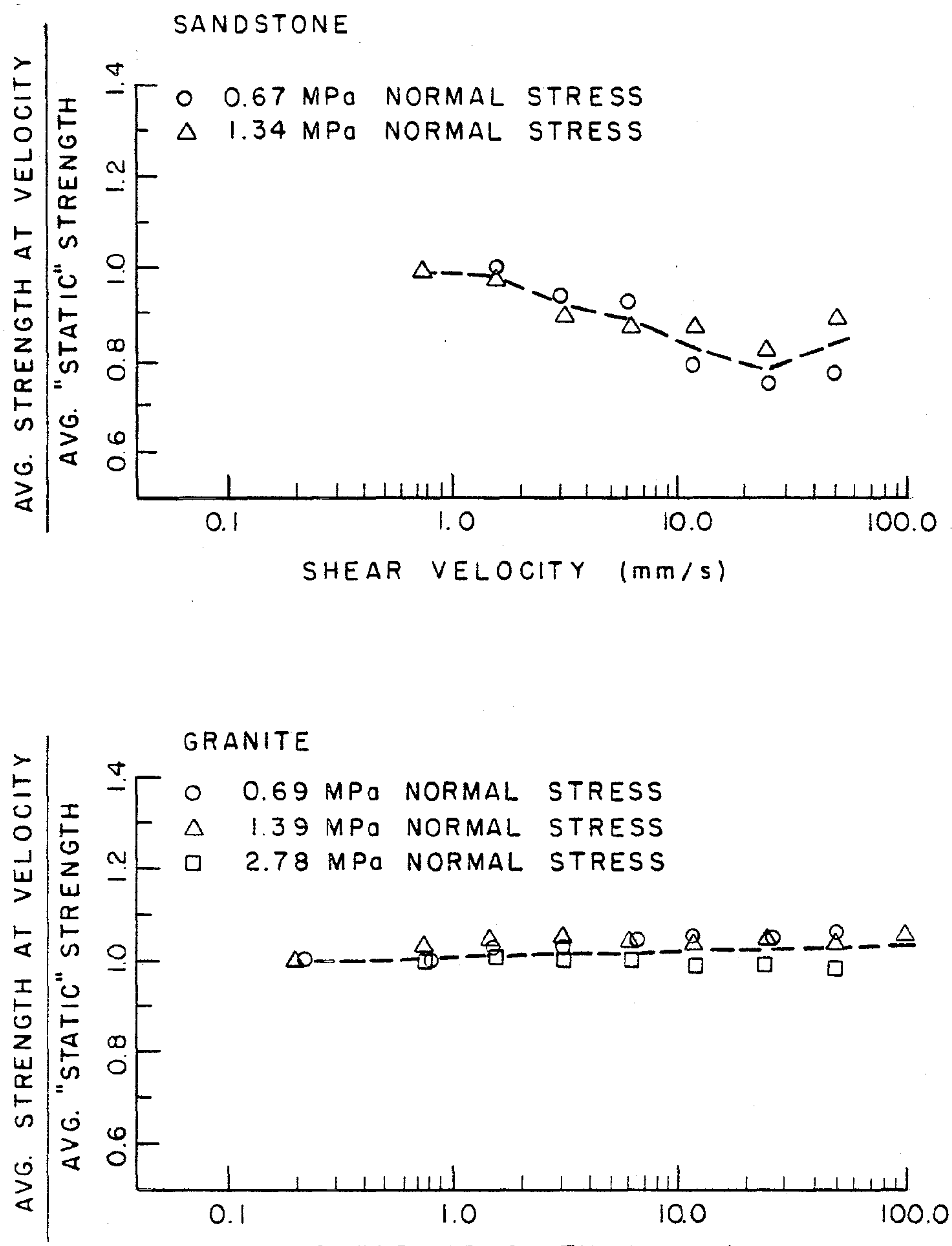

Figure 4.13 Normalized Shear Strength vs. Shear Velocity for Tests on Sandstone and Granite [5].

dependent. The other tests indicate an increase or decrease in strength with increasing shear velocity that is relatively independent of the normal stress. Crawford and Curran [6] propose a velocity dependent shear strength model that is independent of normal stress. Changes in shear strength are assumed to occur only beyond a critical velocity. The shear strength is assumed to vary linearly with the logarithm of velocity beyond this critical velocity.

The relative shear displacement for the samples tested at the University of Colorado under displacement control is given by:

$$d = d_{max} \sin (2 \pi ft + \beta) \tag{4.2}$$

where d_{max} is the displacement amplitude, f is the test frequency, t is time, and β is the phase angle. The relative velocity is given by:

$$v = \frac{dd}{dt} = d_{max} \, 2 \pi f \cos (2 \pi ft + \beta) \tag{4.3}$$

The maximum velocity occurs when $\cos (2 \pi ft + \beta) = 1$ or where the slope of the displacement vs. time curve (see Figure 4.14) is steepest at displacement = 0. Thus:

$$v_{max} = d_{max} 2 \pi f \tag{4.4}$$

The average shear strength at maximum velocity, normalized with respect to the average "static" shear strength which occurs at

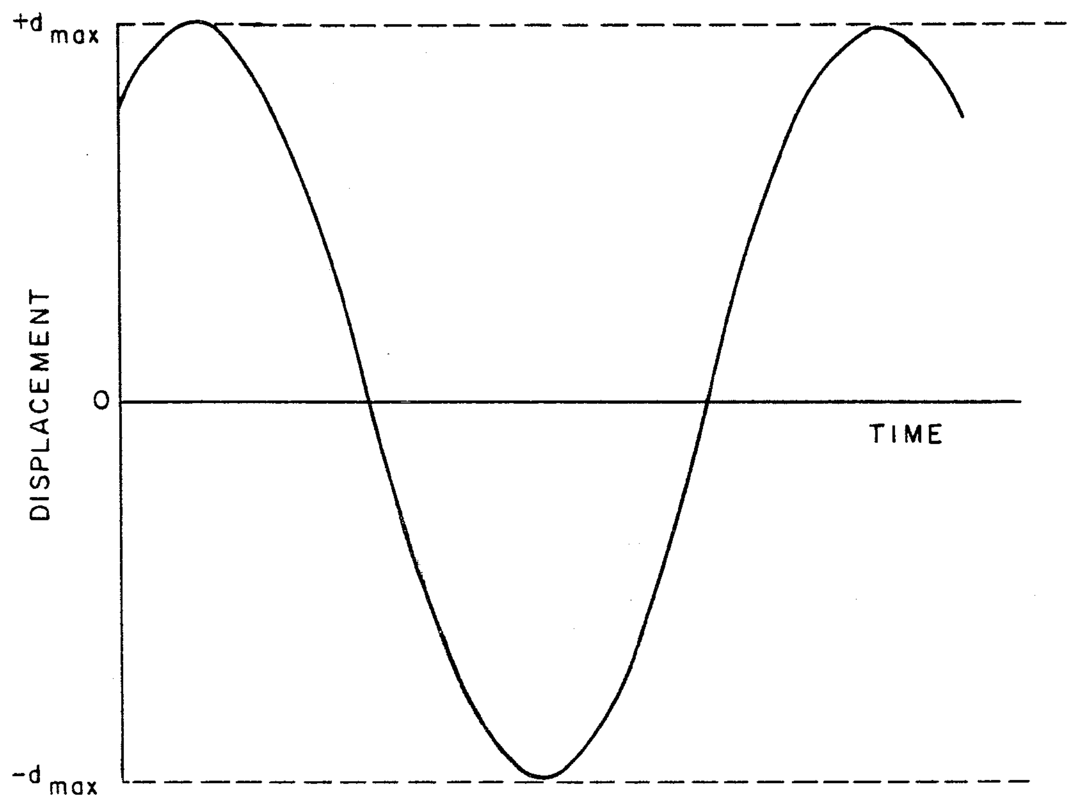

Figure 4.14 Displacement vs. Time for Displacement Controlled Tests (Conceptual).

maximum velocity and a frequency of 0.01 Hz, is plotted in Figures 4.15 through 4.17 for the rough samples [12]. Normalization was performed independently for each displacement amplitude and normal stress. Results presented by Gould [12] indicate that there is essentially no loss in strength of the samples due to

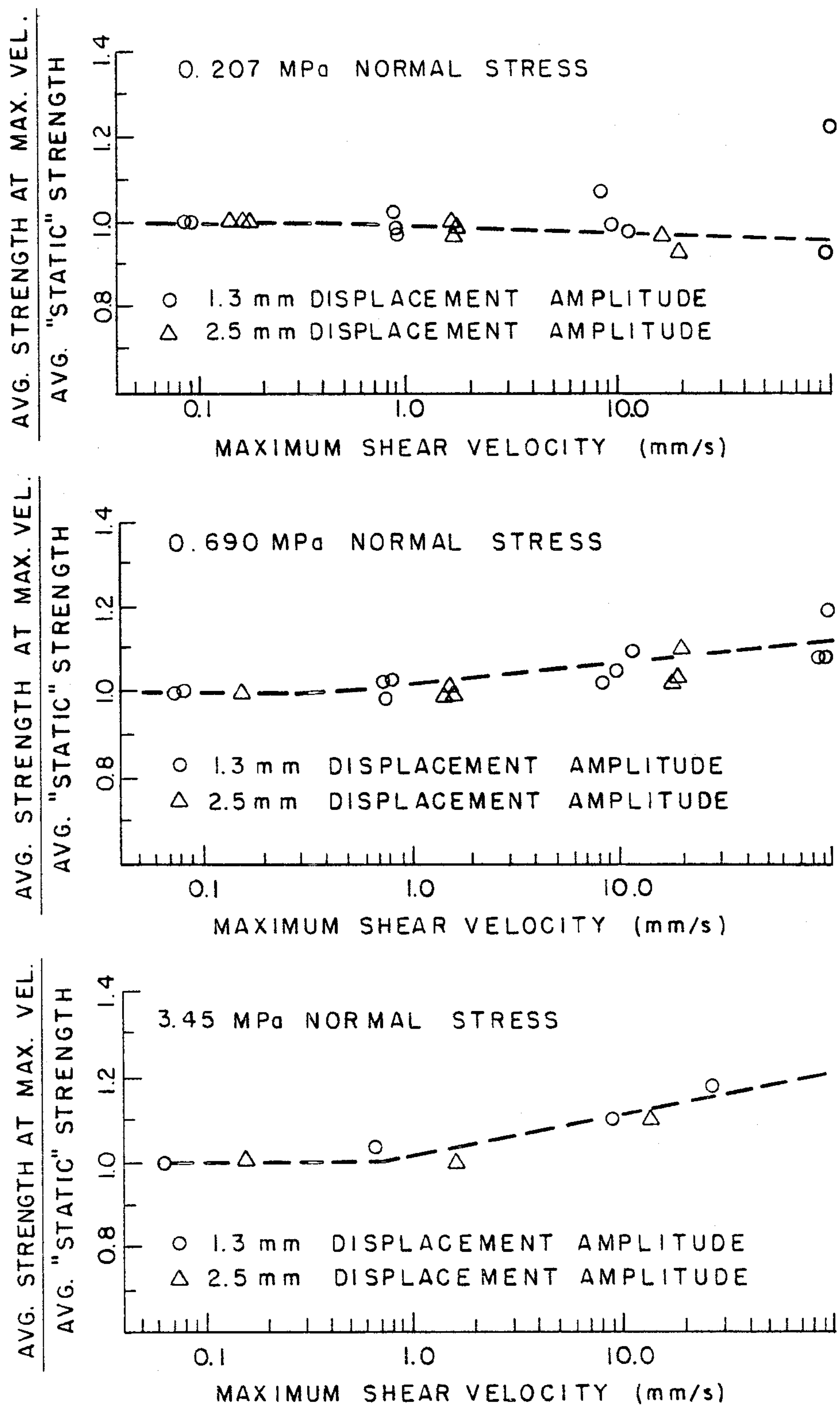

Figure 4.15 Normalized Shear Strength vs. Shear Velocity for Sample C.

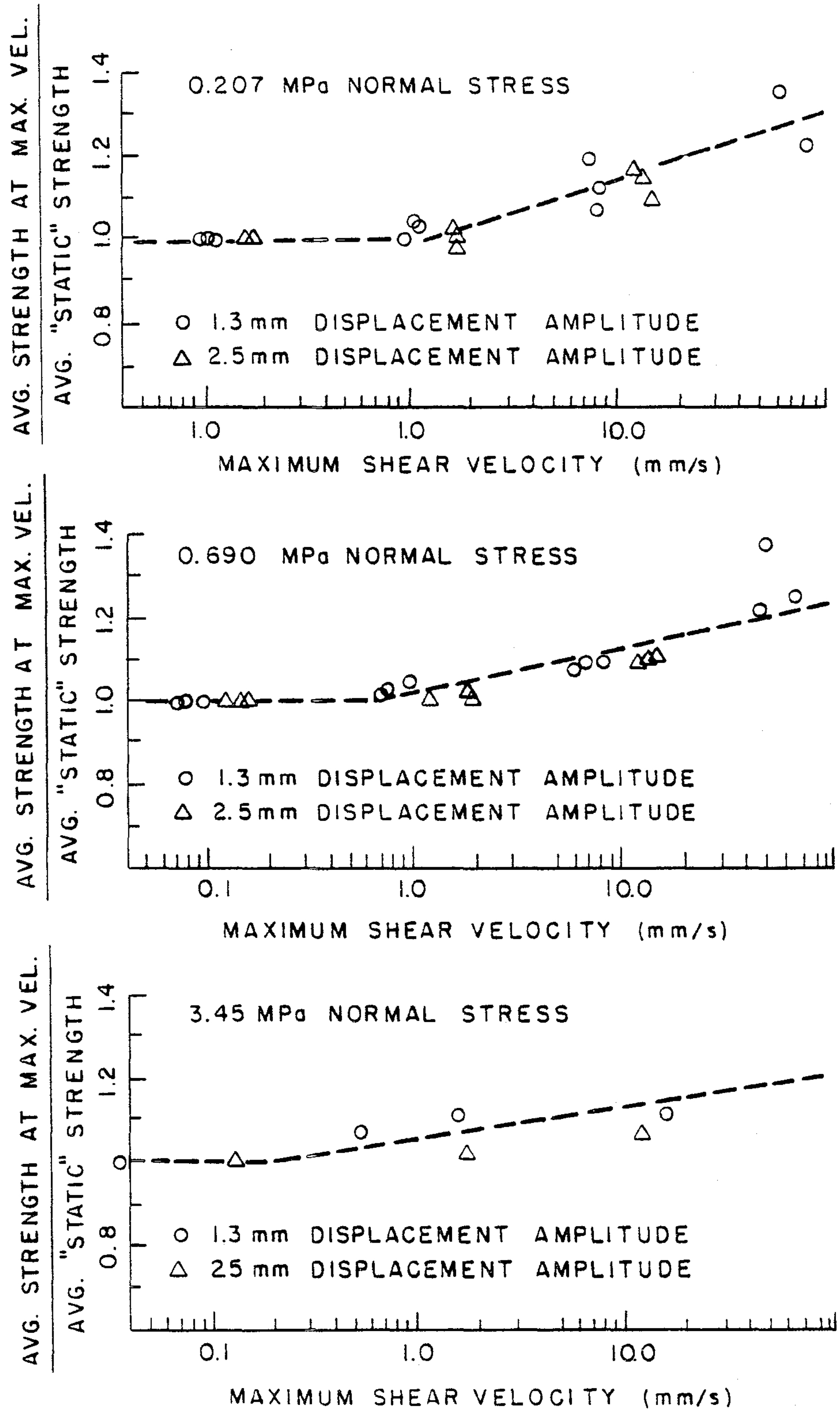

Figure 4.16 Normalized Shear Strength vs. Shear Velocity for Sample D.

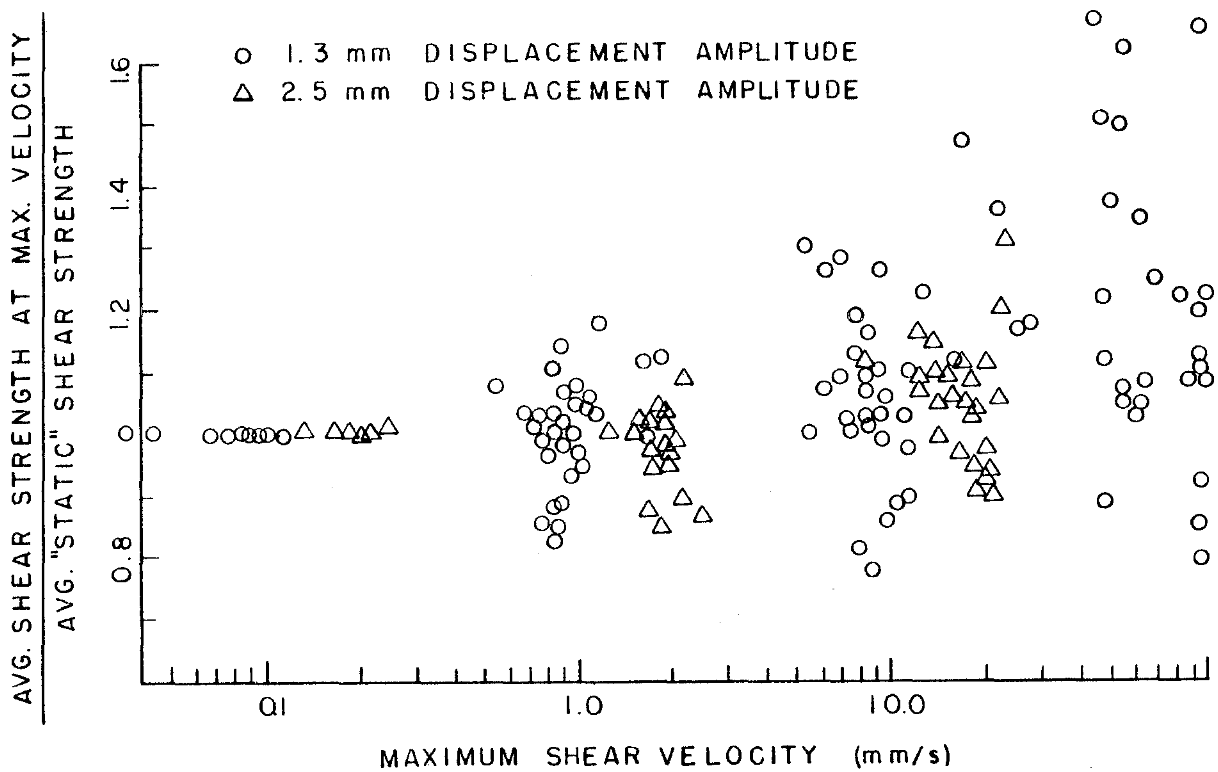

Figure 4.17 Normalized Shear Strength vs. Shear Velocity for Samples A Through E (Excluding Tests at 0.069 MPa Normal Stress).

degradation. This allows a close examination of the shearing rate or velocity effects.

The results from the testing at the University of Colorado indicate deviation from the "static" strength at somewhat lower velocities than those presented by Crawford and Curran [5]. Excluding tests at 0.069 MPa (10 lb/in^2) normal stress, samples C and D show the most consistent results. The results from sample C indicate that the velocity effects may be normal stress dependent (Figure 4.15). However, if the two tests showing increasing strength at 0.207 MPa (30 lb/in^2) normal stress are considered, the dependency on normal stress is less obvious. In addition, the results from sample D indicate that velocity effects are relatively independent of normal stress (Figure 4.16). Trends are not apparent in samples A, B, and E. The data from all five rough samples are shown in Figure 4.17. Although, in general, the strength of the samples seems to increase with increasing shear velocity, the scatter in the data is relatively large. For tests conducted at approximately 2.54 mm (0.1 in) displacement amplitude, there are about the same number of tests showing decreasing strength as increasing strength, as the shear velocity increases. These tests should be the most consistent since the samples have been displaced under the same normal stress but a smaller displacement amplitude beforehand, and the samples should approach a steady-state condition. The indicated changes in strength with velocity, therefore, are probably also influenced by properties of the test and sample geometry. This can be further substantiated by examining the results from a smooth sample. Although a complete series of tests was not performed on a smooth sample, some results are plotted in Figures 4.18 and 4.19. They indicate that the shear strength increases slightly with increasing shear velocity. This is similar to the average response of the rough joints and is not inconsistent with the results of Crawford and Curran. Based on uniaxial compressive strength, the Loveland Sandstone used in the University of Colorado tests is in the middle range of hardness of the rocks tested by Crawford and Curran.

The velocity dependent model proposed by Crawford and Curran [6] therefore seems to be appropriate for the average response of clean rock joints. An increase or decrease in shear strength with respect to the static shear strength can be made according to:

$$\text{for } v \leq v_c \quad \tau_d = \tau_s \tag{4.5}$$
$$\text{for } v > v_c \quad \tau_d = \tau_s \left[1 + m \left(\log_{10} v - \log_{10} v_c\right)\right]$$

in which v is the relative velocity across a sliding joint, v_c is the critical velocity, τ_d is the dynamic shear strength of the joints, τ_s is the static shear strength of the joint, and m is the change in increase or decrease of shear strength divided by the change in $\log_{10}$ (velocity), defined by the slope of a line similar to those shown in Figures 4.15 and 4.16.

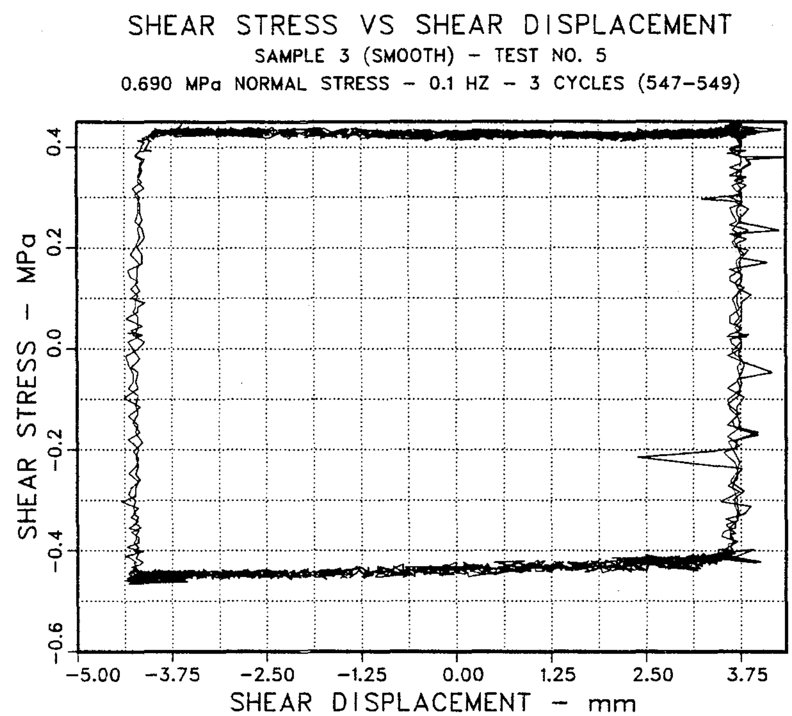

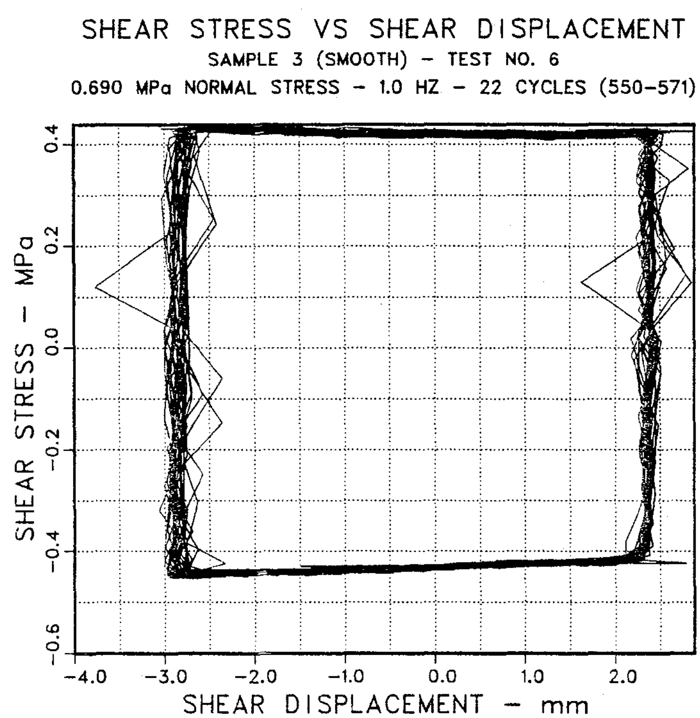

Figure 4.18 Typical Shear Stress vs. Shear Displacement Curves for Smooth Sample 3.

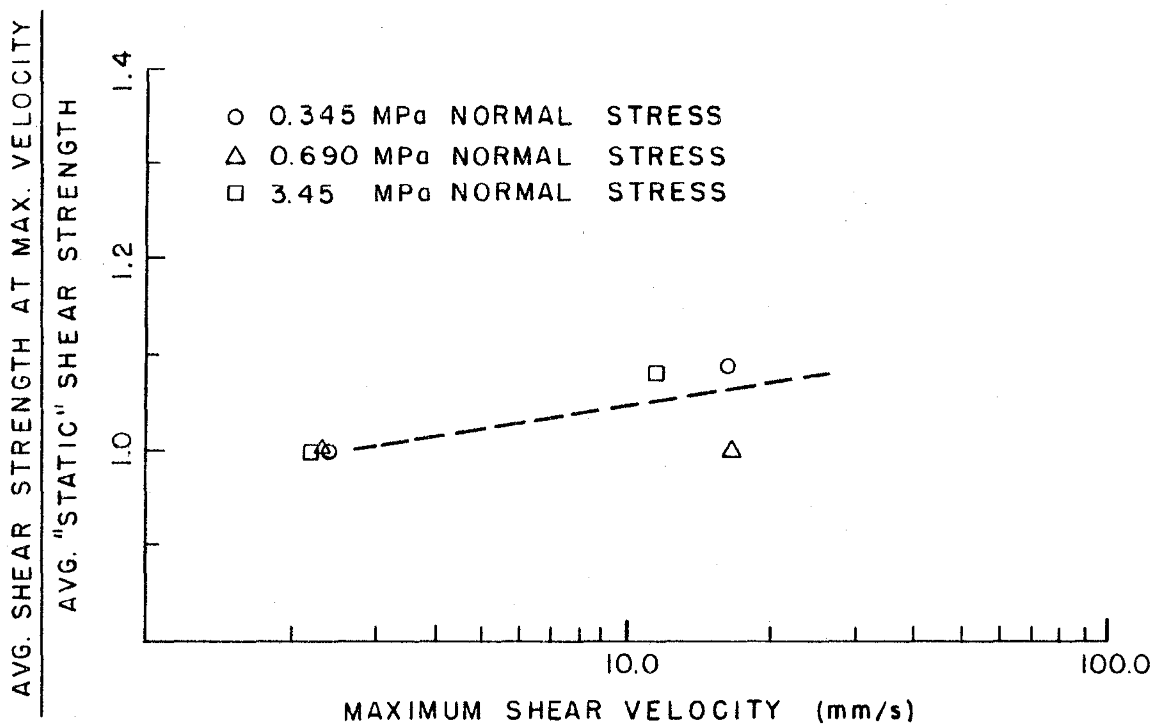

Figure 4.19 Normalized Shear Strength vs. Shear Velocity for Smooth Sample 3.

CHAPTER V

DYNAMIC LIMIT EQUILIBRIUM ANALYSIS

5.1 Response History Analysis

The three-dimensional limit equilibrium approach described in Chapter III can be readily extended to study the stability of rock masses subjected to time-varying forces, such as those created by an earthquake, if these forces are digitized at discrete time steps. At each time step during the earthquake, three-dimensional time-varying forces, such as dynamic loads from a dam and inertia forces acting opposite to the ground acceleration, are added to the static forces. Force resolution is performed and a factor of safety computed at each time step as appropriate. The large number of time steps usually encountered in a dynamic analysis necessitates the use of a computer program, such as that described in the Appendix.

As an example, consider the potential localized instability created by a powerplant excavation at the base of an arch dam as shown in Figure 5.1. Two diverging fault planes cross the foundation from upstream to downstream. A prominent and continuous joint set dips slightly downstream and daylights in the powerplant excavation between the fault planes. A potentially unstable rock wedge including a plane contacting the heel of the

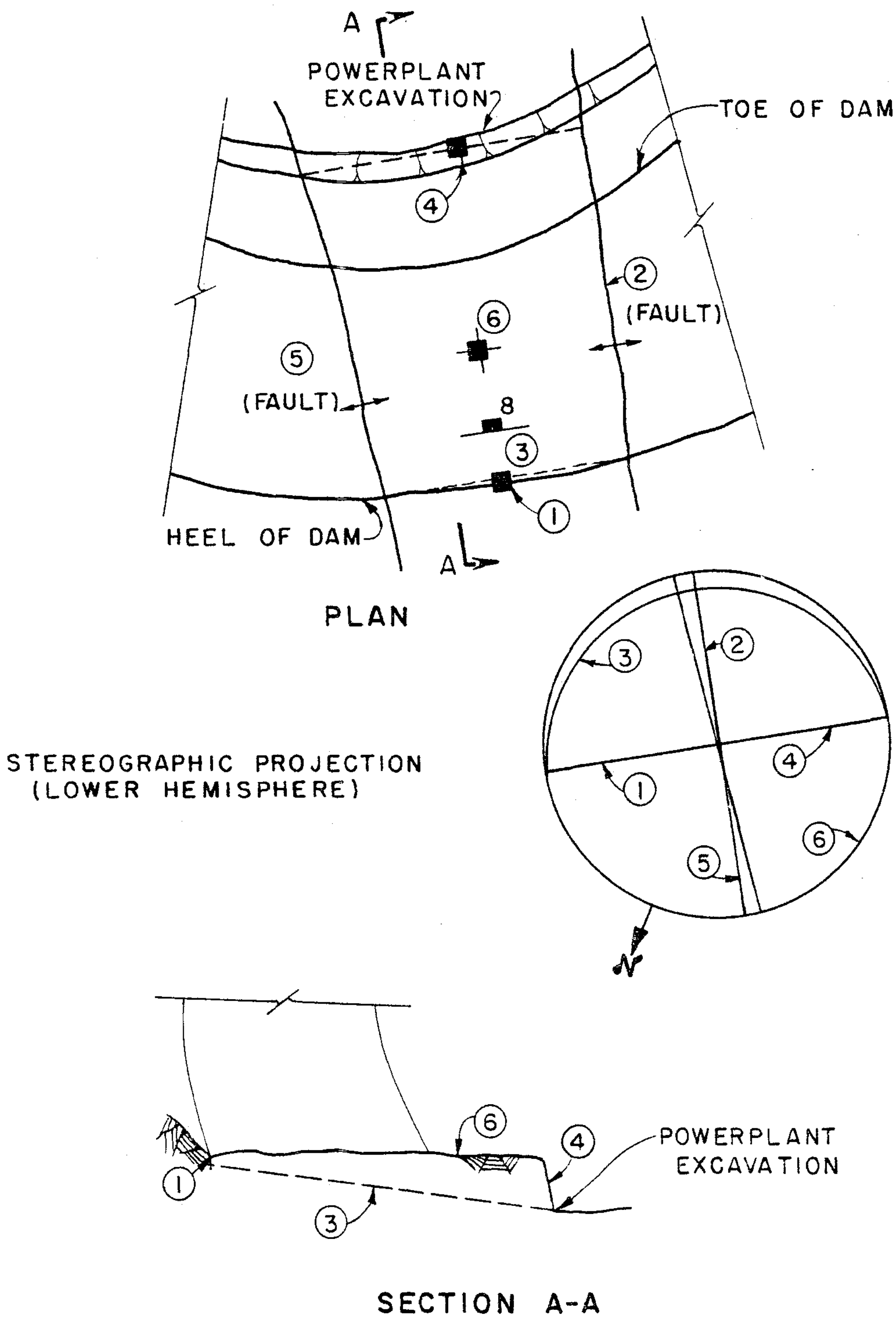

Figure 5.1 Example of a Potentially Unstable Rock Mass.

dam and daylighting at the base of the powerplant excavation can be considered as a worst case. An isometric view of the resulting potentially unstable rock mass is shown in Figure 5.2. The orientations of the planes forming the rock mass are summarized in Table 5.1 along with shear strengths and water forces. The static forces acting on the block are summarized in Table 5.2. The shear strength of the fault planes is approximated by the nonlinear failure envelope shown in Figure 5.3. In reality, the water forces acting normal to each plane are dependent on the stresses transmitted by the dam. An increase in stress closes the discontinuities and changes the seepage characteristics of the rock mass. However, coupled stress-flow problems are difficult to solve, particularly when there are a large number of discontinuities where flow can occur, such as a jointed rock mass. Therefore, a more practical approach utilizes an equivalent continuum seepage analysis with anisotropic permeability to represent preferred directions of flow. The water forces shown in Table 5.1 were determined in this manner.

In addition to the static forces, the dam is subjected to a Richter Magnitude 6.5 earthquake represented by three synthetic accelerograms shown in Figure 5.4 [27]. Three-dimensional forces acting on the potentially unstable rock mass are computed at each time step during the earthquake from a finite element analysis of the dam utilizing the method described by Scott and Dreher [24]. The resulting histories of forces are shown in Figure 5.5. Inertia forces acting on the rock wedge opposite to the directions

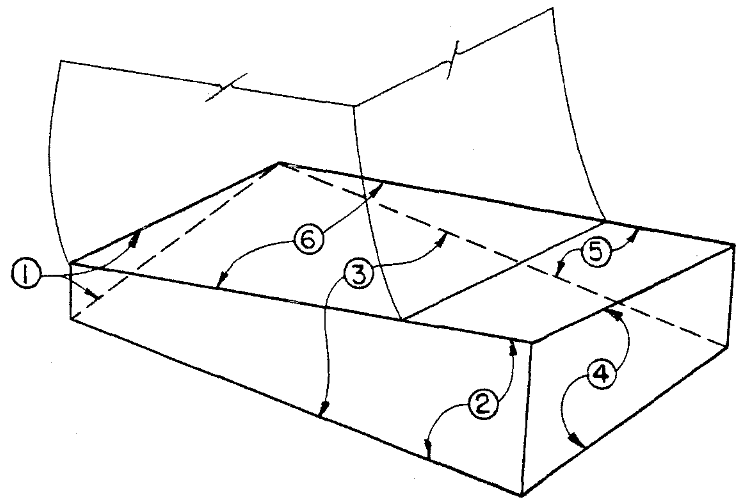

Figure 5.2 Isometric View of Example Wedge.

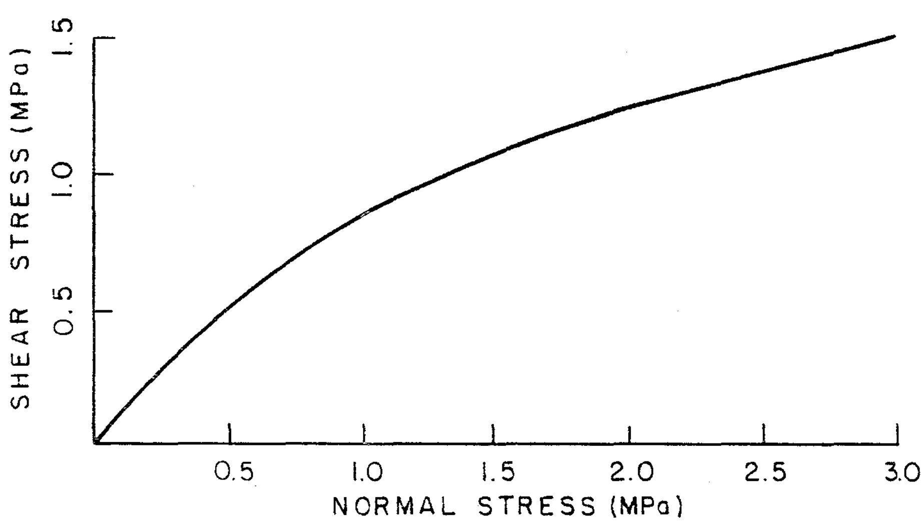

Figure 5.3 Nonlinear Shear Strength Envelope.

Table 5.1 Summary of Planes for Example Rock Mass (See Figure 5.2)

Plane	Strike	Dip	Water Force (MN)	Area (m^2)	Shear Strength
1	N57°E	90°	225	111	Ø = 45°
2	N30°W	90°	202	408	Figure 5.3
3	N57°E	8°SE	1606	4617	JRC = 15 JCS = 86 MPa Ø = 30°
4	N58°E	90°	0	-	0
5	N35°W	90°	94	552	Figure 5.3
6	Horizontal		0	-	0

Table 5.2 Static Forces Acting on Example Rock Mass

	Cross Canyon* (MN)	Upstream/Downstream* (MN)	Vertical (MN)
Dam	-574	4893	8363
Weight			1134

* NOTE: +x is directed in the cross canyon direction toward the left abutment (looking downstream) and +y is directed downstream.

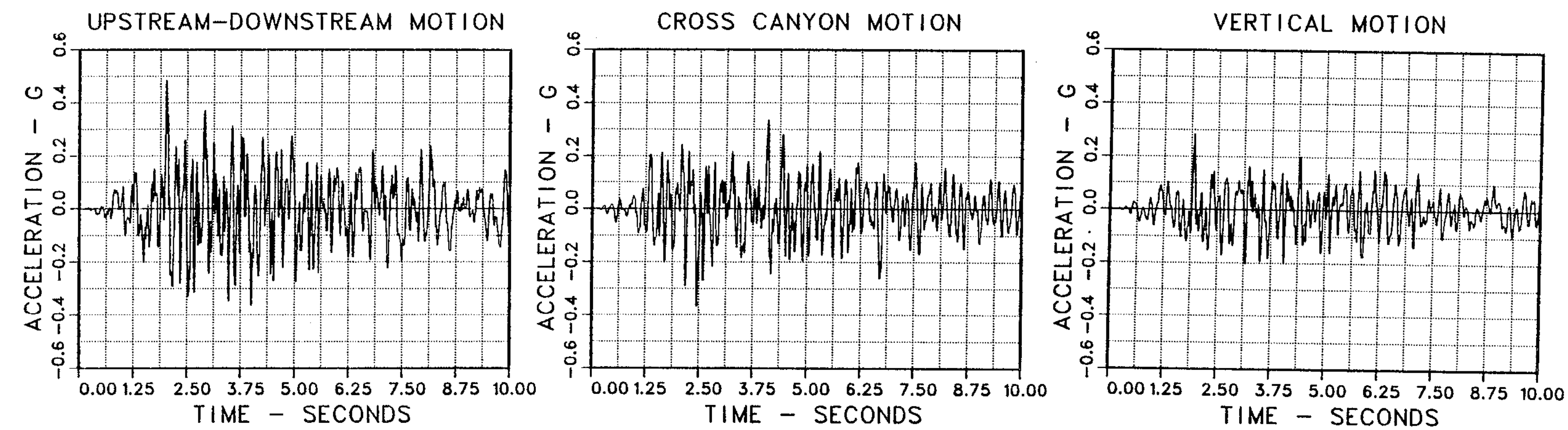

Figure 5.4 Synthetic Ground Accelerations for Richter M6.5 Earthquake [27].

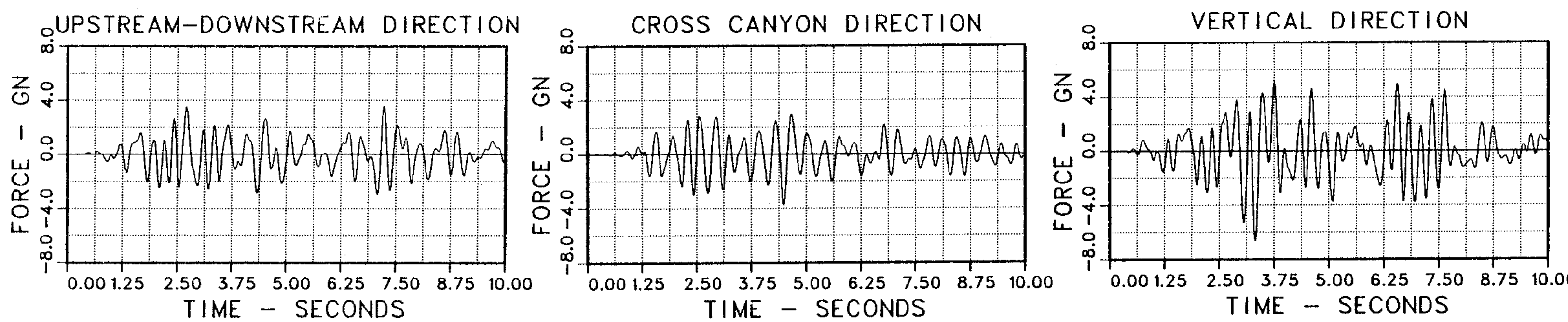

Figure 5.5 Loads From Dam During Richter M6.5 Earthquake [24].

of ground acceleration are also computed for each time step by multiplying the values of acceleration by the mass of the rock block and changing the sign of the resulting force.

The potential mode of sliding as determined from force resolution at each time step, is plotted against time in Figure 5.6. The potential mode of instability changes during the earthquake due to the time-varying forces. The factor of safety against sliding of the example rock mass is plotted against time in Figure 5.7. The factor of safety drops below 1.0 twice during the earthquake. However, the total time the factor of safety is below 1.0 is less than 0.1 second, and it may not be reasonable to assume complete failure.

5.2 Permanent Cumulative Displacement

The permanent displacement of a rock mass can be estimated when the factor of safety against sliding is less than 1.0 for a period of time. Von Thun and Harris [30] describe a method for estimating cumulative permanent displacements of slopes subjected to time-varying forces in two directions. The material shear strength is assumed to follow rigid-perfect plastic behavior, ignoring elastic shear deformation. Movement is considered to occur only when the shear strength of the resisting plane is exceeded.

This method can be extended to three dimensions to estimate permanent deformations of rock masses. Displacement occurs

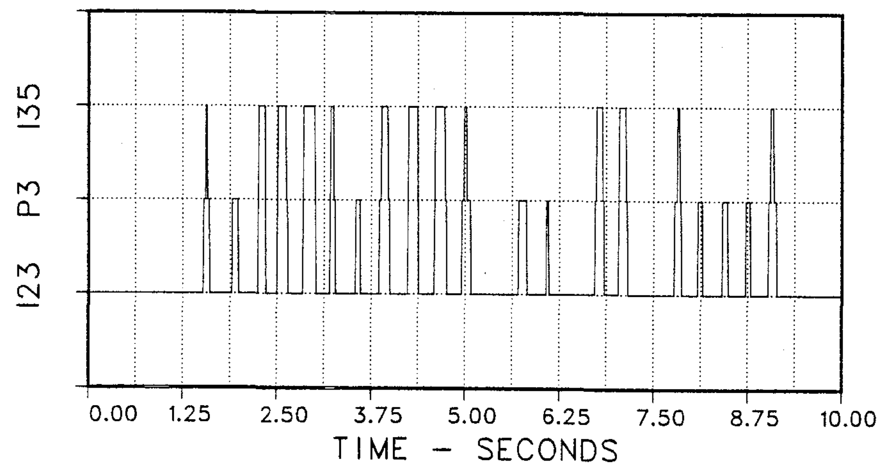

Figure 5.6 Modes of Potential Instability vs. Time - I23 Represents Sliding on the Intersection of Planes 2 and 3, P3 Represents Sliding on Plane 3, and I35 Represents Sliding on the Intersection of Planes 3 and 5 (See Figure 5.2).

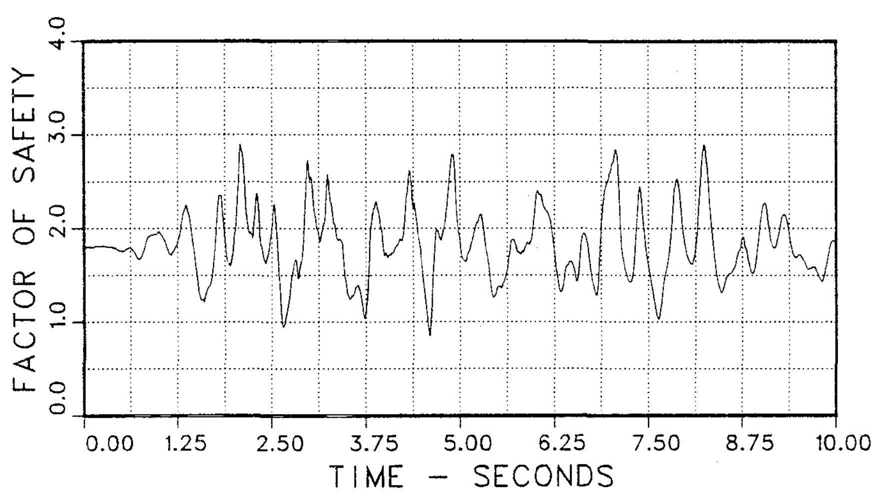

Figure 5.7 Factor of Safety Against Sliding vs. Time.

only when the factor of safety drops below 1.0. Linear interpolation between input time steps may be utilized to find the exact time at which movement initiates, if it does not occur at an even time step, as shown in Figure 5.8. The time of impending motion,

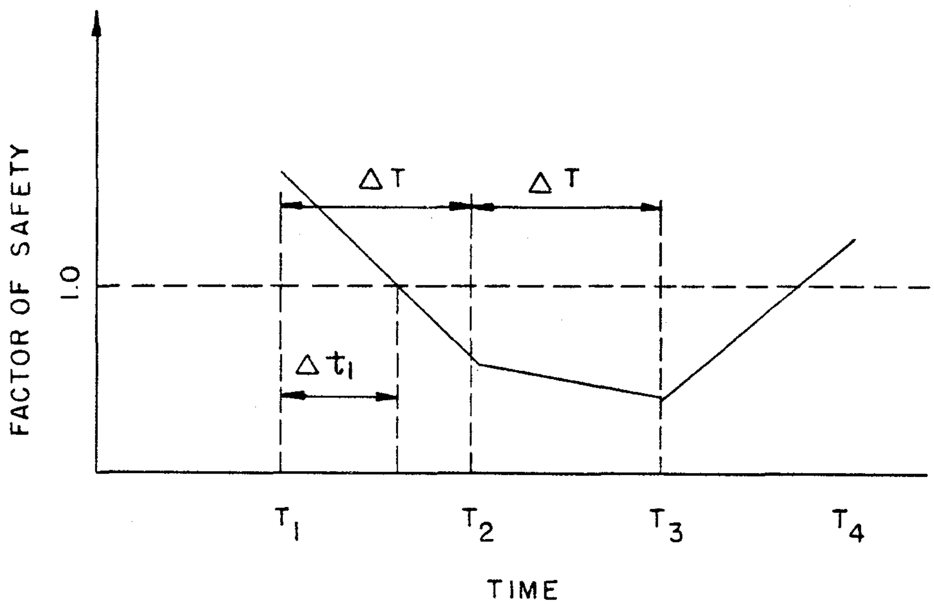

Figure 5.8 Linear Interpolation Between Input Time Steps.

when the factor of safety is just equal to 1.0, is determined by:

$$S_f\ (T_1 + \Delta t_1) = S_f(T_1) + \frac{S_f(T_2) - S_f(T_1)}{\Delta T}\ \Delta t_1 = 1.0 \qquad (5.1)$$

$$\Delta t_1 = [1.0 - S_f(T_1)]\ \frac{\Delta T}{S_f(T_2) - S_f(T_1)} \qquad (5.2)$$

in which the factor of safety at time T_1 is greater than 1.0, the factor of safety at time T_2 is less than 1.0, Δt_1 is defined in

Figure 5.8, and ΔT is the time between T_1 and T_2. When the safety factor drops below 1.0, the unbalanced force acting on the unstable rock mass at any time step is given by:

$$F_u = D - R \tag{5.3}$$

in which D is the driving force and R is the resisting force, both of which vary with time. Movement occurs in the direction of the driving force. For the case of sliding on a single plane, the resisting force is a function of the normal stress and shear strength of the single plane, and the driving force is represented by the magnitude and direction of the shear force in the plane. In the case of sliding on an intersection, the resisting force is a function of the normal stress and shear strength for both planes forming the intersection, and the driving force is the component of the resultant force in the direction of the intersection. In case of lifting, the resisting force is zero and the driving force is the total resultant acting on the wedge.

When sliding occurs, the effects of post-peak shear strength behavior must be considered. Thus, residual strengths should be used to estimate resisting forces once movement begins. In addition, if sliding occurs along the intersection of two planes, the shear strengths utilized in the analysis must be developed at compatible displacements.

The relative acceleration between the unstable mass and the underlying rock at a particular instant in time is given by:

$$a = \frac{F_u}{M} \tag{5.4}$$

where M is the mass of the unstable rock. Assuming the acceleration varies linearly between input time steps:

$$a(t) = a(T_{n-1}) + \frac{a(T_n) - a(T_{n-1})}{\Delta T} t \tag{5.5}$$

where ΔT is the time step between T_{n-1} and T_n, and t varies from 0 to ΔT. The relative velocity for each time step, calculated by integration of the relative acceleration is:

$$\begin{aligned} v(T_n) &= v(T_{n-1}) + \int_0^{\Delta T} a(t)\, dt \\ &= v(T_{n-1}) + \left[a(T_{n-1})\, t + \frac{a(T_n) - a(T_{n-1})}{\Delta T} \frac{t^2}{2} \right]_0^{\Delta T} \\ &= v(T_{n-1}) + \frac{\Delta T}{2} [a(T_{n-1}) + a(T_n)] \end{aligned} \tag{5.6}$$

Another integration yields the relative displacement for the time step.

$$\begin{aligned} d(T_n) &= d(T_{n-1}) + \int_0^{\Delta T} \int_0^{\Delta T} a(t)\, dt \\ &= d(T_{n-1}) + \left[v(T_{n-1}) t + a(T_{n-1}) \frac{t^2}{2} + \frac{a(T_n) - a(T_{n-1})}{\Delta T} \frac{t^3}{6} \right]_0^{\Delta T} \\ &= d(T_{n-1}) + v(T_{n-1})\ \Delta T + [2a(T_{n-1}) + a(T_n)] \frac{\Delta T^2}{6} \end{aligned} \tag{5.7}$$

Movement stops when the relative velocity becomes zero. The exact time that movement stops, as shown in Figure 5.9, may be determined by quadratic interpolation between input time steps, since velocity is a quadratic function of time. Inserting Δt_2 (see Figure 5.9) into equation (5.6), setting the equation equal to zero, and solving by the quadratic formula yields:

$$\Delta t_2 = \frac{-a(T_{n-1}) \pm \left[a(T_{n-1})^2 - \frac{2}{\Delta T}\left[a(T_n) - a(T_{n-1})\right] v(T_{n-1})\right]^{1/2}}{\frac{1}{\Delta T}\left[a(T_n) - a(T_{n-1})\right]} \tag{5.8}$$

The solution which lies in the interval between 0 and ΔT is used to calculate the time at which movement stops. The total displacement magnitude and direction is determined by vector addition of

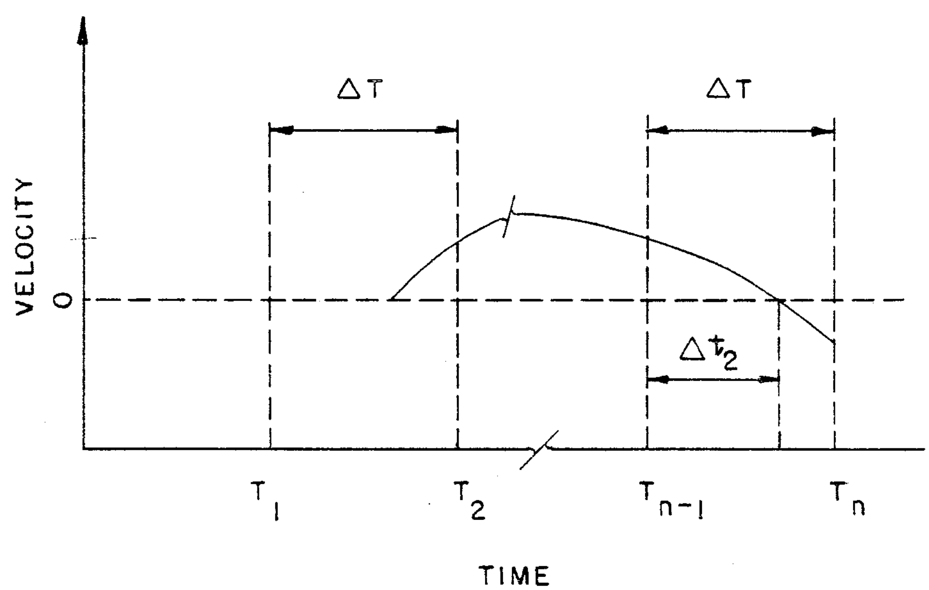

Figure 5.9. - Quadratic Interpolation Between Input Time Steps.

the displacements at each time step. The direction of movement at each time step is determined by the direction cosines of the shear force. In the case of sliding on a single plane they are given by:

$$\{C_m\} = \begin{Bmatrix} C_{mx} \\ C_{my} \\ C_{mz} \end{Bmatrix} = \frac{1}{(F_{sx}^2 + F_{sy}^2 + F_{sz}^2)^{1/2}} \begin{Bmatrix} F_{sx} \\ F_{sy} \\ F_{sz} \end{Bmatrix} \tag{5.9}$$

In the case of sliding along the intersection of two planes the direction cosines of the movement are given by (see Chapter III):

$$\{C_m\} = \{C_i\} \tag{5.10}$$

The process is repeated for each cycle in which the factor of safety drops below 1.0, and displacements are accumulated vectorally. The displacement calculated in this manner is approximate and only appropriate for small displacements, since the mode of instability is assumed to change instantaneously without repositioning of the block.

5.3 Effects of Dynamic Material Behavior

The method described in the previous section results in calculation of the relative velocity for sliding planes at each time step during a dynamic analysis. Shear strengths can, therefore, be revised during the analysis according to the relative velocity calculated for the previous time step, and the velocity dependent shear strength criteria described by equation (4.5).

For the example problem described in previous sections, cumulative displacements were calculated considering no change in strength with velocity. Values of critical velocity and m which envelope the results from the University of Colorado dynamic direct shear tests conducted at displacement amplitudes of 2.54 mm (0.1 in) were also considered for plane 3 only. The results, shown in Table 5.3, indicate that velocity effects can be an important consideration in estimating cumulative permanent displacements of potentially unstable rock masses.

Table 5.3 Velocity Effects on Cumulative Permanent Displacements of Example Rock Mass

Critical Velocity (mm/s)	m	Cumulative Permanent Displacement (mm)
-	0	10.6
0.3	0.119	0.5
0.2	-0.052	51.1

The example problem is based on work performed for Auburn Dam. However, details were modified for illustration purposes.

CHAPTER VI

SUMMARY, CONCLUSIONS, AND SUGGESTIONS FOR FURTHER STUDY

The behavior of rock discontinuities under static loading conditions has received much attention and research in recent years. Research into the behavior of such discontinuities subjected to dynamic loading is just beginning. Crawford and Curran [5] studied the effects of shear velocity on the shear strength of clean rock joints utilizing a sophisticated servocontrolled dynamic direct shear apparatus. A similar machine was developed at the University of Colorado as described by Gould [12]. The results from testing in both machines indicate that shearing velocity can have a pronounced effect on discontinuity shear strength. The effects seem to be independent of the normal stress across the discontinuity. The strength appears to increase or decrease linearly with the logarithm of velocity beyond a critical threshold velocity. However, there is a relatively large amount of scatter in the data, and further verification work is warranted. The approach adopted in this research has been to examine changes from static behavior of rock joints, when they are subjected to dynamic loads. Although this is probably a good first approach, further research may lead to comprehensive material models for dynamic loading.

When evaluating the effects of earthquakes is important, response history analyses for rock masses can be performed. The three-dimensional limit equilibrium approach is a cost effective means of performing such analyses for masses bounded by planar discontinuities. If the dynamic loads and accelerations are digitized for each time step during an earthquake, analytical computer techniques can be utilized. At each time step during the earthquake, an analysis is performed. Dynamic and static forces, including water forces acting normal to the discontinuities, are summed and resolved. The potential mode of instability and factor of safety against sliding are determined. If the factor of safety drops below 1.0 for short periods of time during the earthquake, cumulative permanent displacements can be estimated by double integration of the relative acceleration. The effects of relative shearing velocity can be included and appear to have a significant effect on the estimated displacement.

The rigid block analysis is appropriate when the potentially unstable rock mass is bounded by planar discontinuities. The ratio of normal stiffness to shear stiffness of the discontinuities must also be large, which is usually the case in nature. Localized stress concentrations cannot be considered using this method. The permanent displacement calculated for dynamic analyses is approximate and only appropriate for small displacements, since the mode of instability is assumed to change instantaneously without repositioning of the block. The major weakness in the analytical approach is the treatment of water forces. Currently they are assumed to be constant throughout the earthquake. However, it is reasonable to expect that the dynamic loads may cause an increase in stress in certain areas of the rock, resulting in closing of discontinuities and an increase in water pressure. Similarly, once movement starts, the discontinuities can be expected to dilate, thus reducing water pressures.

Research is continuing at the University of Colorado to examine changes in water pressures and effects of water during dynamic shearing of sandstone joints subjected to constant normal stress. The effects of cycling in load control rather than displacement control are also being studied. Different rock types may behave differently, and dynamic studies of joints in several rock types are warranted. Joints containing infilling may also behave differently and should be studied under dynamic loading. In reality, the normal load acting across a discontinuity is not constant during an earthquake. Further testing where the normal load is cycled at various phase angles to the shear load are also justified.

Research into the behavior of jointed rock masses during dynamic earthquake loading is just beginning. It is hoped that the need for such research is realized and that further work can be performed.

BIBLIOGRAPHY

1. Barney, K. R., "Madison Canyon Slide," Civil Engineering, Vol. 30, No. 8, 1960, pp. 72-75.

2. Barton, N., "The Shear Strength of Rock and Rock Joints," Int. J. Rock Mech. Min. Sci. & Geomech. Abstr., Vol. 13, 1976, pp. 255-279.

3. Barton, N., and V. Choubey, "The Shear Strength of Rock Joints in Theory and Practice," Rock Mechanics, Vol. 10, 1977, pp. 1-54.

4. Barton, N., and S. Bandis, "Some Effects of Scale on the Shear Strength of Joints," Int. J. Rock Mech. Min. Sci. & Geomech. Abstr., Vol. 17, 1980, pp. 69-73.

5. Crawford, A. M., and J. H. Curran, "The Influence of Shear Velocity on the Frictional Resistance of Rock Discontinuities," Int. J. Rock Mech. Min. Sci. & Geomech. Abstr., Vol. 18, 1981, pp. 505-515.

6. Crawford, A. M., and J. H. Curran, "The Influence of Rate and Displacement - Dependent Shear Resistance on the Response of Rock Slopes to Seismic Loads," Int. J. Rock Mech. Min. Sci. & Geomech. Abstr., Vol. 19, 1982, pp. 1-8.

7. Design and Analysis of Auburn Dam, U.S. Department of the Interior, Bureau of Reclamation, Denver, 1977.

8. Fairhurst, C., "On the Validity of the Brazilian Test for Brittle Materials," Int. J. Rock Mech. and Min. Sci., Vol. 1, 1964, pp. 535-546.

9. Finn, W.D.L., "Liquefaction Potential: Developments Since 1976," International Conference on Recent Advances in Geotechnical Earthquake Engineering and Soil Dynamics, St. Louis, Vol. II, 1981, pp. 655-682.

10. Goodman, R. E., and Y. Onishi, "Undrained Shear Testing of Jointed Rock," Rock Mechanics, Vol. 5, 1973, pp. 129-149.

11. Goodman, R. E., Methods of Geological Engineering, West Publishing Co., St. Paul, Minn., 1976.

12. Gould, M., Development of a High Capacity Dynamic Direct Shear Apparatus and Its Application to Testing of Sandstone Rock Joints, Master's Thesis, University of Colorado, 1982.

13. Hendron, A. J., E. J. Cording, and A. K. Aiyer, "Analytical and Graphical Methods for the Analysis of Slopes in Rock Masses," NCG Technical Report No. 36, Available from NTIS, Springfield, Va., 1971.

14. Hardin, B. O., "The Nature of Stress - Strain Behavior of Soils," Proc. ASCE Specialty Conference on Earthquake Engineering and Soil Dynamics, Pasadena, Calif., 1978, pp. 3-90.

15. Hoek, E., and J. W. Bray, Rock Slope Engineering, Revised 2nd Edition, Institution of Mining and Metallurgy, London, 1977.

16. Jaeger, J. C., "Friction of Rocks and the Stability of Rock Slopes," Geotechnique, Vol. 21, No. 2, 1971, pp. 97-134.

17. Jansen, R. B., Dams and Public Safety, U.S. Department of the Interior, Bureau of Reclamation, Denver, 1980.

18. Ladanyi, B., and G. Archambault, "Simulation of Shear Behavior of a Jointed Rock Mass," Proc. 11th Symposium on Rock Mechanics, Berkeley, Calif., 1970, pp. 105-125.

19. Londe, P., "Une Methode D'Analyze o'Trois Dimensions De La Stabilite D'une Rive Rocheuse," Annls De Ponts Et Chaus, No. 1, 1965, pp. 37-60.

20. Londe, P., Rock Mechanics and Dam Foundation Design, International Congress on Large Dams, Paris, 1973.

21. Mahtab, M. A., and R. E. Goodman, "Three Dimensional Finite Element Analysis of Jointed Rock Slopes," Final Report to U.S. Bureau of Reclamation, Contract No. 14-06-D-6639, 1969.

22. Newmark, N. M., "Effects of Earthquakes on Dams and Embankments," Geotechnique, Vol. 15, No. 2, 1965, pp. 139-160.

23. Patton, F. D., "Multiple Modes of Shear Failure in Rock," Proc. 1st Int. Congress on Rock Mechanics, Lisbon, Vol. 1, 1966, pp. 509-513.

24. Scott, G. A., and K. J. Dreher, "Dynamic Stability of Concrete Dam Foundations," Proc. 5th Int. Congress on Rock Mechanics, Melbourne, 1983, (in progress).

25. Seed, H. B., "Evaluation of Soil Liquefaction Effects on Level Ground During Earthquakes," Liquefaction Problems in Geotechnical Engineering, ASCE, 1976, pp. 1-104.

26. Silver, M. L., "Load, Deformation and Strength Behavior of Soils under Dynamic Loadings," International Conference on Recent Advances in Geotechnical Earthquake Engineering and Soil Dynamics, St. Louis, Vol. III, 1981, pp. 873-895.

27. Tarbox, G. S., K. J. Dreher, and L. Carpenter, "Seismic Analysis of Concrete Dams," Proc. 13th ICOLD Congress, New Delhi, 1979, pp. 963-994.

28. Von Thun, J. L., "The Practical and Realistic Solution of Rock Slope Stability Problems," Proc. 16th Symposium on Rock Mechanics, Minneapolis, Minn., 1975, pp. 87-98.

29. Von Thun, J. L., "Stability Analysis of Cut Slopes at Auburn Dam," Proc. ASCE Specialty Conference of Rock Engineering for Foundations and Slopes, Boulder, Colo., Vol. 1, 1975, pp. 349-360.

30. Von Thun, J. L., and C. W. Harris, "Estimation of Displacements of Rockfill Dams Due to Seismic Shaking," International Conference on Recent Advances in Geotechnical Earthquake Engineering and Soil Dynamics, St. Louis, Vol. I, 1981, pp. 417-424.

31. Wittke, W., "A Numerical Method of Calculating the Stability of Slopes in Rocks with Systems of Plane Joints," (in German), Rock Mechanics and Engineering Geology, Supplement 1, ISRM, 1964, pp. 101-129.

32. Woods, R. D., "Measurement of Dynamic Soil Properties," Proc. ASCE Specialty Conference on Earthquake Engineering and Soil Dynamics, Pasadena, Calif., 1978, pp. 91-180.

APPENDIX - COMPUTER PROGRAM

A. User's Guide

Consistent units must be used throughout the input tapes.

Input for PROGRAM RIGID from TAPE5

Card 1 FORMAT (5A10, 5X, A5, I5)

Column	Variable	Description
1-50	JOB	Title information to be printed on output.
56-60	IBLOCK	Identification for rigid block being analyzed.
61-65	IPROBN	Nonzero problem identification number.

Card 2 FORMAT (30I1)

Column	Variable	Description
1	IOC(1)	Input 0 for static analysis. Input 1 for dynamic analysis with input time-varying loads and accelerations on TAPE4.
2	IOC(2)	Input 1 for extra output. Input 0 for standard output (0 should be specified for large dynamic runs).
3	IOC(3)	Input 1 if cumulative permanent displacements of unstable rock masses are to be estimated. This can only be specified for dynamic analyses. Input 0 to suppress this option.

Card 3 FORMAT (5F10.0)

Column	Variable	Description
1-10	WT	Weight of rigid block (positive).
11-20	BMASS	Mass of rigid block.
21-30	QX	External static force acting on rigid block in x-direction.
31-40	QY	External static force acting on rigid block in y-direction.
41-50	QZ	External static force acting on rigid block in z-direction.

NOTE: The program uses a right hand cartesian coordinate system with x and y forming a horizontal plane and +z directed vertically downward.

Card 4 FORMAT (2F10.0)

Column	Variable	Description
1-10	CC	Cohesion of treatment concrete.
11-20	TPHIC	Tangent of the friction angle of treatment concrete in the planes of discontinuities.

NOTE: Treatment concrete can only be considered if the area of the plane is also specified (see card 6A). Resistance due to concrete treatment will only be considered if a positive normal force acts on the treated plane. In dynamic analyses, the concrete cohesion will be set to zero once the factor of safety drops below 1.0.

Card 5 FORMAT (F5.1)

Column	Variable	Description
1-5	XAXIS	Clockwise angle (degrees) from north to +x axis.

One set of cards 6A through 6H for each plane forming the block (up to 19 planes may be input).

Card 6A FORMAT (I5, 2F10.0, I5, 4F10.0)

Column	Variable	Description
1-5	I	Plane identification number (sequential - no missing numbers).
6-15	STRIKE(I)	Clockwise angle (degrees) from north to strike direction vector.
16-25	DIP(I)	Dip angle (degrees) measured down to the right from horizontal looking in the direction of the strike vector.
26-30	IPHI(I)	Shear strength code. Input 1 if shear strength for plane I is to be represented by cohesion and a friction angle. Input 2 if the shear strength is to be represented by a normal stress vs. shear strength curve. Input 3 if Barton's shear strength criterion is to be used. Input 4 to use Ladanyi and Archambault's criterion for clean rough joints. Input 5 to use Ladanyi and Archambault's criteria for filled joints[1]. Input 6 to use Jaeger's criterion.
31-40	UP(I)	Water uplift force acting normal to plane I.
41-50	AREA(I)	Area of planar face of plane I (needed if cohesion, Barton's parameters, Ladanyi and Archambault's parameters, Jaeger's criterion, or shear strength curve is specified) including concrete treatment area.

---

[1]Ladanyi, B., and G. Archambault, "Shear Strength and Deformability of Filled Indented Joints," Int. Symposium on the Geotechnics of Structurally Complex Formations, Capri, Vol. 1, 1977, pp. 317-326.

Column	Variable	Description
51-60	AREAC(I)	Area of treatment concrete in plane I (may be specified only if AREA(I) is also specified).
61-70	PHIR(I)	Residual friction angle (degrees) to be used once movement initiates. Input only if IOC(1) and IOC(3) are 1. Input 0 if strength is to remain unchanged.
71-75	IVEL(I)	Input 1 if effects of velocity on shear strength are to be considered when estimating permanent cumulative displacements. Input 0 to suppress this option.

NOTE: The strike and dip must be described such that the plane normal is directed into the block. The normal direction is found by crossing the strike vector into the dip vector through an angle of 90°. The strike must be changed by 180° if the normal is not directed into the block, and the dip must be changed appropriately.

Skip card 6B if IPHI(I) is not equal to 1.

Card 6B FORMAT (2F10.0)

Column	Variable	Description
1-10	PHI(I)	Friction angle (degrees) for plane I.
11-20	COHESN(I)	Cohesion value for plane I (units must be compatible with area units).

Skip cards 6C and 6D if IPHI(I) is not equal to 2.

Card 6C FORMAT (I5)

Column	Variable	Description
1-5	NSSP	Number of points used to describe shear strength curve for plane I.

Cards 6D FORMAT (2F10.0)

One card for each of NSSP points.

Column	Variable	Description
1-10	SIG(J,I)	Normal stress for shear strength point J, plane I (units must be compatible with area units).
11-20	TAU(J,I)	Shear strength (stress) for point J, plane I (units must be compatible with area units).

Skip card 6E if IPHI(I) is not equal to 3.

Card 6E FORMAT (3F10.0)

Column	Variable	Description
1-10	FJRC(I)	Joint roughness coefficient, JRC, for Barton's shear strength criterion.
11-20	FJCS(I)	Unconfined compressive strength of joint wall rock, JCS, for Barton's shear strength criterion.
21-30	PHI(I)	Residual friction angle (degrees) of joint for Barton's shear strength criterion.

Skip card 6F if IPHI(I) is not equal to 4.

Card 6F FORMAT (3F10.0)

Column	Variable	Description
1-10	PHI(I)	Friction angle (degrees) of asperities for Ladanyi and Archambault's shear strength criterion.
11-20	FJCS(I)	Compressive strength of joint wall rock for Ladanyi and Archambault's shear strength criterion.
21-30	FIA(I)	"i" angle (degrees) of asperities for Ladanyi and Archambault's shear strength criterion.

Skip card 6G if IPHI(I) is not equal to 5.

Card 6G FORMAT (4F10.0)

Column	Variable	Description
1-10	FJRC(I)	Thickness of filled joint for Ladanyi and Archambault's shear strength criteria.
11-20	AM(I)	Amplitude of roughness of filled joint for Ladanyi and Archambault's shear strength criteria.
21-30	COHESN(I)	Undrained cohesion of infilling material for Ladanyi and Archambault's shear strength criteria.
31-40	PHIU(I)	Undrained friction angle (degrees) of infilling material for Ladanyi and Archambault's shear strength criteria.

Skip card 6H if IPHI(I) is not equal to 6.

Card 6H FORMAT (3F10.0)

Column	Variable	Description
1-10	COHESN(I)	Cohesion of asperities for Jaeger's criterion.
11-20	PHI(I)	Residual friction angle (degrees) of wall rock for Jaeger's criterion.
21-30	AM(I)	Exponent b for Jaeger's criterion (positive value).

Skip card 7 if IVEL(I) is not equal to 1.

Card 7 FORMAT (2F10.0)

Column	Variable	Description
1-10	CRITV(I)	Critical velocity. No change in shear strength occurs below this relative velocity.
11-20	SLOG(I)	Slope of line defining change in shear strength with increasing velocity, defined as (change from static strength)/($\log_{10}$ velocity).

The input for plane description cards must end with 20 in columns 4 and 5.

Card 8 FORMAT (20I1).

Enter a 1 in each column corresponding to the plane identification number of any plane that can contribute no resistance to sliding.

Another problem may be started here. Otherwise terminate the run with a blank card.

Input for PROGRAM RIGID from TAPE4

TAPE4 is used to supply time-varying forces and ground accelerations for response history dynamic analyses.

Card 1 FORMAT (2I5)

Column	Variable	Description
1-5	NTS4	Number of time steps with forces and accelerations on TAPE4 (It is recommended that each time step be less than or equal to about 0.02 second).
6-10	IB	Block identification number.

Card(s) 2 FORMAT (7E14.6) Need NTS4 cards

Column	Variable	Description
1-14	TIME	Time during the earthquake.
15-28	FX	x-direction force at time TIME.
29-42	FY	y-direction force at time TIME.
43-56	FZ	z-direction force at time TIME.
57-70	AX	x-direction ground acceleration at time TIME.
71-84	AY	y-direction ground acceleration at time TIME.
85-98	AZ	z-direction ground acceleration at time TIME.

Files used by PROGRAM RIGID

TAPE4 - File containing time-varying forces and ground accelerations representing earthquake loading.

TAPE5 - File containing program input.

TAPE6 - Printer formatted ouput file.

TAPE7 - Formatted output file containing information that can be used for plotting. Consult listing of SUBROUTINE SRBFS for further details.

PROGRAM RIGID was developed on a CDC CYBER/170 computer and is written in FORTRAN. Modifications may be required to run the program on other machines. The program can be run in time-share or batch modes using the NOS operating system.

THE FOLLOWING IS AN EXAMPLE OF A CCL (CYBER CONTROL LANGUAGE) PROCEDURE FILE THAT MAY BE USED TO RUN PROGRAM RIGID. THE PROCEDURE FILE IS STORED UNDER THE NAME PRORIG ON A PERMANENT FILE.

```
.PROC,PRORIG2,INPUT,ABC,TAPE4,TAPE7.
HEADING,ABC.  NAME
HEADING,ABC.  RIGID
GET,RIGID/UN=ERO2219.
GET,INPUT,TAPE4/NA.
FTN,I=RIGID,B=RIGBIN,L=O.
RIGBIN,INPUT,ABC,TAPE4,TAPE7.
REPLACE,TAPE7/NA.
REWIND,ABC.
REPLACE,ABC.
ROUTE,ABC,DC=LP.
RETURN,RIGID,RIGBIN,INPUT,TAPE4.
DAYFILE,OP=I.
REVERT.OK
EXIT.
REWIND,ABC.
REPLACE,ABC.
ROUTE,ABC,DC=LP.
DAYFILE,OP=I.
REVERT.ERROR
```

TO RUN THE PROGRAM TYPE:

```
BEGIN,PRORIG,PRORIG,PFNI,PFNO,PFN4,PFN7
```

WHERE PFNI IS THE NAME OF THE PERMANENT FILE CONTAINING THE TAPE5 INPUT,PFNO IS THE NAME OF A PERMANENT FILE WHERE THE OUTPUT IS TO BE SAVED, PFN4 IS THE NAME OF THE PERMANENT FILE CONTAINING THE TAPE4 INPUT IF ANY, AND PFN7 IS A PERMANENT FILE WHERE THE INFORMATION FOR PLOTTING IS TO BE SAVED, IF ANY.

B. PROGRAM LISTING

```
      PROGRAM RIGID
     +(INPUT,OUTPUT,TAPE4,TAPE7,TAPE5=INPUT,TAPE6=OUTPUT)
C
C     COMPUTES THE FACTOR OF SAFETY AGAINST MOVEMENT OF A RIGID BLOCK
C
C
      COMMON   NPL, IOC(30) ,JOB(5),IPROBN,DATE,IBLOCK,IPAGE,XAXIS
      COMMON /FOUR/ WT,BMASS,QX,QY,QZ,TPHIC,CC,FXU,FYU,FZU
      COMMON /SIX/ FSM1,FACTOS,TIMM1,TIME,IFLAG3,ZCS(3)
C
C     COMMENCE BY READING IN HEADING AND CONTROL DATA
C
      REWIND 4
  100 READ(5,1020)(JOB(I),I=1,5), IBLOCK,IPROBN
      IF(EOF(5)) 150,110
  110 IF(IPROBN.EQ.0) GO TO 150
      READ(5,1030)(IOC(I),I=1,30)
C
C     CONTINUE BY HEADING THE FIRST PAGE
C
      CALL UDATE(DATE)
      CALL DPAGE(0 )
      IF(IOC(2).EQ.1)CALL DPAGE(2)
      IF(IOC(2).EQ.1)WRITE(6,1000)
      IF(IOC(3).EQ.1)CALL DPAGE(2)
      IF(IOC(3).EQ.1)WRITE(6,1010)
      READ(5,1040)WT,BMASS,QX,QY,QZ
      CALL DPAGE(7)
      WRITE (6,1050)IOC(1),WT,BMASS,QX,QY,QZ
      READ(5,1060)CC,TPHIC
      IF(CC.EQ.0.0.AND.TPHIC.EQ.0.0)GO TO 120
      CALL DPAGE(2)
      WRITE(6,1070)CC,TPHIC
  120 IF(IOC(1).EQ.0)NTS4=1
      IF(IOC(1).EQ.0)GO TO 130
      READ(4,1080)NTS4,IB
      CALL DPAGE(3)
      WRITE(6,1090)NTS4,IB
  130 CONTINUE
C
C
```

```
      CALL DPAGE(4)
      WRITE(6,1210) XAXIS
C
C     CONTINUE READING INPUT WITH PLANE DESCRIPTION
C
      NPL=0
      CALL DPAGE(3)
      WRITE(6,1000)
  100 READ(5,1200) I, STRIKE(I), DIP(I),IPHI(I),UP(I),AREA(I),
     +AREAC(I),PHIR(I),IVEL(I)
      IF(I.EQ.20)GO TO 200
      CALL DPAGE(1)
      WRITE(6,1010)I,STRIKE(I),DIP(I),IPHI(I),UP(I),AREA(I),
     +AREAC(I)
      GO TO (110,120,140,150,150,160)IPHI(I)
  110 READ(5,1020)PHI(I),COHESN(I)
      CALL DPAGE(1)
      WRITE(6,1030)PHI(I),COHESN(I)
      PHI(I)=PHI(I)*0.017453295
      GO TO 170
  120 READ(5,1040)NSSP
      DO 130 J=1,NSSP
        READ(5,1020)SIG(J,I),TAU(J,I)
        CALL DPAGE(1)
        WRITE(6,1050)SIG(J,I),TAU(J,I)
  130 CONTINUE
      GO TO 170
  140 READ(5,1060)FJRC(I),FJCS(I),PHI(I)
      CALL DPAGE(4)
      WRITE(6,1070)FJRC(I),FJCS(I),PHI(I)
      GO TO 170
  150 READ(5,1080)PHI(I),FJCS(I),FIA(I)
      CALL DPAGE(4)
      WRITE(6,1090)PHI(I),FJCS(I),FIA(I)
      PHI(I)=PHI(I)*0.0174532925
      FIA(I)=FIA(I)*0.0174532925
      IF(IPHI(I).EQ.4)GO TO 170
      READ(5,1100)FJRC(I),AM(I),COHESN(I),PHIU(I)
      CALL DPAGE(5)
      WRITE(6,1120)FJRC(I),AM(I),COHESN(I),PHIU(I)
      PHIU(I)=PHIU(I)*0.0174532925
      GO TO 170
  160 READ(5,1080)COHESN(I),PHI(I),AM(I)
      CALL DPAGE(4)
```

```
      WRITE(6,1110)COHESN(I),PHI(I),AM(I)
      PHI(I)=PHI(I)*0.0174532925
  170 CONTINUE
      IF(PHIR(I).NE.0.)CALL DPAGE(2)
      IF(PHIR(I).NE.0.)WRITE(6,1130)PHIR(I)
      PHIR(I)=PHIR(I)*0.0174532925
      IF(IVEL(I).EQ.0)GO TO 180
      CALL DPAGE(2)
      WRITE(6,1140)
      READ(5,1160)CRITV(I),SLOG(I)
      CALL DPAGE(2)
      WRITE(6,1170)CRITV(I),SLOG(I)
  180 NPL=NPL+1
C
C     COMPUTE DIR COSINES OF STRIKE AND DIP
C
      T=(STRIKE(I)-XAXIS)*.0174532925
      Q=DIP(I)*.0174532925
      DCOSS(I,1)=COS(T)
      DCOSS(I,2)=SIN(T)
      DCOSS(I,3)=0.0
      Q1=COS(Q)
      DCOSD(I,1)=-DCOSS(I,2)*Q1
      DCOSD(I,2)=DCOSS(I,1)*Q1
      DCOSD(I,3)=SIN(Q)
C
C     COMPUTE DIR COSINES OF NORMAL
C
      DCOSN(1)=DCOSS(I,2)*DCOSD(I,3)-DCOSD(I,2)*DCOSS(I,3)
      DCOSN(2)=DCOSS(I,3)*DCOSD(I,1)-DCOSD(I,3)*DCOSS(I,1)
      DCOSN(3)=DCOSS(I,1)*DCOSD(I,2)-DCOSD(I,1)*DCOSS(I,2)
      ZZ=SQRT(DCOSN(1)**2+DCOSN(2)**2+DCOSN(3)**2)
      DO 190 J=1,3
        DCOSN(J)=DCOSN(J)/ZZ
  190 DIS(I,J)=DCOSN(J)
      IF(IOC(2).EQ.1)CALL DPAGE(5)
      IF(IOC(2).EQ.1)WRITE(6,1220)I,(DCOSS(I,J),J=1,3),
     +(DCOSD(I,J),J=1,3),(DIS(I,J),J=1,3)
      GO TO 100
  200 CONTINUE
C
C     COMMENCE BY INITIALIZING
C
      READ( 5,1150) (IFREFC(J),J=1,20)
```

```
C
C
C     COLLECT COMPONENTS OF WATER FORCE AND STORE INTO FXU,FYU,FZU
C
      FXU=0.
      FYU=0.
      FZU=0.
      DO 210 I =1,NPL
        FXU  =  DIS(I,1) * UP(I) + FXU
        FYU =  DIS(I,2) * UP(I)+FYU
        FZU=DIS(I,3) * UP(I) +FZU
  210 CONTINUE
      CALL DPAGE(5)
      WRITE(6,1180)FXU,FYU,FZU
      V=0.
      RETURN
C
C     FORMATS
C
 1000 FORMAT(1H0,* PLANE   STRIKE      DIP      CODE*,
     +        *    WATER FORCE    AREA     CONC. AREA*,
     +        *                  SHEAR STRENGTH*/)
 1010 FORMAT(1X,I5,2F10.1,3X,I5,5X,E10.4,2X,E10.4,2X,E10.4)
 1020 FORMAT(2F10.0)
 1030 FORMAT(1H ,75X,*PHI =*,F10.2,5X,*COHESION =*,F10.2)
 1040 FORMAT(I5)
 1050 FORMAT(1H ,75X,*NORMAL STRESS *,F10.2,5X,*SHEAR STRENGTH *,F10.2)
 1060 FORMAT(3F10.0)
 1070 FORMAT(1H ,75X*BARTON'S SHEAR STRENGTH PARAMETERS*/
     +        76X,*JRC =*,F10.2/76X,*JCS =*,F10.2/76X,*PHI =*,F10.2)
 1080 FORMAT(3F10.0)
 1090 FORMAT(1H ,75X,*LADANYI AND ARCHAMBAULT'S PARAMETERS*,
     +        * (CLEAN JOINTS)*/
     +        76X,*PHI =*,F10.2/76X,*WALL COMPR. STRENGTH =*F10.2/
     +        76X,*ROUGHNESS ANGLE =*,F10.2)
 1100 FORMAT(4F10.0)
 1110 FORMAT(76X,*JAEGER'S SHEAR STRENGTH CRITERIA*/
     +        76X,*COHESION =*,F10.2/76X,*PHI =*,F10.2/
     +        76X,*EXPONENT =*,F10.2)
 1120 FORMAT(1H ,75X,*ADDITIONAL PARAMETERS FOR FILLED JOINTS*/
     +        76X,*INFILLING THICKNESS =*,F10.2/
     +        76X,*WALL ROCK AMPLITUDE =*,F10.2/
     +        76X,*INFILLING COHESION (UNDRAINED) =*,F10.2/
     +        76X,*INFILLING PHI (UNDRAINED) =*,F10.2)
```

```
 1130 FORMAT(76X,*RESIDUAL PHI =*,F10.2,* WILL BE*/
     +        77X,* USED ONCE MOVEMENT INITIATES*)
 1140 FORMAT(76X,*EFFECTS OF VELOCITY ON SHEAR STRENGTH WILL*/
     +        77X,* BE CONSIDERED FOR PERM. DISPLACEMENTS*)
 1150 FORMAT(20I1)
 1160 FORMAT(2F10.0)
 1170 FORMAT(76X,*CRITICAL VELOCITY =*,F8.4/
     +        76X,*CHANGE IN STRENGTH/LOG VELOCITY =*,F8.4)
 1180 FORMAT(// 2X,    12HWATER FORCES, 10X,2H X, 10X,2H Y, 10X,2H Z//
     +        21X,E10.4,2(2X,E10.4))
 1190 FORMAT( F5.1)
 1200 FORMAT(I5,2F10.0,I5,4F10.0,I5)
 1210 FORMAT( / 2X,   30HAZIMUTH FROM NORTH TO X-AXIS =, F5.1, // )
 1220 FORMAT(*  UNIT VECTOR DIRECTION COSINES FOR PLANE*,I5/
     +        *     STRIKE - X,Y,Z *,3E11.4/
     +        *     DIP - X,Y,Z *,3E11.4/
     +        *     NORMAL - X,Y,Z *,3E11.4/)
      END
      SUBROUTINE SRBFS
C
C     COMPUTES FACTOR OF SAFETY AGAINST SLIDING
C
C
      COMMON   NPL, IOC(30) ,JOB(5),IPROBN,DATE,IBLOCK,IPAGE,XAXIS
      COMMON /ONE/ STRIKE(20),DIP(20),
     +DIS(20,4),DCOSS(20,3),DCOSD(20,3),
     +DCOSN(3)
      COMMON /TWO/   A(3,3)
      COMMON /THREE/  TT(5),QQ(5),ZZ(5)
      COMMON /FOUR/ WT,BMASS,QX,QY,QZ,TPHIC,CC,FXU,FYU,FZU
      COMMON /FIVE/  PHI(20), COHESN(20), Z(3) , IFREFC(20),AREA(20),
     +IPHI(20),SIG(20,20),TAU(20,20),UP(20),AREAC(20),FJRC(20),
     +FJCS(20),FIA(20),AM(20),PHIU(20),PHIR(20),
     +IVEL(20),CRITV(20),SLOG(20),V
      COMMON /SIX/ FSM1,FACTOS,TIMM1,TIME,IFLAG3,ZCS(3)
C
      IF(IOC(2).EQ.1)CALL DPAGE(5)
      IF(IOC(2).EQ.1)WRITE(6,1090)
      FX=AX=0.
      FY=AY=0.
      FZ=AZ=0.
      TIME=0.
      IF(IOC(1).EQ.0)GO TO 100
C
```

```
C      COMPONENTS OF ALL TIME VARYING FORCES ARE READ IN HERE
C
       READ(4,1000) TIME,FX,FY,FZ,AX,AY,AZ
C
  100  FX=FXU+QX+FX-AX*BMASS
       FY=FYU+QY+FY-AY*BMASS
       FZ=FZU+QZ+WT+FZ-AZ*BMASS
       FXYZ=SQRT(FX**2+FY**2+FZ**2)
       IFLAG1 =0
       IFLAG2=0
       DO 170 I = 1,NPL
         IF(IFREFC(I).EQ.1) GO TO 170
         DO 110  J=1,3
           A(1,J) = DCOSS(I,J)
           A(2,J) = DCOSD(I,J)
  110    A(3,J) = DIS(I,J )
         DO 120  J=1,3
  120    TT(J)=-A(J,1)*FX - A(J,2)*FY- A(J,3)*FZ
         IF(IOC(2).EQ.1)CALL DPAGE(5)
         IF(IOC(2).EQ.1)WRITE(6,1150) I,TT(1),TT(2),TT(3)
         IF(TT(3).GT.O.)GO TO 130
         IF(IOC(2).EQ.1)CALL DPAGE(1)
         IF(IOC(2).EQ.1)WRITE(6,1110) I
         GO TO 170
  130    TTT = SQRT(TT(1)**2+TT(2)**2)
         IFLAG1=1
         IF(IOC(2).EQ.1)CALL DPAGE(2)
         IF(IOC(2).EQ.1)WRITE(6,1160) TTT
         IF(TTT.GT.O.) GO TO 140
         IF(IOC(2).EQ.1)CALL DPAGE(2)
         IF(IOC(2).EQ.1)WRITE(6,1140) I
         GO TO 170
  140    D1 = TT(2)/TTT
         DO  = TT(1)/TTT
         Z(1) = (A(1,1)*DO + A(2,1)*D1) * TTT
         Z(2) = (A(1,2)*DO + A(2,2)*D1) * TTT
         Z(3) = (A(1,3)*DO + A(2,3)*D1) * TTT
         IF(IOC(2).EQ.1)CALL DPAGE(2)
         IF(IOC(2).EQ.1)WRITE(6,1170)I,(Z(K),K=1,3)
         ZCS(1)=-Z(1)/TTT
         ZCS(2)=-Z(2)/TTT
         ZCS(3)=-Z(3)/TTT
         CALL MOVE(EZ)
         IF(EZ.NE.O.) GO TO 170
```

```
      AA = 1.5707963
      IF(DO.EQ.O.) GO TO 150
      AA = ATAN(ABS(D1/DO))
      IF(DO.GT.O.) GO TO 150
      AA = 3.1415927 - AA
 150  IF(D1.GT.O.) GO TO 160
      AA = -AA
 160  AA =  AA * 57.2958
C
C     COMPUTE FACTOR OF SAFETY FOR ONE PLANE
C
      IFLAG2=1
      CALL RESFRC(I,TT(3),RESIST)
      IF(IOC(2).EQ.1)CALL DPAGE(2)
      IF(IOC(2).EQ.1)WRITE(6,1010)I,RESIST,TTT
      FACTOS=ABS(RESIST/TTT)
      CALL DPAGE(3)
      WRITE(6,1100)TIME,FX,FY,FZ
      WRITE(6,1120)FACTOS,I,TT(3),TTT,AA
      WRITE(7,1020)TIME,FACTOS,I,FX,FY,FZ
      IF(IOC(1).EQ.O.OR.IOC(3).EQ.O)GO TO 170
      IF(FACTOS.LT.1.O.OR.IFLAG3.EQ.1)CALL DYNMOVE(TTT,RESIST)
      TIMM1=TIME
      FSM1=FACTOS
 170 CONTINUE
    IF(IFLAG2.EQ.1)GO TO 230
    IF(IFLAG1.EQ.1)GO TO 190
    CALL DPAGE(3)
    WRITE(6,1100)TIME,FX,FY,FZ
    WRITE(6,1030)
    FACTOS=O.O
    WRITE(7,1040)TIME,FACTOS,FX,FY,FZ
    IF(IOC(1).EQ.O.OR.IOC(3).EQ.O)GO TO 180
    IF(FXYZ.EQ.O.)GO TO 240
    ZCS(1)=FX/FXYZ
    ZCS(2)=FY/FXYZ
    ZCS(3)=FZ/FXYZ
    RESIST=O.
    CALL DYNMOVE(FXYZ,RESIST)
    TIMM1=TIME
    FSM1=FACTOS
 180 GO TO 230
 190 NP=NPL-1
    DO 220 I=1,NP
```

```
      IP1=I+1
      DO 220 K= IP1,NPL
        IF(IFREFC(I).EQ.1) GO TO 220
        IF(IFREFC(K).EQ.1) GO TO 220
        DO 200 J=1,3
          TT(J) = DIS(I,J)
200     QQ(J) = DIS(K,J)
        Z(1) = TT(2)* QQ(3) -QQ(2)* TT(3)
        Z(2) = TT(3)* QQ(1) -QQ(3)* TT(1)
        Z(3) = TT(1)* QQ(2) -QQ(1)* TT(2)
        ZZZ = SQRT(Z(1)**2 + Z(2)**2 +Z(3)**2)
        Z(1)= Z(1)/ZZZ
        Z(2)= Z(2)/ZZZ
        Z(3)= Z(3)/ZZZ
        IF(IOC(2).EQ.1)CALL DPAGE(3)
        IF(IOC(2).EQ.1)WRITE(6,1180)I,K,(Z(L),L=1,3)
        ZCS(1)=Z(1)
        ZCS(2)=Z(2)
        ZCS(3)=Z(3)
        DO 210 J =1,3
          A(J,1) = TT(J)
          A(J,2) = QQ(J)
210     A(J,3) = Z(J)
        CALL MATINV(     3,0,DET,IFLOW)
        F1=A(1,1)*FX +A(1,2)*FY +A(1,3)*FZ
        F1 =- F1
        IF(F1.LT..01) GO TO 220
        F2=A(2,1)*FX +A(2,2)*FY + A(2,3)*FZ
        F2 =- F2
        IF(F2.LT..01) GO TO 220
        F3 = A(3,1)*FX + A(3,2)*FY +  A(3,3)* FZ
        F3 = -F3
        Z(1) = Z(1)*F3
        Z(2) = Z(2)*F3
        Z(3) = Z(3)*F3
        IF(IOC(2).EQ.1)CALL DPAGE(5)
        IF(IOC(2).EQ.1)WRITE(6,1190)I,F1,K,F2,(Z(L),L=1,3)
        F3 = -F3
        CALL  MOVE(EZ)
        IF(EZ.NE.O.) GO TO 220
        IFLAG1=2
C
C       COMPUTE FACTOR OF SAFETY FOR TWO PLANES
C
```

```
          CALL RESFRC(I,F1,F)
          CALL RESFRC(K,F2,FF)
          IF(IOC(2).EQ.1)CALL DPAGE(2)
          IF(IOC(2).EQ.1)WRITE(6,1050)I,F,K,FF,F3
          F=F+FF
          FACTOS =  ABS(F/F3)
          CALL DPAGE(3)
          WRITE(6,1100)TIME,FX,FY,FZ
          WRITE(6,1130)FACTOS,I,F1,K,F2,I,K,F3
          WRITE(7,1060)TIME,FACTOS,I,K,FX,FY,FZ
          IF(IOC(1).EQ.0.OR.IOC(3).EQ.0)GO TO 220
          IF(FACTOS.LT.1.0.OR.IFLAG3.EQ.1)CALL DYNMOVE(F3,F)
          TIMM1=TIME
          FSM1=FACTOS
  220 CONTINUE
      IF(IFLAG1.EQ.2)GO TO 230
      CALL DPAGE(3)
      WRITE(6,1100)TIME,FX,FY,FZ
      WRITE(6,1070)
      FACTOS=99999.
      WRITE(7,1080)TIME,FACTOS,FX,FY,FZ
      IF(IOC(1).EQ.0.OR.IOC(3).EQ.0)GO TO 230
      IF(FXYZ.EQ.0.)GO TO 240
      ZCS(1)=FX/FXYZ
      ZCS(2)=FY/FXYZ
      ZCS(3)=FZ/FXYZ
      DRIVE=0.
      IF(IFLAG3.EQ.1)CALL DYNMOVE(DRIVE,FXYZ)
      TIMM1=TIME
      FSM1=FACTOS
  230 RETURN
  240 CALL DPAGE(2)
      WRITE(6,1200)
      STOP
C
C     FORMATS
C
 1000 FORMAT(7E14.6)
 1010 FORMAT(/10X,* RESISTING*,I3,E14.6,*   DRIVING*,E14.6)
 1020 FORMAT(2F10.2,5H     1,5X,I5,3E10.4)
 1030 FORMAT(1H ,*  ROCK WEDGE IS LIFTED *)
 1040 FORMAT(2F10.2,5H     0,10X,3E10.4)
 1050 FORMAT(/10X,*RESISTING*,I3,E14.6,*   RESISTING*,I3,E14.6,
     +       *   DRIVING*,E14.6)
```

```
1060 FORMAT(2F10.2,5H    2,2I5,3E10.4)
1070 FORMAT(1H ,*  ROCK WEDGE IS STABLE*)
1080 FORMAT(2F10.2,5H   99,10X,3E10.4)
1090 FORMAT( // 2X,  34HBEGIN THE FACTOR OF SAFETY PROGRAM//)
1100 FORMAT(1HO,* TIME =*,F6.2,5X,* TOTAL X,Y,Z FORCES  *,3E10.4)
1110 FORMAT(15X,     8HSURFACE ,I2,2X,  13HIS IN TENSION)
1120 FORMAT(1H *  FACTOR OF SAFETY =*,F7.2,*   PLANE*,I3,*   NORMAL =*,
    +       E10.4,*   SHEAR =*,E10.4,*   ALPHA =*,E10.4)
1130 FORMAT(1H *  FACTOR OF SAFETY =*,F7.2,*   PLANE*,I3,*   NORMAL =*,
    +       E10.4,*   PLANE*,I3,*   NORMAL =*,E10.4,*   I*,2I1,
    +       * SHEAR =*,
    +       E10.4)
1140 FORMAT(15X,     8HSURFACE ,I2,    15H HAS ZERO SHEAR/)
1150 FORMAT(/10X,*COMPONENTS OF FORCE FOR PLANE*,I5/
    +       10X,*PARALLEL TO STRIKE *,E10.4/
    +       10X,*PARALLEL TO DIP *,E10.4/
    +       10X,*NORMAL TO PLANE *,E10.4)
1160 FORMAT(  10X,   19HTHE SHEAR FORCE IS ,F14.0,  /)
1170 FORMAT(10X,*GLOBAL SHEAR FORCE COMPONENTS*/
    +       10X,*PLANE*,I5,*   X,Y,Z *,3E11.4)
1180 FORMAT(/10X,*DIRECTION COSINES OF INTERSECTION*/
    +       10X,*PLANES*,2I5,*   X,Y,Z *,3E11.4)
1190 FORMAT(/10X,*NORMAL FORCE PLANE*,I5,E13.4/
    +       10X,*NORMAL FORCE PLANE*,I5,E13.4/
    +       10X,*GLOBAL INTERSECTION SHEAR FORCE*
    +       /10X,*X,Y,Z *,3E11.4)
1200 FORMAT(/*  STOP - ZERO FORCE ACTING ON BLOCK*)
     END
     SUBROUTINE RESFRC(I,XNORM,RESIST)
     COMMON   NPL, IOC(30) ,JOB(5),IPROBN,DATE,IBLOCK,IPAGE,XAXIS
     COMMON /FOUR/ WT,BMASS,QX,QY,QZ,TPHIC,CC,FXU,FYU,FZU
     COMMON /FIVE/  PHI(20), COHESN(20), Z(3) , IFREFC(20),AREA(20),
    +IPHI(20),SIG(20,20),TAU(20,20),UP(20),AREAC(20),FJRC(20),
    +FJCS(20),FIA(20),AM(20),PHIU(20),PHIR(20),
    +IVEL(20),CRITV(20),SLOG(20),V
     COMMON /SEVEN/ IFLAG4
C
C    COMPUTE RESISTANCE FOR SINGLE PLANE BASED ON SHEAR STRENGTH,
C    AREAS, AND NORMAL FORCE
C
     AREA(I)=AREA(I)-AREAC(I)
     IF(AREA(I).NE.O.)SIGMA=XNORM/(AREA(I)+AREAC(I))
     IF(IFLAG4.NE.1)GO TO 100
     CC=O.
```

```
      IF(PHIR(I).EQ.O.)GO TO 100
      PHI(I)=PHIR(I)
      GO TO 110
  100 GO TO (110,130,160,170,170,190)IPHI(I)
  110 IF(AREAC(I).NE.O.)GO TO 120
      RESIST=AREA(I)*COHESN(I)+TAN(PHI(I))*XNORM
      IF(IVEL(I).NE.1)GO TO 230
      IF(V.LE.CRITV(I))GO TO 230
      CALL RESVEL(RESIST,I)
      GO TO 230
  120 CONTINUE
      TAUR=COHESN(I)+TAN(PHI(I))
      GO TO 200
  130 IF(AREA(I).EQ.O.)GO TO 220
      J=1
  140 IF(SIGMA.GE.SIG(J,I).AND.SIGMA.LE.SIG(J+1,I))GO TO 150
      J=J+1
      IF(J.GT.20)CALL DPAGE(2)
      IF(J.GT.20)WRITE(6,1000)I
      IF(J.GT.20)STOP
      GO TO 140
  150 TAUR=TAU(J,I)+(SIGMA-SIG(J,I))/(SIG(J+1,I)-SIG(J,I))
     +*(TAU(J+1,I)-TAU(J,I))
      GO TO 200
  160 IF(AREA(I).EQ.O.)GO TO 220
      FEI=(FJRC(I)*ALOG10(FJCS(I)/SIGMA)+PHI(I))*O.0174532925
      TAUR=SIGMA*TAN(FEI)
      GO TO 200
  170 IF(AREA(I).EQ.O.)GO TO 220
      TR=FJCS(I)*((SQRT(1.+10.)-1.)/10.)
     +*((1.+10.*SIGMA/FJCS(I))**O.5)
      VDOT=((1.-SIGMA/FJCS(I))**4.)*TAN(FIA(I))
      AS=1.-((1.-SIGMA/FJCS(I))**1.5)
      TAUR=(SIGMA*(1.-AS)*(VDOT+TAN(PHI(I)))+AS*TR)
     +/(1.-(1.-AS)*VDOT*TAN(PHI(I)))
      IF(IPHI(I).EQ.4)GO TO 200
      FM=(1.-2./3.*FJRC(I)/AM(I))**2
      FIA(I)=FIA(I)/O.0174532925
      STRAT=SIGMA/FJCS(I)
      IF(FIA(I).LT.15.O.AND.STRAT.LT.O.1)GO TO 180
      IF(COHESN(I).GT.O.O.AND.FIA(I).GE.15.O.AND.FIA(I).LE.30.O
     +.AND.STRAT.LT.O.5)GO TO 180
      FIA(I)=FIA(I)*O.0174532925
      C=COHESN(I)+SIGMA*TAN(PHIU(I))
```

```
      TAUR=FM*(TAUR-C)+C
      GO TO 200
  180 FIA(I)=FIA(I)*0.0174532925
      FIE=ATAN(FM*TAN(FIA(I)))
      TAUR=COHESN(I)/(1.-TAN(FIE)*TAN(PHIU(I)))
     ++SIGMA*TAN(PHIU(I)+FIE)
      GO TO 200
  190 IF(AREA(I).EQ.O.)GO TO 220
      TAUR=COHESN(I)*(1-EXP(-AM(I)*SIGMA))
     ++SIGMA*TAN(PHI(I))
  200 RESIST=TAUR*AREA(I)
      IF(IVEL(I).NE.1)GO TO 210
      IF(V.LE.CRITV(I))GO TO 210
      CALL RESVEL(RESIST,I)
  210 RESIST=RESIST+(TPHIC*SIGMA+CC)*AREAC(I)
      IF(IOC(2).EQ.1)CALL DPAGE(2)
      IF(IOC(2).EQ.1)WRITE(6,1010)I,SIGMA,TAUR
      GO TO 230
  220 CALL DPAGE(2)
      WRITE(6,1020)
  230 RETURN
 1000 FORMAT(1HO,* STOP -- SHEAR STRENGTH NOT FOUND - PLANE*,I5)
 1010 FORMAT(/10X,*PLANE*,I3,*    NORM. STRESS*,E14.6,
     +       *   SHEAR STRENGTH*,E14.6)
 1020 FORMAT(1HO,* ---ERROR--- ZERO AREA IN SUBROUTINE RESFRC*)
      END
      SUBROUTINE RESVEL(RESIST,I)
      COMMON /FIVE/  PHI(20), COHESN(20), Z(3) , IFREFC(20),AREA(20),
     +IPHI(20),SIG(20,20),TAU(20,20),UP(20),AREAC(20),FJRC(20),
     +FJCS(20),FIA(20),AM(20),PHIU(20),PHIR(20),
     +IVEL(20),CRITV(20),SLOG(20),V
C
C ROUTINE TO ACCOUNT FOR VELOCITY EFFECTS ON SHEAR STRENGTH
C
      IF(V.EQ.O..OR.CRITV(I).EQ.O.)GO TO 10
      RESIST=RESIST*(SLOG(I)*(ALOG10(V)-ALOG10(CRITV(I)))+1.)
      RETURN
   10 CALL DPAGE(2)
      WRITE(6,1000)
      STOP
 1000 FORMAT(/*  STOP - ZERO VELOCITY IN RESVEL*)
      END
      SUBROUTINE MOVE(EZ)
C
```

```
C      SUBROUTINE  TO  CHECK CAPABILITY OF MOVEMENT OF BLOCK
C
       COMMON   NPL, IOC(30) ,JOB(5),IPROBN,DATE,IBLOCK,IPAGE,XAXIS
       COMMON /ONE/ STRIKE(20),DIP(20),
      +DIS(20,4),DCOSS(20,3),DCOSD(20,3),
      +DCOSN(3)
       COMMON /TWO/   A(3,3)
       COMMON /FOUR/ WT,BMASS,QX,QY,QZ,TPHIC,CC,FXU,FYU,FZU
       COMMON /FIVE/  PHI(20), COHESN(20), Z(3) , IFREFC(20),AREA(20),
      +IPHI(20),SIG(20,20),TAU(20,20),UP(20),AREAC(20),FJRC(20),
      +FJCS(20),FIA(20),AM(20),PHIU(20),PHIR(20),
      +IVEL(20),CRITV(20),SLOG(20),V
       DO 100 J = 1,NPL
         IF(IFREFC(J).EQ.1) GO TO 100
         EZ = DIS(J,1)*Z(1)+ DIS(J,2)*Z(2) +DIS(J,3)* Z(3)
         IF(EZ.GT..01) RETURN
  100  CONTINUE
       EZ = 0.
       RETURN
       END
       SUBROUTINE DYNMOVE (DRIVE,RESIST)
       COMMON /FOUR/ WT,BMASS,QX,QY,QZ,TPHIC,CC,FXU,FYU,FZU
       COMMON /FIVE/  PHI(20), COHESN(20), Z(3) , IFREFC(20),AREA(20),
      +IPHI(20),SIG(20,20),TAU(20,20),UP(20),AREAC(20),FJRC(20),
      +FJCS(20),FIA(20),AM(20),PHIU(20),PHIR(20),
      +IVEL(20),CRITV(20),SLOG(20),V
       COMMON /SIX/ FSM1,FACTOS,TIMM1,TIME,IFLAG3,ZCS(3)
       COMMON /SEVEN/ IFLAG4
C
C      COMPUTES CUMULATIVE DISPLACEMENTS FOR DYNAMIC ANALYSES
C
       IFLAG4=1
       IF(IFLAG3.NE.0)GO TO 100
       T1=(1.0-FSM1)*(TIME-TIMM1)/(FACTOS-FSM1)
       TMOVE=TIMM1+T1
       CALL DPAGE(2)
       WRITE(6,1000)TMOVE
       DT=TIME-TMOVE
       AM1=0.
       VM1=0.
       DX=0.
       DY=0.
       DZ=0.
       IFLAG3=1
```

```
      GO TO 110
  100 DT=TIME-TIMM1
      IF(BMASS.EQ.O.)GO TO 150
  110 A=(DRIVE-RESIST)/BMASS
      V=VM1+DT/2.*(AM1+A)
      IF(V.LE.O.)GO TO 130
  120 D=VM1*DT+(2*AM1+A)*DT**2/6.
      AM1=A
      VM1=V
      DXD=D*ZCS(1)
      DYD=D*ZCS(2)
      DZD=D*ZCS(3)
      CALL DPAGE(1)
      WRITE(6,1010)DXD,DYD,DZD
      DX=DX+DXD
      DY=DY+DYD
      DZ=DZ+DZD
      DXYZ=SQRT(DX**2+DY**2+DZ**2)
      IF(IFLAG3.EQ.O)CALL DPAGE(4)
      IF(IFLAG3.EQ.O)WRITE (6,1020)TMOVE,DX,DY,DZ,DXYZ
      RETURN
  130 IF(DT.EQ.O.)GO TO 150
      XNSQ=SQRT(AM1**2-2./DT*(A-AM1)*VM1)
      DENOM=1/DT*(A-AM1)
      IF(DENOM.EQ.O.)GO TO 150
      T2=(-AM1+XNSQ)/DENOM
      IF(T2.GE.O.O.AND.T2.LE.DT)GO TO 140
      T2=(-AM1-XNSQ)/DENOM
      IF(T2.GE.O.O.AND.T2.LE.DT)GO TO 140
      CALL DPAGE(1)
      WRITE(6,1030)
      STOP
  140 IFLAG3=O
      A=AM1+(A-AM1)*T2/DT
      DT=T2
      TMOVE=TIMM1+T2
      V=O.
      GO TO 120
  150 CALL DPAGE(2)
      WRITE(6,1040)
      STOP
 1000 FORMAT(/*  MOVEMENT STARTS AT TIME*,F10.3)
 1010 FORMAT(*  INCREMENTAL X,Y,Z.MOVEMENTS FOR TIME STEP *,3E10.4)
 1020 FORMAT(/*  MOVEMENT STOPS AT TIME *F10.3/
```

```
     +         *  TOTAL X,Y,Z COMPONENTS OF MOVEMENT *,3E10.4/
     +         *  TOTAL MOVEMENT FOR THIS CYCLE *,E10.4)
 1030 FORMAT(*  STOP - TIME OF ZERO VELOCITY NOT FOUND*)
 1040 FORMAT(/*  STOP - ZERO DENOMINATOR IN DYNMOVE*)
      END
      SUBROUTINE MATINV(N,M, DETERM, IFLOW)
C
      COMMON /TWO/   A(3,3)
      DIMENSION IPIVOT( 20),B(20,1) , INDEX( 20,2)
C
C     ROUTINE TO INVERT A MATRIX
C
C     INITIALIZATION
C
      IFLOW=0
      DETERM=1.0
      DO 100 J=1,N
  100 IPIVOT(J)=0
      DO 300 I=1,N
C
C       SEARCH FOR PIVOT ELEMENT
C
        AMAX=0.0
        DO 150 J=1,N
          IF (IPIVOT(J)-1) 110, 150, 110
  110     DO 140 K=1,N
            IF(IPIVOT(K)-1) 120, 140, 350
  120       IF (ABS(AMAX)-ABS(A(J,K)))  130,  130, 140
  130       IROW=J
            ICOLUM=K
            AMAX=A(J,K)
  140     CONTINUE
  150   CONTINUE
        IPIVOT(ICOLUM)=IPIVOT(ICOLUM)+1
C
C       INTERCHANGE ROWS TO PUT PIVOT ELEMENT ON DIAGONAL
C
        IF (IROW-ICOLUM) 160, 200, 160
  160   DETERM=-DETERM
        DO 170 L=1,N
          SWAP=A(IROW,L)
          A(IROW,L)=A(ICOLUM,L)
  170   A(ICOLUM,L)=SWAP
        IF(M) 200, 200, 180
```

```
  180   DO 190 L=1, M
          SWAP=B(IROW,L)
          B(IROW,L)=B(ICOLUM,L)
  190   B(ICOLUM,L)=SWAP
  200   INDEX(I,1)=IROW
        INDEX(I,2)=ICOLUM
        PIVOT    =A(ICOLUM,ICOLUM)
        DETERM=DETERM*PIVOT
        IF(ABS(DETERM).GT.1.0E-50 ) GO TO 210
        CALL DPAGE(1)
        WRITE(6,1000) DETERM, I
        DETERM = 1.0
        IF(DETERM.EQ.0.) GO TO 360
C
C       DIVIDE PIVOT ROW BY PIVOT ELEMENT
C
  210   A(ICOLUM,ICOLUM)=1.0
        DO 220 L=1,N
  220   A (ICOLUM,L)=A (ICOLUM,L)/PIVOT
        IF(M) 250, 250, 230
  230   DO 240 L=1,M
  240   B(ICOLUM,L)=B(ICOLUM,L)/PIVOT
C
C       REDUCE NON-PIVOT ROWS
C
  250   DO 300 L1=1,N
          IF(L1-ICOLUM) 260, 300, 260
  260     T=A(L1,ICOLUM)
          A(L1,ICOLUM)=0.0
          DO 270 L=1,N
  270     A(L1,L)=A(L1,L)-A(ICOLUM,L)*T
          IF(M) 300, 300, 280
  280     DO 290 L=1,M
  290     B(L1,L)=B(L1,L)-B(ICOLUM,L)*T
  300 CONTINUE
C
C     INTERCHANGE COLUMNS
C
      DO 330 I=1,N
        L=N+1-I
        IF (INDEX(L,1)-INDEX(L,2)) 310, 330, 310
  310   JROW=INDEX(L,1)
        JCOLUM=INDEX(L,2)
        DO 320 K=1,N
```

```
          SWAP=A(K,JROW)
          A(K,JROW)=A(K,JCOLUM)
          A(K,JCOLUM)=SWAP
  320   CONTINUE
  330 CONTINUE
      IFLOW=0
  340 RETURN
  350 IFLOW=2
      GO TO 340
  360 IFLOW=1
      GO TO 340
 1000 FORMAT(2X,16HTHE DETERMINANT=,E16.8,  7H AT THE, I4,  6H ROUND)
      END
      SUBROUTINE DPAGE(IZ)
      COMMON   NPL, IOC(30) ,JOB(5),IPROBN,DATE,IBLOCK,IPAGE,XAXIS
      DATA( MAXLCT=55)
C
C     ROUTINE TO NUMBER AND FORMAT PAGES
C
      IX= IZ
      IF(IX) 130, 100, 120
  100 IPAGE= 0
  110 IPAGE= IPAGE + 1
      LNCT= IX
      WRITE(6,1000) IPROBN,IBLOCK,IPAGE,(JOB(I),I=1,5), DATE
      RETURN
  120 LNCT= LNCT + IX
      IF(LNCT.LE.MAXLCT) RETURN
      GO TO 110
  130 IX= -IX
      IF(IX.EQ.1) IX=0
      IF(LNCT.NE.0) GO TO 110
      LNCT= IX
      RETURN
C
C     FORMATS
C
 1000 FORMAT(1H1/ 56X, 20HRIGID BLOCK ANALYSIS,37X,14HPROBLEM NUMBER,I5
     +       /51X,24H FOR RIGID BLOCK NUMBER ,
     +       A5,43X,4HPAGE,I5,
     +       /1X,11HJOB TITLE -,1X,5A10,55X, 4HDATE,1X,A9 ///)
      END
      SUBROUTINE UDATE(IATE)
C
```

```
C      ROUTINE TO EXTRACT DATE
C
       INTEGER DATE
       IATE =  DATE(I)
       RETURN
       END
```

C. EXAMPLE PROBLEM

THE FOLLOWING IS AN EXAMPLE TAPE5 INPUT FILE FOR A DYNAMIC ANALYSIS OF THE EXAMPLE PROBLEM DESCRIBED IN CHAPTER V, INCLUDING CALCULATION OF PERMANENT CUMULATIVE DISPLACEMENTS AND VELOCITY EFFECTS ON SHEAR STRENGTH (NOTE: ENGLISH UNITS ARE USED HERE - LB,IN).

```
COLUMN
12345678901234567890123456789012345678901234567890123456789012345678901234567890

BLOCK H STABILITY - AUBURN ARCH - POWERPLANT AREA          1     1
101
  2.55E+08  6.60E+05 -1.29E+08  1.10E+09  1.88E+09
       O.        O.
 66.5
    1      237.        90.     1  5.06E+07  1.71E+05        O.        O.    O
      45.        O.
    2      150.        90.     2  4.53E+07  1.25E+06        O.        O.    O
    7
       O.        O.
      50.       52.
     100.       93.
     150.      125.
     250.      171.
     500.      235.
    1000.      369.
    3      237.       172.     3  3.61E+08  7.16E+06        O.        O.    1
      15.    12500.       30.
   O.0118     O.119
    4       58.        90.     1        O.        O.        O.        O.    O
       O.        O.
    5      325.        90.     2  2.12E+07  8.57E+05        O.        O.    O
    7
       O.        O.
      50.       52.
     100.       93.
     150.      125.
     250.      171.
     500.      235.
    1000.      369.
    6        O.        O.      1        O.        O.        O.        O.    O
       O.        O.
   20
  1 1
```

THE FOLLOWING IS A PORTION OF THE INPUT FROM TAPE4 FOR THE
EXAMPLE PROBLEM DESCRIBED IN CHAPTER V (ENGLISH UNITS - LB,IN)

```
COLUMN
12345678901234567890123456789012345678901234567890123456789012345678901234567890123456789012345678901234567890

  999     1
  .100000E-01  0.            0.            0.            0.            0.            0.
  .200000E-01  0.            0.            0.            0.            0.            0.
  .300000E-01  0.            0.            0.            0.            0.            0.
  .400000E-01  -.220398E+03  .875073E+03   .282737E+03   0.            -.386040E-01  0.
  .500000E-01  -.174391E+04  .693781E+04   .222211E+04   0.            -.772080E-01  0.
  .600000E-01  -.651046E+04  .225782E+05   .871484E+04   .386040E-01   -.772080E-01  -.386040E-01
  .700000E-01  -.188582E+05  .492888E+05   .246626E+05   .772080E-01   -.772080E-01  -.888178E-15
  .800000E-01  -.423596E+05  .837678E+05   .416803E+05   .154416E+00   -.621725E-14  .386040E-01
  .900000E-01  -.801647E+05  .114505E+06   .457821E+05   .193020E+00   .115812E+00   .772080E-01
  .100000E+00  -.130543E+06  .124082E+06   .236819E+05   .193020E+00   .270228E+00   .772080E-01
  .110000E+00  -.185298E+06  .935805E+05   -.320290E+05  .772080E-01   .347436E+00   .115812E+00
  .120000E+00  -.225255E+06  .687799E+04   -.130984E+06  -.115812E+00  .540456E+00   .154416E+00
  .130000E+00  -.221903E+06  -.159881E+06  -.279941E+06  -.308832E+00  .772080E+00   .772080E-01
  .140000E+00  -.148849E+06  -.426520E+06  -.465962E+06  -.501852E+00  .849288E+00   .772080E-01
  .150000E+00  .133587E+05   -.792214E+06  -.673001E+06  -.694872E+00  .772080E+00   .199840E-13
  .160000E+00  .278699E+06   -.123948E+07  -.864857E+06  -.100370E+01  .100370E+01   -.193020E+00
  .170000E+00  .671510E+06   -.177342E+07  -.993820E+06  -.131254E+01  .135114E+01   -.347436E+00
  .180000E+00  .121418E+07   -.240699E+07  -.102399E+07  -.146695E+01  .138974E+01   -.424644E+00
  .190000E+00  .190205E+07   -.312179E+07  -.921375E+06  -.142835E+01  .142835E+01   -.694872E+00
  .200000E+00  .270401E+07   -.388748E+07  -.634189E+06  -.135114E+01  .165997E+01   -.772080E+00
  .210000E+00  .358492E+07   -.468456E+07  -.160550E+06  -.123533E+01  .138974E+01   -.540456E+00
  .220000E+00  .449173E+07   -.544821E+07  .449130E+06   -.810684E+00  .540456E+00   -.308832E+00
  .230000E+00  .532577E+07   -.605097E+07  .114564E+07   -.386040E-01  -.308832E+00  -.140332E-12
  .240000E+00  .595115E+07   -.636121E+07  .185731E+07   .115812E+01   -.111952E+01  .579060E+00
  .250000E+00  .620435E+07   -.626612E+07  .246655E+07   .250926E+01   -.200741E+01  .108091E+01
  .260000E+00  .592707E+07   -.567701E+07  .287909E+07   .339715E+01   -.227764E+01  .115812E+01
  .270000E+00  .504111E+07   -.460531E+07  .305213E+07   .370598E+01   -.146695E+01  .135114E+01
  .280000E+00  .357626E+07   -.320615E+07  .290974E+07   .393761E+01   -.656268E+00  .154416E+01
  .290000E+00  .159808E+07   -.165673E+07  .240675E+07   .416923E+01   -.347436E+00  .115812E+01
  .300000E+00  -.814378E+06  -.812922E+05  .162817E+07   .339715E+01   .193020E+00   .810684E+00
  .310000E+00  -.346132E+07  .136990E+07   .659392E+06   .127393E+01   .772080E+00   .887892E+00
  .320000E+00  -.599308E+07  .253113E+07   -.466119E+06  -.165997E+01  .617664E+00   .424644E+00
  .330000E+00  -.800858E+07  .332103E+07   -.159404E+07  -.459388E+01  .501852E+00   -.540456E+00
  .340000E+00  -.914414E+07  .368421E+07   -.248916E+07  -.656268E+01  .146695E+01   -.965100E+00
  .350000E+00  -.915999E+07  .352094E+07   -.301710E+07  -.679430E+01  .154416E+01   -.154416E+01
  .360000E+00  -.807507E+07  .291707E+07   -.297906E+07  -.586781E+01  -.104231E+01  -.281809E+01
  .370000E+00  -.615736E+07  .229303E+07   -.203606E+07  -.451667E+01  -.432365E+01  -.285670E+01
```

.962000E+01	-.899928E+08	.771567E+08	-.264950E+09	.241661E+02	-.143221E+02	-.234712E+02
.963000E+01	-.106471E+09	.864493E+08	-.267716E+09	.156346E+02	-.226219E+02	-.299181E+02
.964000E+01	-.125084E+09	.102044E+09	-.254466E+09	.606083E+01	-.243591E+02	-.308060E+02
.965000E+01	-.143909E+09	.122757E+09	-.226253E+09	-.374459E+01	-.177192E+02	-.291846E+02
.966000E+01	-.160629E+09	.146090E+09	-.185905E+09	-.123147E+02	-.116970E+02	-.269070E+02
.967000E+01	-.173016E+09	.169383E+09	-.137254E+09	-.209234E+02	-.125463E+02	-.191090E+02
.968000E+01	-.179032E+09	.190453E+09	-.853479E+08	-.299567E+02	-.131254E+02	-.849288E+01
.969000E+01	-.176913E+09	.207279E+09	-.357415E+08	-.338171E+02	-.123919E+02	-.208462E+01
.970000E+01	-.165848E+09	.218350E+09	.700163E+07	-.305358E+02	-.192634E+02	.409202E+01
.971000E+01	-.146276E+09	.223370E+09	.392271E+08	-.265596E+02	-.296479E+02	.133570E+02
.972000E+01	-.119172E+09	.222687E+09	.577352E+08	-.247838E+02	-.331608E+02	.184913E+02
.973000E+01	-.856299E+08	.216517E+09	.607727E+08	-.214252E+02	-.359017E+02	.184527E+02
.974000E+01	-.472287E+08	.205522E+09	.485000E+08	-.164067E+02	-.450123E+02	.189546E+02
.975000E+01	-.606809E+07	.191230E+09	.223133E+08	-.121989E+02	-.512661E+02	.164067E+02
.976000E+01	.356103E+08	.175248E+09	-.150109E+08	-.652408E+01	-.508029E+02	.737336E+01
.977000E+01	.753678E+08	.158945E+09	-.591787E+08	.320413E+01	-.528489E+02	-.694872E+00
.978000E+01	.110407E+09	.143938E+09	-.105626E+09	.149784E+02	-.554353E+02	-.613804E+01
.979000E+01	.137957E+09	.131692E+09	-.150240E+09	.258647E+02	-.475601E+02	-.141677E+02
.980000E+01	.155877E+09	.122559E+09	-.189281E+09	.334311E+02	-.342804E+02	-.193406E+02
.981000E+01	.163001E+09	.116049E+09	-.220365E+09	.357859E+02	-.275247E+02	-.164839E+02
.982000E+01	.159123E+09	.111826E+09	-.242952E+09	.345506E+02	-.243591E+02	-.138202E+02
.983000E+01	.144740E+09	.109778E+09	-.256994E+09	.323115E+02	-.168699E+02	-.148625E+02
.984000E+01	.120950E+09	.109364E+09	-.262431E+09	.269070E+02	-.463248E+01	-.141677E+02
.985000E+01	.897235E+08	.109261E+09	-.259928E+09	.151328E+02	.123533E+02	-.146695E+02
.986000E+01	.540302E+08	.107433E+09	-.250476E+09	-.463248E+00	.335855E+02	-.180667E+02
.987000E+01	.174399E+08	.101479E+09	-.235265E+09	-.155960E+02	.508801E+02	-.132798E+02
.988000E+01	-.164822E+08	.894033E+08	-.217172E+09	-.280265E+02	.574814E+02	.772080E+00
.989000E+01	-.447792E+08	.704300E+08	-.200362E+09	-.356315E+02	.572497E+02	.103845E+02
.990000E+01	-.656344E+08	.451203E+08	-.187713E+09	-.359789E+02	.551265E+02	.140519E+02
.991000E+01	-.785605E+08	.149211E+08	-.180320E+09	-.294162E+02	.498378E+02	.189546E+02
.992000E+01	-.842341E+08	-.180596E+08	-.178472E+09	-.192634E+02	.393761E+02	.201899E+02
.993000E+01	-.841761E+08	-.509590E+08	-.180978E+09	-.103845E+02	.254014E+02	.145151E+02
.994000E+01	-.801457E+08	-.805147E+08	-.184986E+09	-.559758E+01	.108477E+02	.104231E+02
.995000E+01	-.735567E+08	-.103830E+09	-.187707E+09	-.204601E+01	-.274088E+01	.822265E+01
.996000E+01	-.656373E+08	-.118646E+09	-.186767E+09	.525014E+01	-.159435E+02	.138974E+01
.997000E+01	-.579233E+08	-.123180E+09	-.179378E+09	.151328E+02	-.273316E+02	-.579060E+01
.998000E+01	-.519383E+08	-.116563E+09	-.163247E+09	.211164E+02	-.301497E+02	-.949658E+01
.999000E+01	-.482797E+08	-.997842E+08	-.137566E+09	.197652E+02	-.197266E+02	-.156346E+02

```
THE FOLLOWING IS A PORTION OF THE PROGRAM OUTPUT FOR THE EXAMPLE
PROBLEM DESCRIBED BY THE PREVIOUS INPUT.

                                            RIGID BLOCK ANALYSIS                              PROBLEM NUMBER    1
                                          FOR RIGID BLOCK NUMBER     1                                  PAGE    1
JOB TITLE - BLOCK H STABILITY - AUBURN ARCH - POWERPLANT AREA                                    DATE  82/10/15


 CUMULATIVE DYNAMIC  DISPLACEMENTS WILL BE CALCULATED FOR UNSTABLE BLOCKS

 ANALYSIS CODE = 1  O=STATIC, 1=DYNAMIC

 WEIGHT OF BLOCK =  .2550E+09
 MASS OF BLOCK = .6600E+06

 X,Y,Z STATIC LOADS = -.1290E+09 .1100E+10 .1880E+10

 NO. OF TIME STEPS =  999 ON TAPE4
 TAPE4 BLOCK NUMBER    1

 AZIMUTH FROM NORTH TO X-AXIS = 66.5


 PLANE   STRIKE     DIP     CODE   WATER FORCE    AREA     CONC. AREA              SHEAR STRENGTH

   1     237.0      90.0      1     .5060E+08   .1710E+06  O.
                                                                         PHI =      45.00     COHESION =      0.00
   2     150.0      90.0      2     .4530E+08   .1250E+07  O.
                                                                         NORMAL STRESS       0.00    SHEAR STRENGTH       0.00
                                                                         NORMAL STRESS      50.00    SHEAR STRENGTH      52.00
                                                                         NORMAL STRESS     100.00    SHEAR STRENGTH      93.00
                                                                         NORMAL STRESS     150.00    SHEAR STRENGTH     125.00
                                                                         NORMAL STRESS     250.00    SHEAR STRENGTH     171.00
                                                                         NORMAL STRESS     500.00    SHEAR STRENGTH     235.00
                                                                         NORMAL STRESS    1000.00    SHEAR STRENGTH     369.00
   3     237.0     172.0      3     .3610E+09   .7160E+07  O.
                                                                         BARTON'S SHEAR STRENGTH PARAMETERS
                                                                         JRC =      15.00
                                                                         JCS =  12500.00
                                                                         PHI =      30.00
                                                                         EFFECTS OF VELOCITY ON SHEAR STRENGTH WILL
                                                                           BE CONSIDERED FOR PERM. DISPLACEMENTS
                                                                         CRITICAL VELOCITY =    .0118
                                                                         CHANGE IN STRENGTH/LOG VELOCITY =    .1190
   4      58.0      90.0      1    O.           O.         O.
                                                                         PHI =       0.00     COHESION =      0.00
   5     325.0      90.0      2     .2120E+08   .8570E+06  O.
                                                                         NORMAL STRESS       0.00    SHEAR STRENGTH       0.00
                                                                         NORMAL STRESS      50.00    SHEAR STRENGTH      52.00
                                                                         NORMAL STRESS     100.00    SHEAR STRENGTH      93.00
                                                                         NORMAL STRESS     150.00    SHEAR STRENGTH     125.00
                                                                         NORMAL STRESS     250.00    SHEAR STRENGTH     171.00
                                                                         NORMAL STRESS     500.00    SHEAR STRENGTH     235.00
                                                                         NORMAL STRESS    1000.00    SHEAR STRENGTH     369.00
   6       0.0       0.0      1    O.           O.         O.
                                                                         PHI =       0.00     COHESION =      0.00
```

```
                                                  RIGID BLOCK ANALYSIS                                    PROBLEM NUMBER    1
                                                FCR RIGID BLOCK NUMBER      1                                       PAGE   27
JOB TITLE - BLOCK H STABILITY - AUBURN ARCH - POWERPLANT AREA                                                  DATE  82/10/15

TIME =  4.43        TOTAL X,Y,Z FORCES  -.4218E+09 .1158E+10 .1905E+10
 FACTOR OF SAFETY =    2.07   PLANE  2   NORMAL = .5375E+09   PLANE  3   NORMAL = .1733E+10   I23 SHEAR = .1357E+10

TIME =  4.44        TOTAL X,Y,Z FORCES  -.5414E+09 .1279E+10 .2046E+10
 FACTOR OF SAFETY =    2.01   PLANE  2   NORMAL = .6692E+09   PLANE  3   NORMAL = .1858E+10   I23 SHEAR = .1482E+10

TIME =  4.45        TOTAL X,Y,Z FORCES  -.6489E+09 .1411E+10 .2168E+10
 FACTOR OF SAFETY =    1.94   PLANE  2   NORMAL = .7901E+09   PLANE  3   NORMAL = .1963E+10   I23 SHEAR = .1616E+10

TIME =  4.46        TOTAL X,Y,Z FORCES  -.7384E+09 .1511E+10 .2266E+10
 FACTOR OF SAFETY =    1.89   PLANE  2   NORMAL = .8897E+09   PLANE  3   NORMAL = .2047E+10   I23 SHEAR = .1719E+10

TIME =  4.47        TOTAL X,Y,Z FORCES  -.8063E+09 .1578E+10 .2336E+10
 FACTOR OF SAFETY =    1.86   PLANE  2   NORMAL = .9644E+09   PLANE  3   NORMAL = .2109E+10   I23 SHEAR = .1787E+10

TIME =  4.48        TOTAL X,Y,Z FORCES  -.8661E+09 .1652E+10 .2360E+10
 FACTOR OF SAFETY =    1.81   PLANE  2   NORMAL = .1032E+10   PLANE  3   NORMAL = .2123E+10   I23 SHEAR = .1856E+10

TIME =  4.49        TOTAL X,Y,Z FORCES  -.9090E+09 .1734E+10 .2333E+10
 FACTOR OF SAFETY =    1.73   PLANE  2   NORMAL = .1084E+10   PLANE  3   NORMAL = .2085E+10   I23 SHEAR = .1928E+10

TIME =  4.50        TOTAL X,Y,Z FORCES  -.9054E+09 .1794E+10 .2271E+10
 FACTOR OF SAFETY =    1.65   PLANE  2   NORMAL = .1088E+10   PLANE  3   NORMAL = .2015E+10   I23 SHEAR = .1979E+10

TIME =  4.51        TOTAL X,Y,Z FORCES  -.8656E+09 .1833E+10 .2175E+10
 FACTOR OF SAFETY =    1.57   PLANE  2   NORMAL = .1054E+10   PLANE  3   NORMAL = .1914E+10   I23 SHEAR = .2009E+10

TIME =  4.52        TOTAL X,Y,Z FORCES  -.8223E+09 .1863E+10 .2036E+10
 FACTOR OF SAFETY =    1.47   PLANE  2   NORMAL = .1015E+10   PLANE  3   NORMAL = .1772E+10   I23 SHEAR = .2024E+10

TIME =  4.53        TOTAL X,Y,Z FORCES  -.7687E+09 .1857E+10 .1867E+10
 FACTOR OF SAFETY =    1.39   PLANE  2   NORMAL = .9622E+09   PLANE  3   NORMAL = .1604E+10   I23 SHEAR = .2000E+10

TIME =  4.54        TOTAL X,Y,Z FORCES  -.6866E+09 .1799E+10 .1683E+10
 FACTOR OF SAFETY =    1.33   PLANE  2   NORMAL = .8754E+09   PLANE  3   NORMAL = .1429E+10   I23 SHEAR = .1927E+10

TIME =  4.55        TOTAL X,Y,Z FORCES  -.5876E+09 .1725E+10 .1493E+10
 FACTOR OF SAFETY =    1.26   PLANE  2   NORMAL = .7700E+09   PLANE  3   NORMAL = .1249E+10   I23 SHEAR = .1838E+10

TIME =  4.56        TOTAL X,Y,Z FORCES  -.4759E+09 .1656E+10 .1310E+10
 FACTOR OF SAFETY =    1.18   PLANE  2   NORMAL = .6525E+09   PLANE  3   NORMAL = .1076E+10   I23 SHEAR = .1758E+10

TIME =  4.57        TOTAL X,Y,Z FORCES  -.3405E+09 .1579E+10 .1147E+10
 FACTOR OF SAFETY =    1.11   PLANE  2   NORMAL = .5102E+09   PLANE  3   NORMAL = .9237E+09   I23 SHEAR = .1675E+10

TIME =  4.58        TOTAL X,Y,Z FORCES  -.1929E+09 .1491E+10 .1001E+10
 FACTOR OF SAFETY =    1.03   PLANE  2   NORMAL = .3548E+09   PLANE  3   NORMAL = .7884E+09   I23 SHEAR = .1585E+10

TIME =  4.59        TOTAL X,Y,Z FORCES  -.5001E+08 .1405E+10 .8728E+09
 FACTOR OF SAFETY =     .95   PLANE  2   NORMAL = .2038E+09   PLANE  3   NORMAL = .6711E+09   I23 SHEAR = .1498E+10

MOVEMENT STARTS AT TIME      4.584
INCREMENTAL X,Y,Z MOVEMENTS FOR TIME STEP  .8396E-04 .7369E-03 .1041E-03
```

```
                                          RIGID BLOCK ANALYSIS                              PROBLEM NUMBER    1
                                        FOR RIGID BLOCK NUMBER      1                                 PAGE   28
JOB TITLE - BLOCK H STABILITY - AUBURN ARCH - POWERPLANT AREA                                 DATE  82/10/15

TIME =  4.60       TOTAL X,Y,Z FORCES    .9096E+08 .1308E+10 .7851E+09
 FACTOR OF SAFETY =    1.00    PLANE  2    NORMAL = .5341E+08    PLANE  3    NORMAL = .5953E+09    I23 SHEAR = .1407E+10
INCREMENTAL X,Y,Z MOVEMENTS FOR TIME STEP  .8417E-03 .7388E-02 .1044E-02

TIME =  4.61       TOTAL X,Y,Z FORCES    .2208E+09 .1206E+10 .7497E+09
 FACTOR OF SAFETY =    1.04    PLANE  3    NORMAL = .5718E+09    SHEAR = .1318E+10    ALPHA =-.8918E+02
INCREMENTAL X,Y,Z MOVEMENTS FOR TIME STEP  .1371E-02 .7523E-02 .1075E-02

TIME =  4.62       TOTAL X,Y,Z FORCES    .3226E+09 .1128E+10 .7560E+09
 FACTOR OF SAFETY =    1.14    PLANE  3    NORMAL = .5859E+09    PLANE  5    NORMAL = .8838E+08    I35 SHEAR = .1264E+10
INCREMENTAL X,Y,Z MOVEMENTS FOR TIME STEP  .2265E-03 .1113E-02 .1596E-03

MOVEMENT STOPS AT TIME        4.614
TOTAL X,Y,Z COMPONENTS OF MOVEMENT  .2523E-02 .1676E-01 .2382E-02
TOTAL MOVEMENT FOR THIS CYCLE   .1712E-01

TIME =  4.63       TOTAL X,Y,Z FORCES    .4076E+09 .1076E+10 .7994E+09
 FACTOR OF SAFETY =    1.08    PLANE  3    NORMAL = .6337E+09    PLANE  5    NORMAL = .1818E+09    I35 SHEAR = .1236E+10

TIME =  4.64       TOTAL X,Y,Z FORCES    .4832E+09 .1016E+10 .8848E+09
 FACTOR OF SAFETY =    1.23    PLANE  3    NORMAL = .7243E+09    PLANE  5    NORMAL = .2674E+09    I35 SHEAR = .1205E+10

TIME =  4.65       TOTAL X,Y,Z FORCES    .5313E+09 .9624E+09 .1005E+10
 FACTOR OF SAFETY =    1.41    PLANE  3    NORMAL = .8494E+09    PLANE  5    NORMAL = .3246E+09    I35 SHEAR = .1179E+10

TIME =  4.66       TOTAL X,Y,Z FORCES    .5564E+09 .9485E+09 .1148E+10
 FACTOR OF SAFETY =    1.56    PLANE  3    NORMAL = .9918E+09    PLANE  5    NORMAL = .3513E+09    I35 SHEAR = .1190E+10

TIME =  4.67       TOTAL X,Y,Z FORCES    .5828E+09 .9551E+09 .1310E+10
 FACTOR OF SAFETY =    1.68    PLANE  3    NORMAL = .1151E+10    PLANE  5    NORMAL = .3751E+09    I35 SHEAR = .1224E+10

TIME =  4.68       TOTAL X,Y,Z FORCES    .5950E+09 .9481E+09 .1487E+10
 FACTOR OF SAFETY =    1.82    PLANE  3    NORMAL = .1326E+10    PLANE  5    NORMAL = .3876E+09    I35 SHEAR = .1244E+10

TIME =  4.69       TOTAL X,Y,Z FORCES    .5691E+09 .9489E+09 .1659E+10
 FACTOR OF SAFETY =    1.95    PLANE  3    NORMAL = .1498E+10    PLANE  5    NORMAL = .3612E+09    I35 SHEAR = .1264E+10

TIME =  4.70       TOTAL X,Y,Z FORCES    .5289E+09 .9890E+09 .1820E+10
 FACTOR OF SAFETY =    1.99    PLANE  3    NORMAL = .1653E+10    PLANE  5    NORMAL = .3131E+09    I35 SHEAR = .1317E+10

TIME =  4.71       TOTAL X,Y,Z FORCES    .4974E+09 .1054E+10 .1971E+10
 FACTOR OF SAFETY =    1.98    PLANE  3    NORMAL = .1794E+10    PLANE  5    NORMAL = .2687E+09    I35 SHEAR = .1395E+10

TIME =  4.72       TOTAL X,Y,Z FORCES    .4569E+09 .1119E+10 .2105E+10
 FACTOR OF SAFETY =    1.97    PLANE  3    NORMAL = .1920E+10    PLANE  5    NORMAL = .2154E+09    I35 SHEAR = .1469E+10

TIME =  4.73       TOTAL X,Y,Z FORCES    .3952E+09 .1181E+10 .2214E+10
 FACTOR OF SAFETY =    1.94    PLANE  3    NORMAL = .2021E+10    PLANE  5    NORMAL = .1420E+09    I35 SHEAR = .1532E+10

TIME =  4.74       TOTAL X,Y,Z FORCES    .3210E+09 .1232E+10 .2300E+10
 FACTOR OF SAFETY =    1.90    PLANE  3    NORMAL = .2101E+10    PLANE  5    NORMAL = .5876E+08    I35 SHEAR = .1579E+10

TIME =  4.75       TOTAL X,Y,Z FORCES    .2368E+09 .1263E+10 .2362E+10
 FACTOR OF SAFETY =    1.88    PLANE  3    NORMAL = .2160E+10    SHEAR = .1601E+10    ALPHA =-.8910E+02
```

```
                                        RIGID BLOCK ANALYSIS                                    PROBLEM NUMBER    1
                                      FOR RIGID BLOCK NUMBER      1                                      PAGE   29
JOB TITLE - BLOCK H STABILITY - AUBURN ARCH - POWERPLANT AREA                                  DATE  82/10/15


 TIME =  4.76       TOTAL X,Y,Z FORCES   .1511E+09 .1281E+10 .2393E+10
  FACTOR OF SAFETY =    1.88   PLANE  3   NORMAL = .2190E+10   SHEAR = .1610E+10   ALPHA =-.9222E+02

 TIME =  4.77       TOTAL X,Y,Z FORCES   .7913E+08 .1293E+10 .2390E+10
  FACTOR OF SAFETY =    1.91   PLANE  2   NORMAL = .5186E+08   PLANE  3   NORMAL = .2187E+10   I23 SHEAR = .1614E+10

 TIME =  4.78       TOTAL X,Y,Z FORCES   .9045E+07 .1292E+10 .2362E+10
  FACTOR OF SAFETY =    1.95   PLANE  2   NORMAL = .1216E+09   PLANE  3   NORMAL = .2160E+10   I23 SHEAR = .1601E+10

 TIME =  4.79       TOTAL X,Y,Z FORCES  -.7368E+08 .1274E+10 .2304E+10
  FACTOR OF SAFETY =    1.99   PLANE  2   NORMAL = .2021E+09   PLANE  3   NORMAL = .2107E+10   I23 SHEAR = .1566E+10

 TIME =  4.80       TOTAL X,Y,Z FORCES  -.1489E+09 .1245E+10 .2219E+10
  FACTOR OF SAFETY =    2.02   PLANE  2   NORMAL = .2741E+09   PLANE  3   NORMAL = .2028E+10   I23 SHEAR = .1517E+10

 TIME =  4.81       TOTAL X,Y,Z FORCES  -.2042E+09 .1201E+10 .2117E+10
  FACTOR OF SAFETY =    2.05   PLANE  2   NORMAL = .3248E+09   PLANE  3   NORMAL = .1934E+10   I23 SHEAR = .1453E+10

 TIME =  4.82       TOTAL X,Y,Z FORCES  -.2588E+09 .1136E+10 .2008E+10
  FACTOR OF SAFETY =    2.11   PLANE  2   NORMAL = .3724E+09   PLANE  3   NORMAL = .1836E+10   I23 SHEAR = .1368E+10

 TIME =  4.83       TOTAL X,Y,Z FORCES  -.3133E+09 .1061E+10 .1893E+10
  FACTOR OF SAFETY =    2.19   PLANE  2   NORMAL = .4188E+09   PLANE  3   NORMAL = .1733E+10   I23 SHEAR = .1272E+10

 TIME =  4.84       TOTAL X,Y,Z FORCES  -.3491E+09 .9914E+09 .1784E+10
  FACTOR OF SAFETY =    2.26   PLANE  2   NORMAL = .4472E+09   PLANE  3   NORMAL = .1635E+10   I23 SHEAR = .1184E+10

 TIME =  4.85       TOTAL X,Y,Z FORCES  -.3718E+09 .9261E+09 .1691E+10
  FACTOR OF SAFETY =    2.34   PLANE  2   NORMAL = .4630E+09   PLANE  3   NORMAL = .1553E+10   I23 SHEAR = .1105E+10

 TIME =  4.86       TOTAL X,Y,Z FORCES  -.3911E+09 .8629E+09 .1610E+10
  FACTOR OF SAFETY =    2.44   PLANE  2   NORMAL = .4755E+09   PLANE  3   NORMAL = .1481E+10   I23 SHEAR = .1029E+10

 TIME =  4.87       TOTAL X,Y,Z FORCES  -.3963E+09 .8065E+09 .1538E+10
  FACTOR OF SAFETY =    2.53   PLANE  2   NORMAL = .4747E+09   PLANE  3   NORMAL = .1418E+10   I23 SHEAR = .9629E+09

 TIME =  4.88       TOTAL X,Y,Z FORCES  -.3881E+09 .7590E+09 .1488E+10
  FACTOR OF SAFETY =    2.62   PLANE  2   NORMAL = .4615E+09   PLANE  3   NORMAL = .1375E+10   I23 SHEAR = .9101E+09

 TIME =  4.89       TOTAL X,Y,Z FORCES  -.3746E+09 .7180E+09 .1459E+10
  FACTOR OF SAFETY =    2.71   PLANE  2   NORMAL = .4437E+09   PLANE  3   NORMAL = .1352E+10   I23 SHEAR = .8673E+09

 TIME =  4.90       TOTAL X,Y,Z FORCES  -.3420E+09 .6860E+09 .1438E+10
  FACTOR OF SAFETY =    2.78   PLANE  2   NORMAL = .4078E+09   PLANE  3   NORMAL = .1335E+10   I23 SHEAR = .8365E+09

 TIME =  4.91       TOTAL X,Y,Z FORCES  -.2880E+09 .6674E+09 .1425E+10
  FACTOR OF SAFETY =    2.79   PLANE  2   NORMAL = .3521E+09   PLANE  3   NORMAL = .1323E+10   I23 SHEAR = .8225E+09

 TIME =  4.92       TOTAL X,Y,Z FORCES  -.2392E+09 .6617E+09 .1426E+10
  FACTOR OF SAFETY =    2.78   PLANE  2   NORMAL = .3029E+09   PLANE  3   NORMAL = .1324E+10   I23 SHEAR = .8224E+09

 TIME =  4.93       TOTAL X,Y,Z FORCES  -.1961E+09 .6703E+09 .1435E+10
  FACTOR OF SAFETY =    2.72   PLANE  2   NORMAL = .2611E+09   PLANE  3   NORMAL = .1332E+10   I23 SHEAR = .8369E+09
```